

Restes de supernova

Anne DECOURCHELLE

Service d'Astrophysique / Astrophysique, Instrumentation et Modélisation (UMR AIM)

IRFU, CEA Saclay, France

Restes de supernova : empreintes d'explosion d'étoile dans le milieu interstellaire, ils sont à plusieurs titres des acteurs majeurs de l'évolution des galaxies.

Objectif de ce cours : fournir un état des lieux de ce que nous comprenons de la physique des restes de supernova, des questions ouvertes et des observations clés pour y répondre.

Résumé du cours

Source principale de production des éléments lourds, les supernovae sont le mécanisme effectif de distribution de ces éléments dans le milieu interstellaire et gouvernent ainsi l'enrichissement chimique galactique. L'observation de restes de supernova permet d'accéder à la quantité d'éléments synthétisés, à leur mélange et dispersion, et apporte des contraintes sur le type de supernovae et le mécanisme d'explosion.

Source principale d'énergie pour le milieu interstellaire, ils sont le lieu où l'énergie cinétique déployée par l'explosion est transmise au milieu interstellaire par son chauffage à des dizaines de millions de degrés, par l'accélération de particules au choc et par la génération de turbulence. Ce sont des sites privilégiés pour rendre compte de l'accélération des rayons cosmiques galactiques et comprendre le mécanisme d'accélération en jeu.

Plan du cours

I. Introduction

1. Supernovae et leurs progéniteurs
2. Hydrodynamique des restes de supernova
3. Mécanismes d'émission
4. Moyens d'observation

II. Nucléosynthèse

1. Synthèse des éléments lourds
2. Physique de l'explosion
3. Emission gamma : raies de décroissance radioactive
4. Emission X : raies d'excitation collisionnelle

III. Accélération de particules

1. Origine des rayons cosmiques galactiques
2. Observations de l'accélération de particules dans les restes de supernova : de la radio au TeV
3. Caractérisation de l'accélération
 1. Amplification du champ magnétique au choc
 2. Energie maximale atteinte dans les restes de supernova
 3. Efficacité de l'accélération : rétroaction des particules accélérées

IV. Modélisation des restes de supernovae

V. Conclusions et perspectives

Supernova remnants: key ingredients to understand our Universe



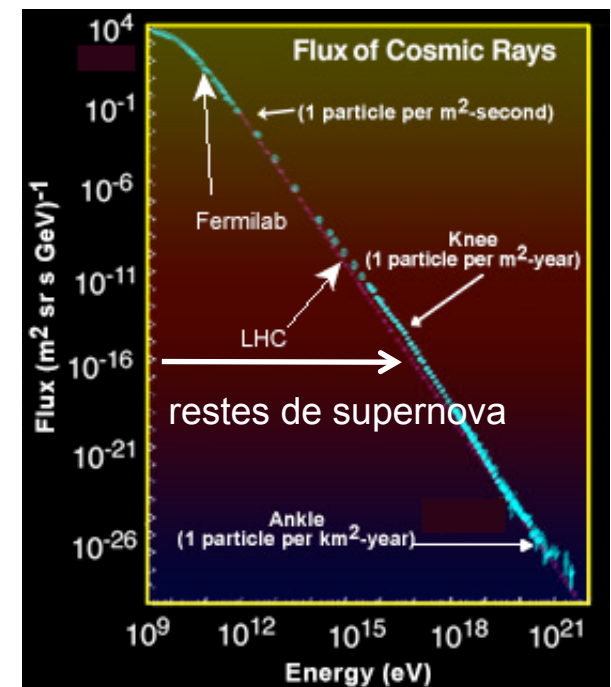
Hot diffuse gas in the Galactic center

Chemical enrichment, heating and
turbulence of the interstellar medium

Physics of supernova explosions



Origin of Galactic Cosmic Rays



I. Introduction

1. Supernovae et leurs progéniteurs
2. Hydrodynamique des restes de supernova
3. Mécanismes d'émission
4. Moyens d'observation

I.1 Supernovae et leurs progéniteurs

“Novæ” : étoiles qui apparaissent
brusquement dans le ciel
“Super” : de brillance gigantesque
⇒ SNe font partie des événements
les plus énergétiques de l’Univers

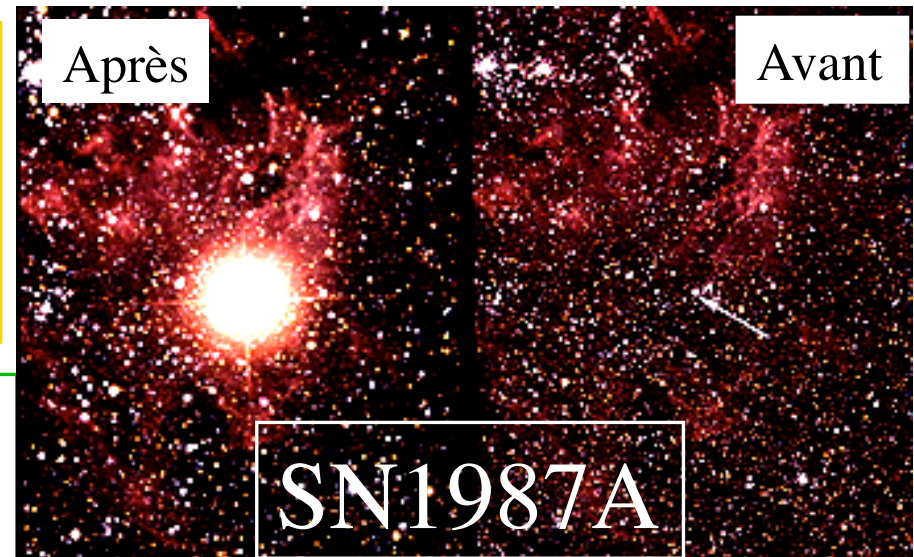
Suivant la masse du progéniteur, 2 types d’explosion :

- étoiles massives libère une énergie instantanée de $\sim 10^{53}$ ergs dont 99 % sous forme de neutrinos
- naines blanches libère $\sim 10^{51}$ ergs

Les 2 mécanismes d’explosion fournissent une énergie cinétique comparable $\sim 10^{51}$ ergs dans la matière éjectée.

⇒ compression, chauffage et accélération de particules du milieu interstellaire/circumstellaire ambiant.

Petite fraction sous la forme de lumière visible



© Anglo-Australian Observatory/Royal Observatory, Edinburgh.

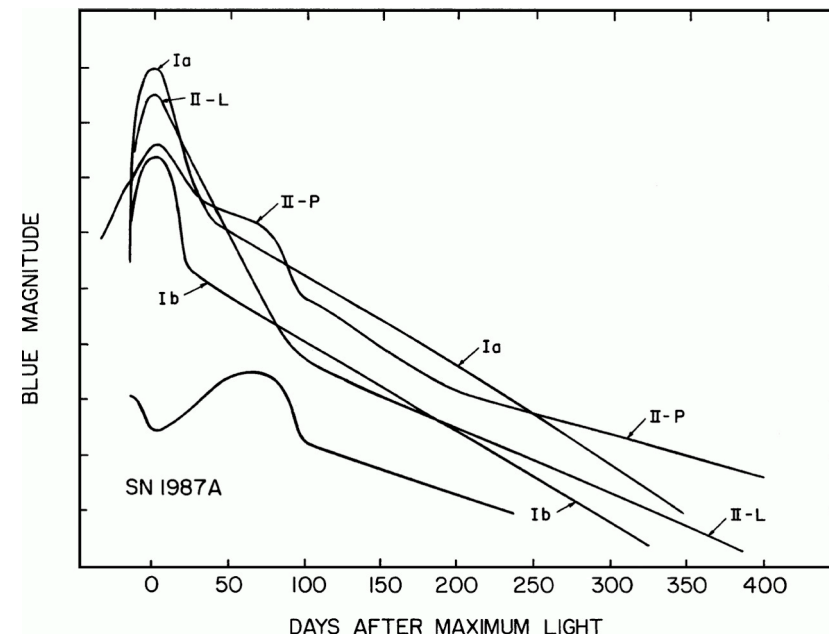
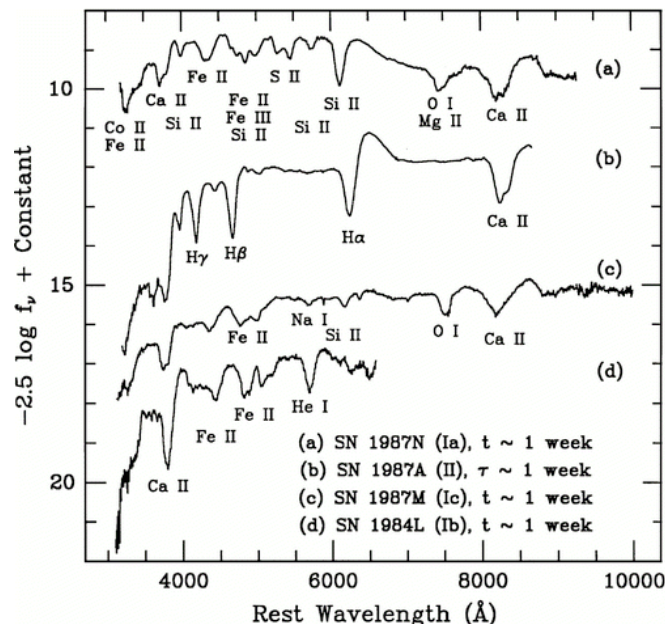
I.1 Types et progéniteurs des supernovae

Lumière visible : provient de la décroissance de noyaux radioactive synthétisés lors de l'explosion (^{56}Ni , ^{56}Co). Les photons gamma sont absorbés par le matériel éjecté et réémis dans le domaine optique.

- Forme de la courbe de lumière
- Présence ou non d'éléments identifiés par des raies en absorption dans le spectre

=> **Classification en différentes catégories des SNe extragalactiques** (Filipenko 1997)

=> signe le mécanisme d'explosion et la perte de masse, donc la nature du progéniteur



Left: Early-time spectra of supernovae for the four major types. t and τ are the time after the observed maximum in the B band and time after core-collapse, respectively. The ordinate unit is "AB magnitudes".

Right: Schematic light curves for supernovae of Types Ia, averaged Ib and Ic, II-L, II-P, and SN 1987A.

I.1 Types et progéniteurs des supernovae

Type I : absence d'hydrogène et d'hélium

- Type Ia : présence de fortes raies du silicium, puis des éléments du groupe du fer
sous-classe homogène => explosion thermonucléaire d'une naine blanche
- Type Ib : forte émission He I
- Type Ic : absence de Si II and He I
sous-classes inhomogènes => effondrement du cœur de binaire en interaction de masse modérée ayant perdu leur enveloppe d'hydrogène et d'hélium.

Type II : présence d'hydrogène

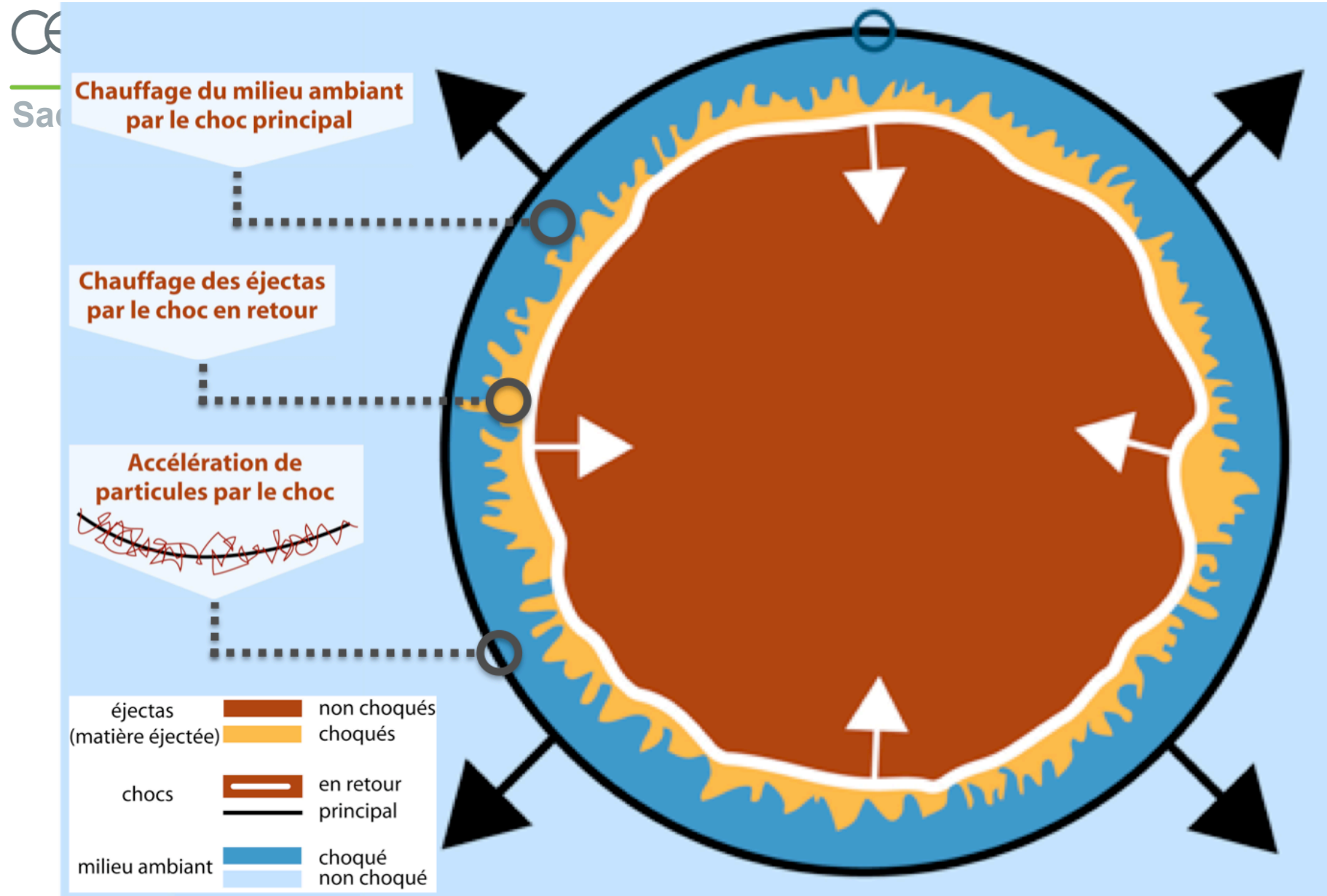
=> effondrement gravitationnel du cœur, plus de dispersion que pour les SNe de type Ia

- Type II-L : « linear » courbe de lumière similaire au Type Ia
- Type II-P « plateau » : période étendue où elle conserve leur brillance maximale
Progéniteur : supergéante rouge
- Type II-n : raies d'émission étroites courbe de lumière lentement décroissante (Schlegel 1990)
Progéniteur : avec un vent circumstellaire très dense (Chevalier 1990)
- Type IIb : caractéristiques spectrales évoluant de Type II à Type Ib (Chevalier & Soderberg 2010)
 - cIIb (progéniteur compact avec une enveloppe d'H < 0.1 Msol)
 - eIIb (progéniteur étendu avec une enveloppe d'H > 0.1 Msol)

SN Ia : observée dans les galaxies spirales et elliptiques

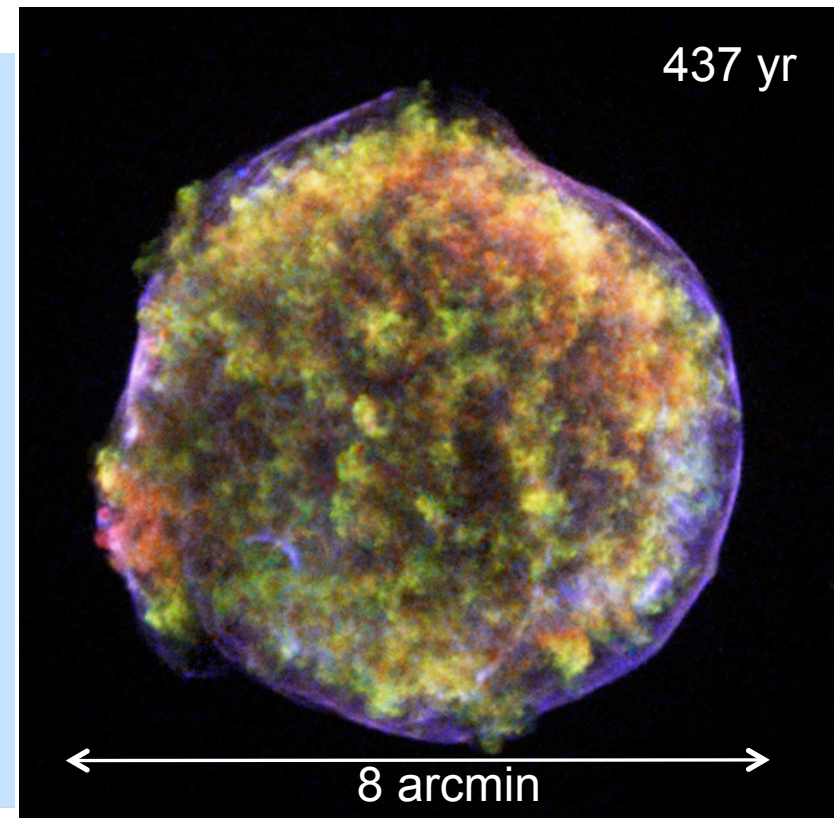
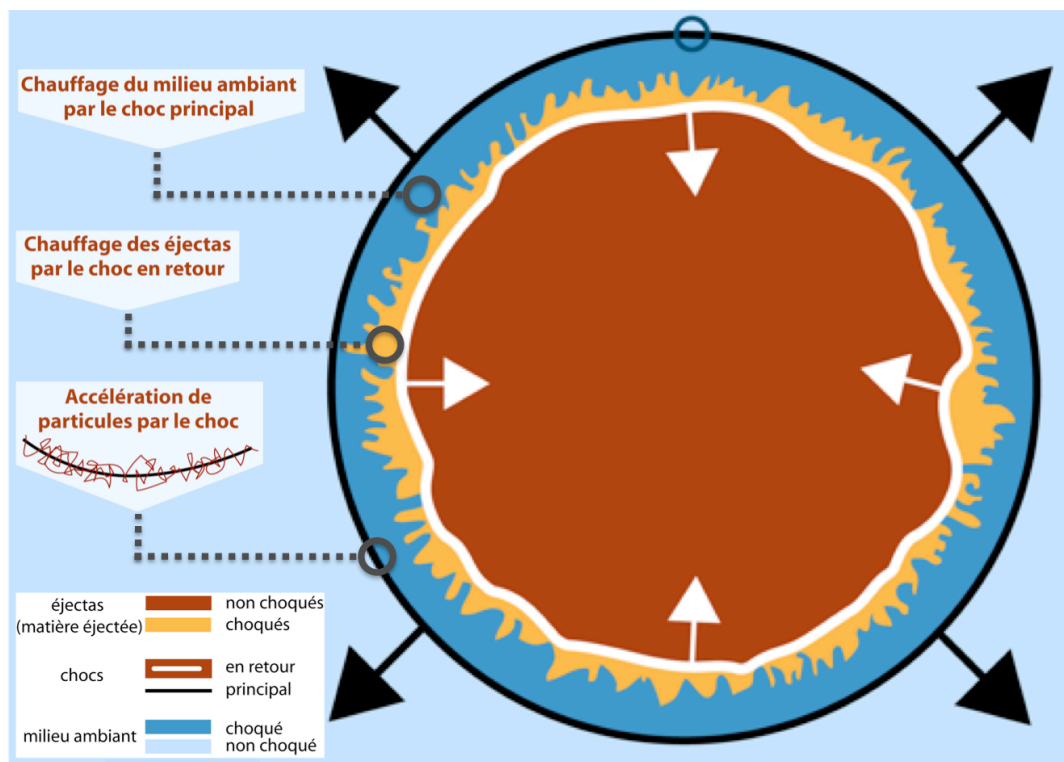
SN II, Ib, Ic : observée dans les galaxies spirales, ds ou près des bras spiraux et des régions HII.
Progéniteur : jeunes étoiles massives

I.2 Hydrodynamique des restes de supernova



I.2 Hydrodynamique des restes de supernova

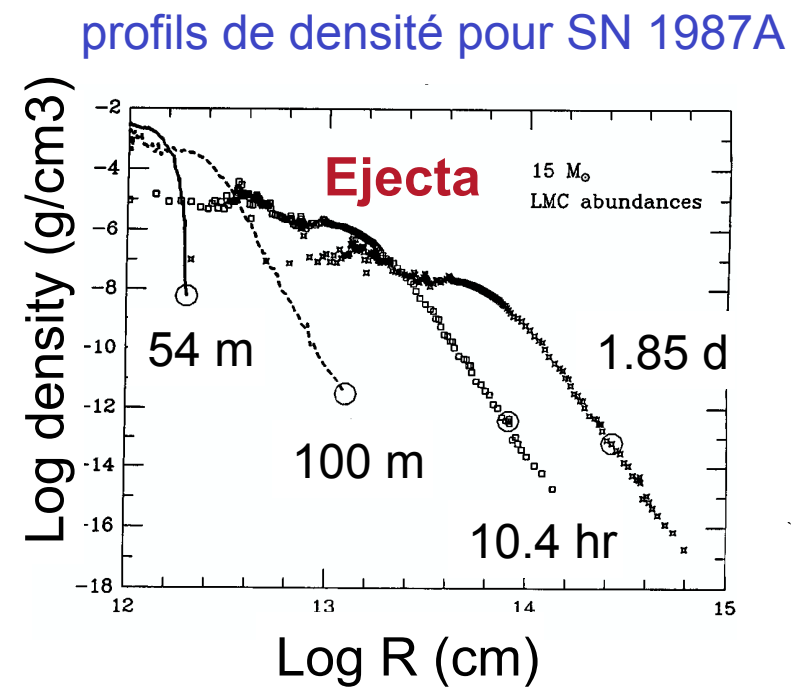
Tycho (SN 1572)
Type Ia



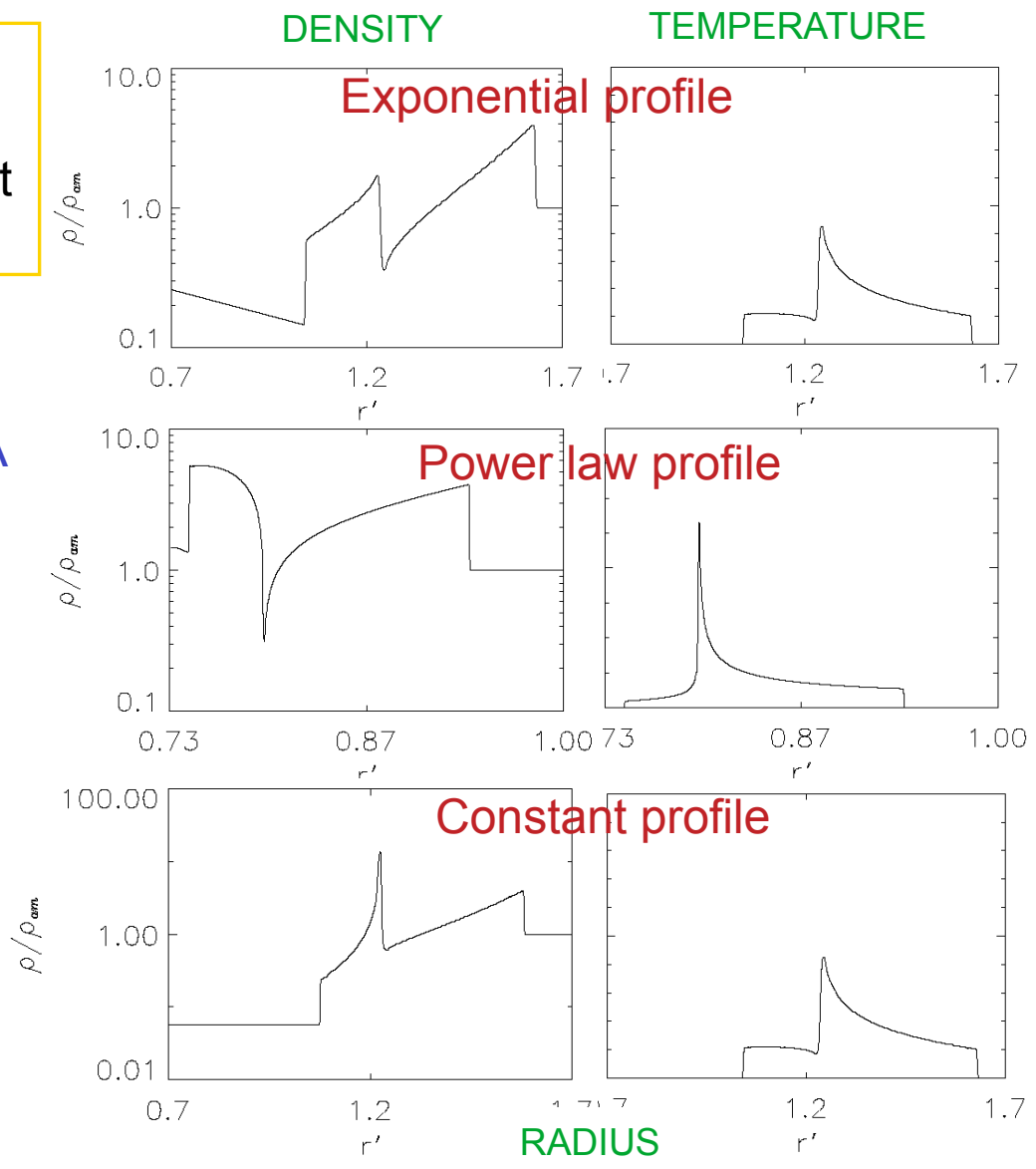
$D \sim 2.0 - 4.5 \text{ kpc}$

I.2 Hydrodynamique des restes de supernova jeunes

La structure d'interaction dépend des profils de densité initiaux des éjecta et du milieu ambiant

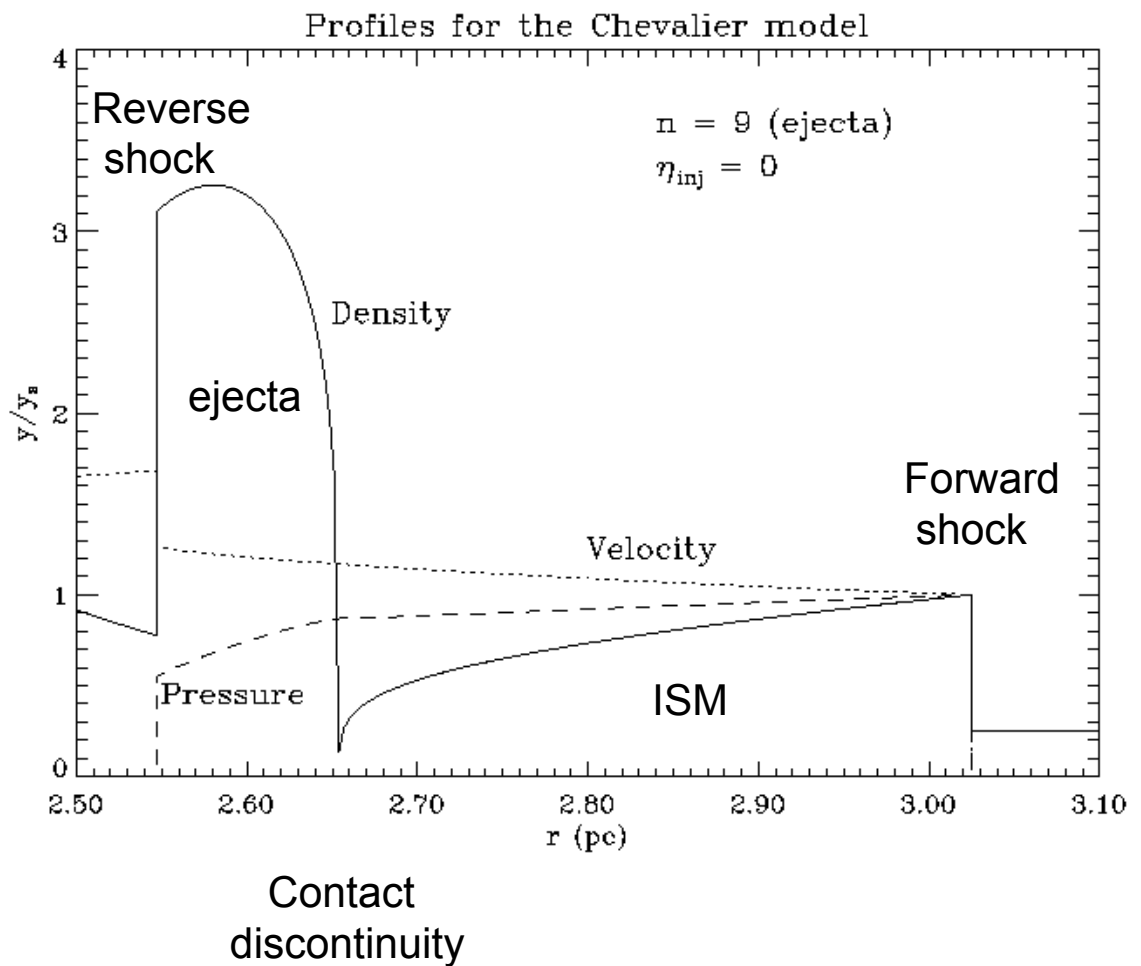
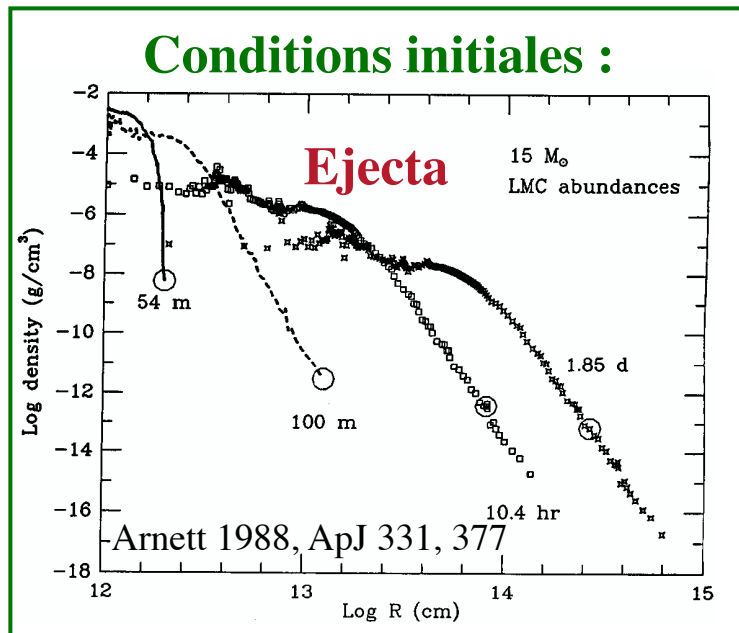


Arnett 1988, ApJ 331, 377



Dwarkadas and Chevalier 1998, ApJ 497, 807

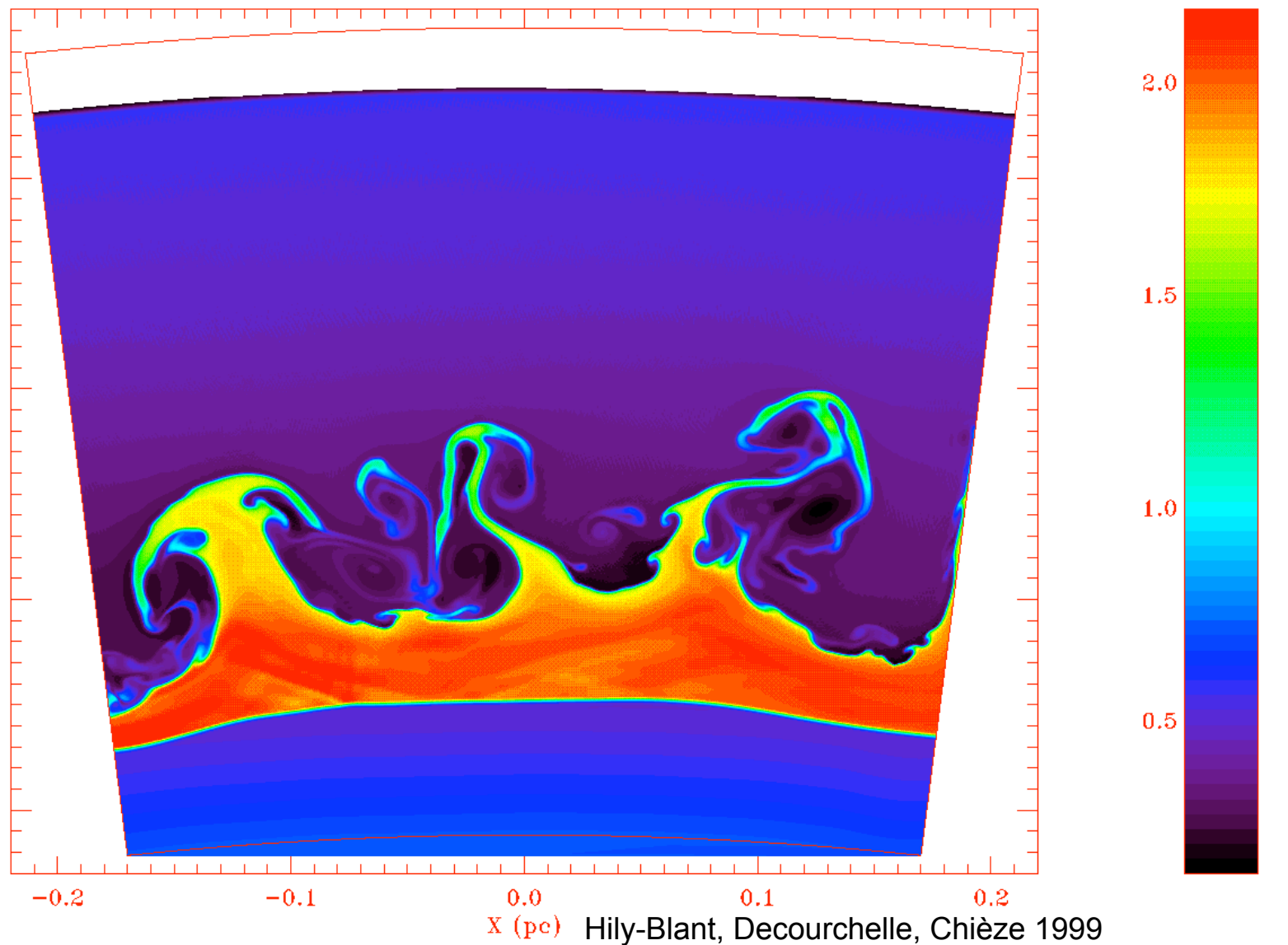
I.2 Solutions hydrodynamiques autosimilaires



Power law density profiles => self-similar solutions
 (Chevalier 1982, ApJ 258, 790)

I.2 Instabilités hydrodynamiques à l'interface

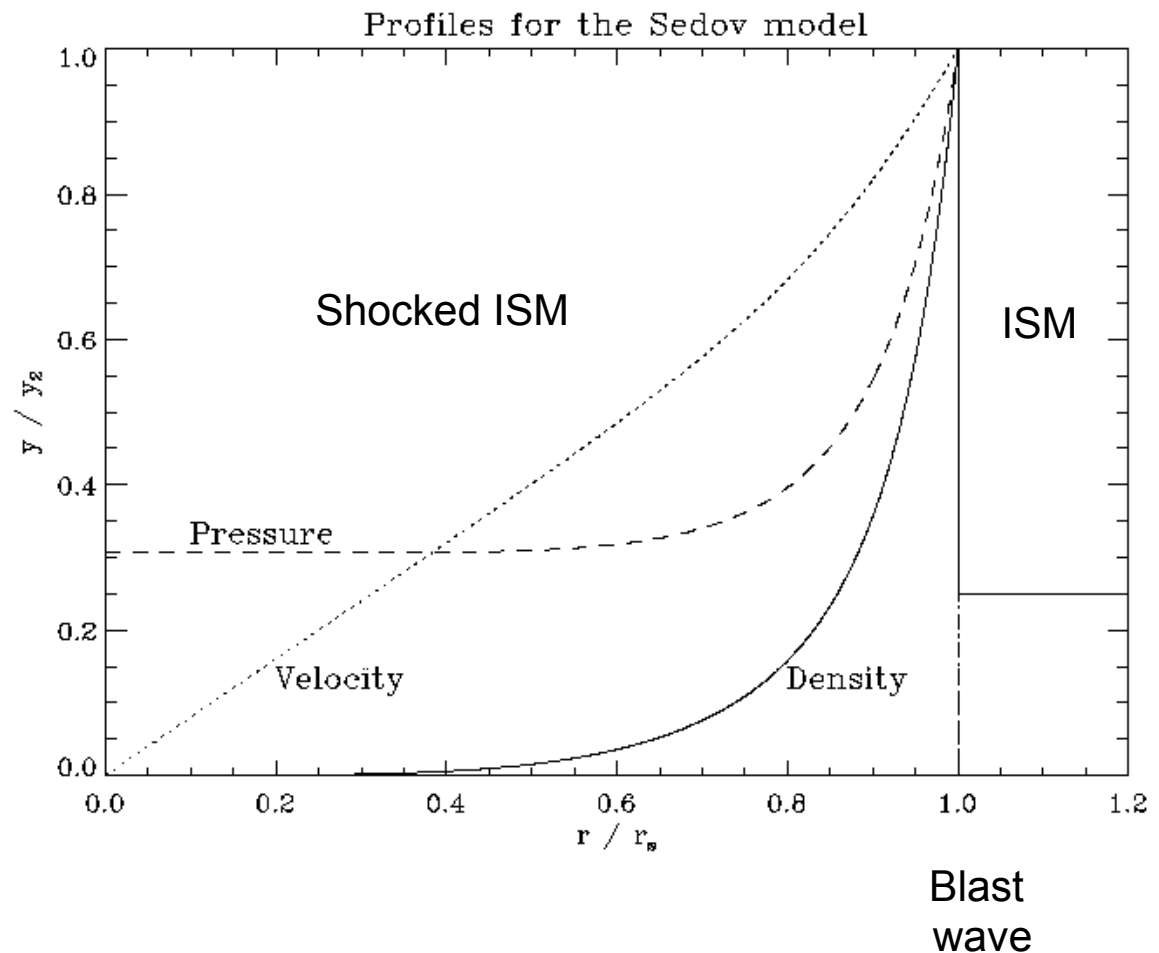
Carte de densité



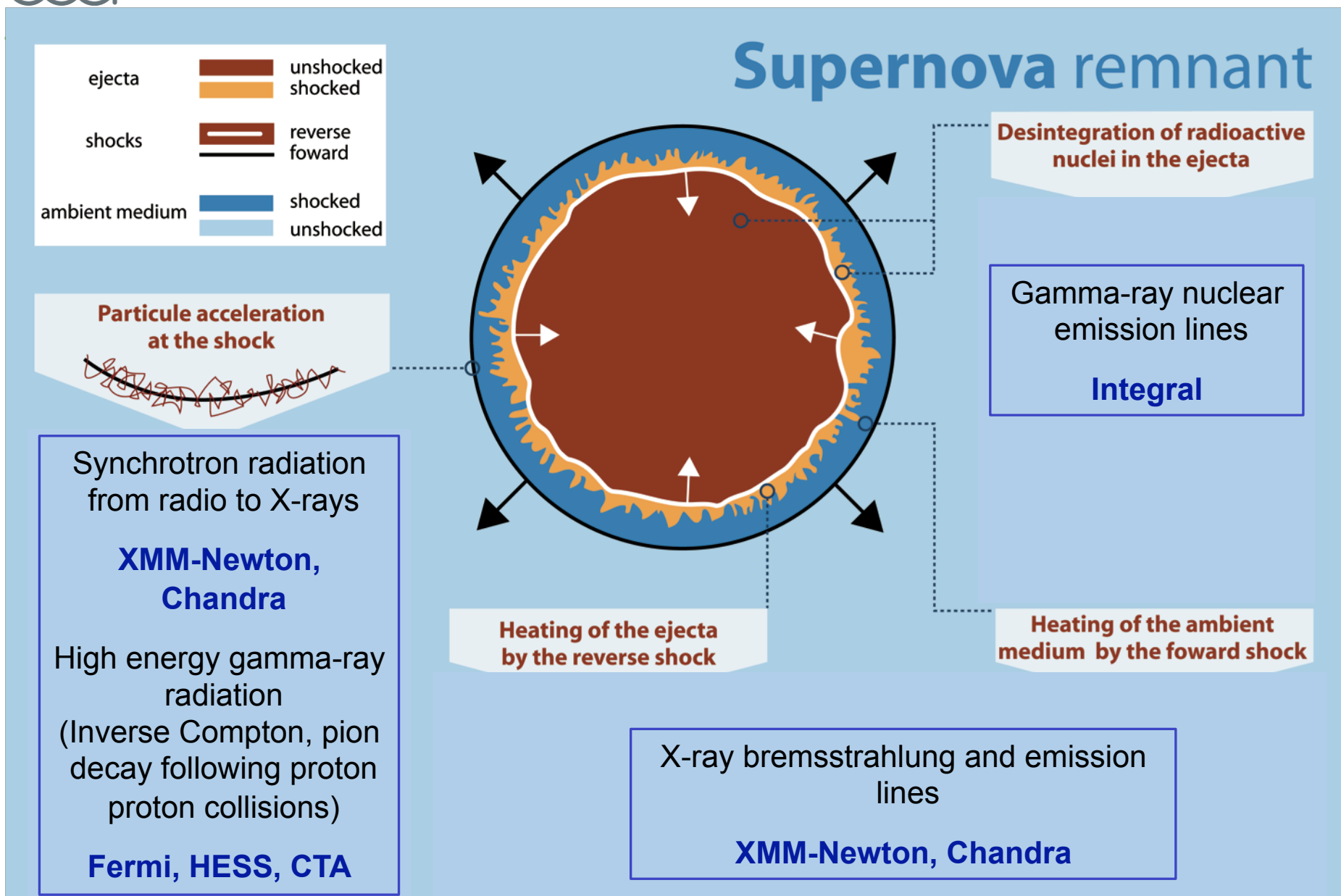
X (pc) Hily-Blant, Decourchelle, Chièze 1999

I.2 Hydrodynamique des restes de supernova matures

- Energie constante (pas de pertes radiatives)
- Densité constante du milieu ambiant ISM
- Solutions autosimilaires (Sedov 1959)



I.3 Mécanismes d'émission : la haute énergie, un domaine de préférence pour comprendre les restes de supernova



I.4 Moyens d'observations : Astronomie X et γ de 100 keV au TeV

Astronomie gamma => cours de Bernard Degrange



A very brief history of X-ray astronomy

1946: First rockets (NRL, USA) => UV and X-ray emission from the Sun, but instrumental sensitivity too low by a factor 10^5 to detect the closest stars

Giacconi => instrumental development/improvement of sensitivity

1962: second flight of ASE experiment => powerful extra-solar X-ray source discovered: **Sco X-1**

Beginning of X-ray astronomy: Physics Nobel prize in 2002

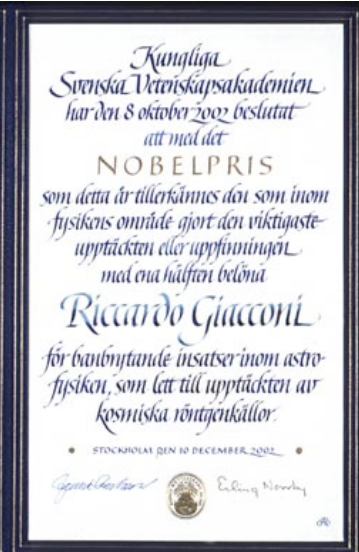
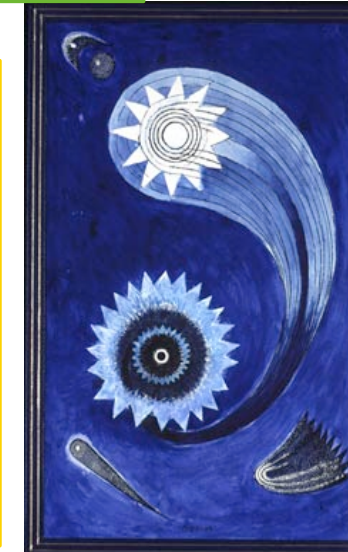
Riccardo Giacconi

Prix Nobel de Physique 2002

1970: Uhuru, first X-ray satellite: 300 sources from its sky survey.

1978-1996: numerous US, european and japanese X-ray satellites with improved detectors (Einstein, Exosat, Ginga, Rosat, Asca, RXTE, SAX)

1999: Chandra and XMM-Newton satellites opened a new area of X-ray astronomy combining spectral and spatial resolution with effective area

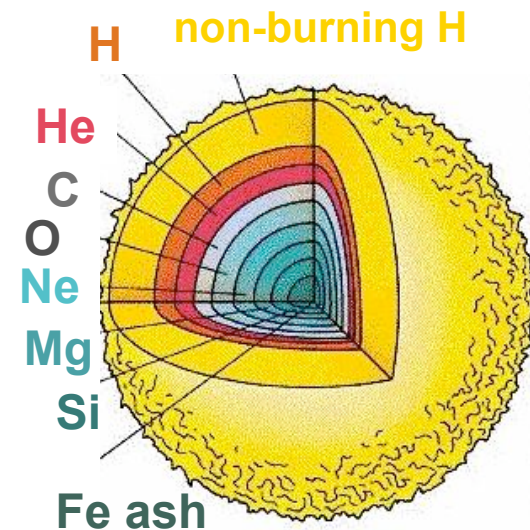


II. Nucléosynthèse

1. Synthèse des éléments lourds
2. Physique de l'explosion
3. Emission gamma : raies de décroissance radioactive
4. Emission X : raies d'excitation collisionnelle

II.1 Synthèse des éléments lourds dans les étoiles et leur dispersion

- Hydrostatic nucleosynthesis in stars**
- fusion of H to He (main sequence, millions years)
 - fusion of He to C and O (giant stars)
 - fusion of C, O, Ne to Mg, Si, S up to Fe (supergiant stars)
- => long timescale, classic onion-skin structure**



- Explosive nucleosynthesis in SNe**
- most of heavy elements from Si to Fe peak
 - only provider of elements heavier than lead and stable isobars
- Very short timescale (s) and large energy (kinetic $\sim 10^{51}$ ergs)**
- => much more diverse distribution of the elements**
- Effective mechanism for dispersing them in the ISM**

=> drive heavy-element enrichment of the interstellar medium in galaxies

II.2 Physics of supernovae: type Ia

Two main types of SN explosions: quantity of synthesized elements depends on the type and on the detailed physics of the explosion

Thermonuclear supernovae: SN Ia

explosion of accreting white dwarf in a binary system when $M_{WD} > 1.4 M_{\odot}$ via mass transfer

⇒ total disruption of WD and complete ejection of synthesized elements

- main provider of Fe (~75 %) and Fe peak nuclei.
- standard candles for cosmology



Open questions

- nature of the companion: normal star (single degenerate) or a white dwarf (double degenerate)?
- Ignition of the burning and burning front propagation ?

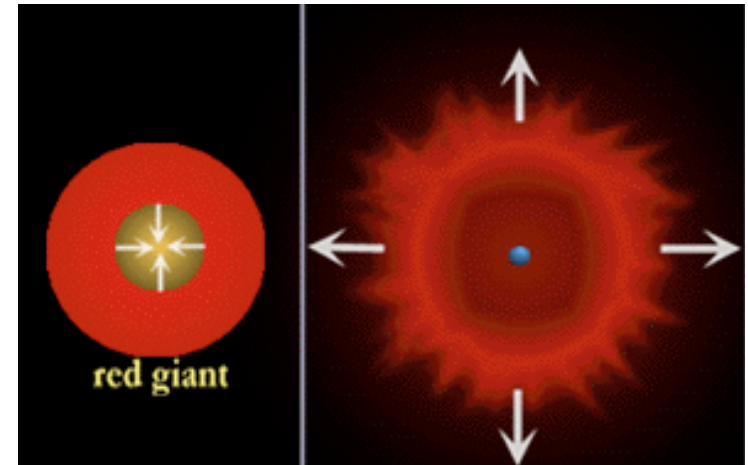
Quantity of synthesized elements depends on:

- accretion rate from the companion star
- physics of propagating flame fronts (slow / fast deflagration, transition to detonation)
=> constraints from the observed ratio between intermediate elements and iron

Core collapse supernovae : SN II, Ib, Ic

Gravitational collapse of Fe core of a massive star after successive stages of hydrostatic burning
=> **neutron star / black hole and envelope ejection**

- main provider of intermediate elements (Si-Ca): 70 %
- responsible for enrichment in very early universe



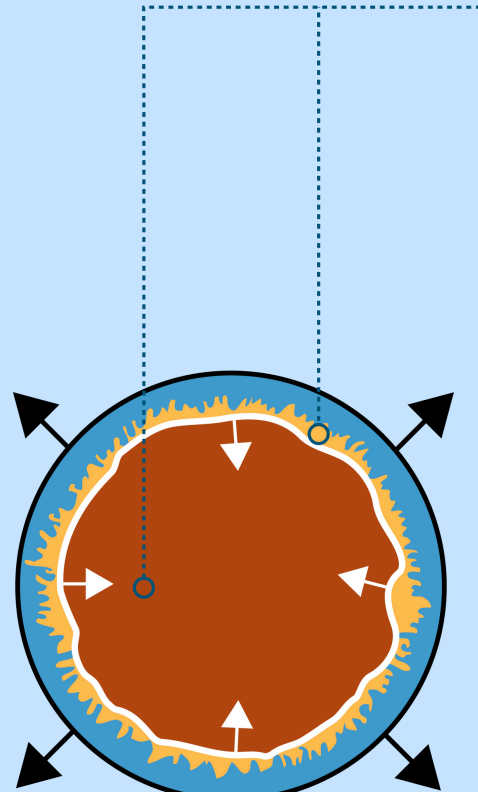
Open questions depending on the progenitor:

- Value of the mass-cut ? unclear on theoretical grounds
- Explosion mechanism: neutrino-driven, MHD-driven (jets)

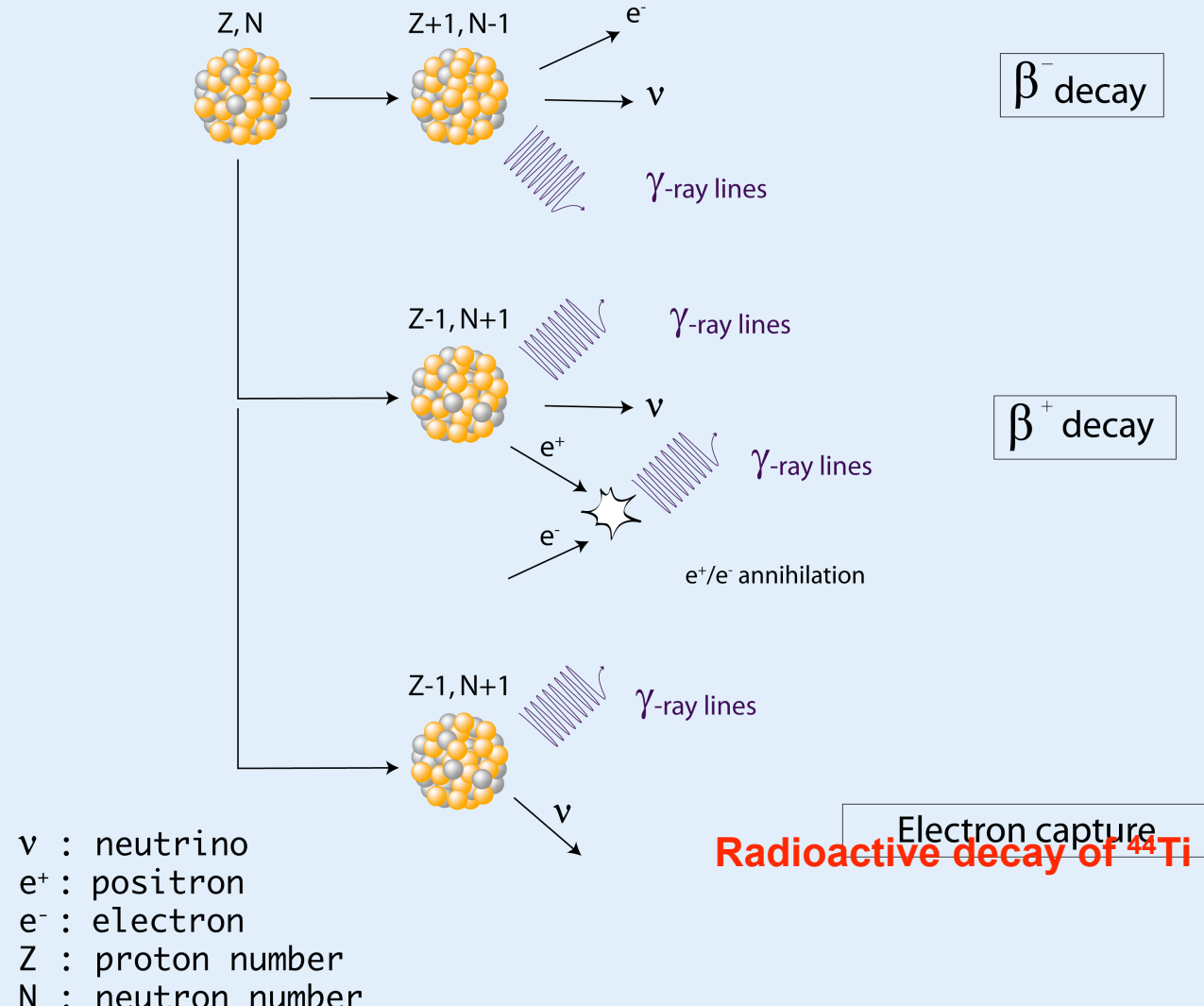
Quantity of synthesized elements depends on:

- **progenitor** for element lighter than Si (essentially produced during hydrostatic evolution and spread away in the explosion)
- **explosion energy and amount of matter accreting onto the core before the explosion** for intermediate elements enhanced through explosive oxygen burning.
- **details of the explosion and mass-cut** between the residual compact object and the ejected envelope for iron-group nuclei

Desintegration of radioactive nuclei in the ejecta



ejecta		unshocked shocked
shocks		reverse forward
ambient medium		shocked unshocked



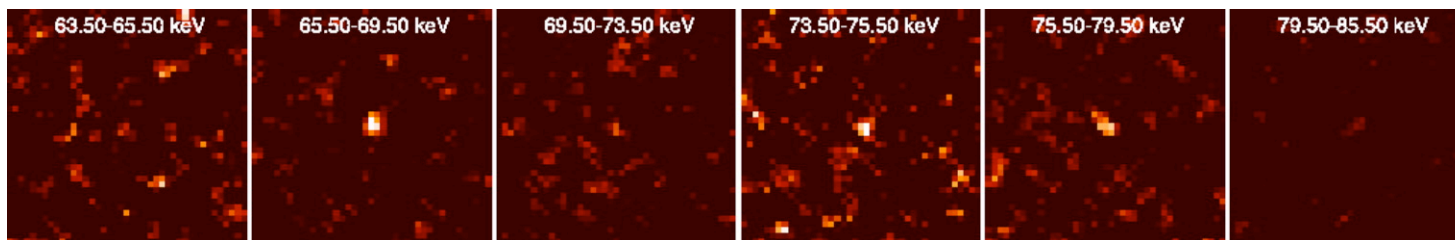
II.3 Emission gamma : raies de décroissance radioactive : ^{44}Ti

Decay-chain by electronic capture: ^{44}Ti (85 yr) \rightarrow ^{44}Sc (5.6 h) \rightarrow $^{44}\text{Ca} \Rightarrow$ 3 γ -ray lines

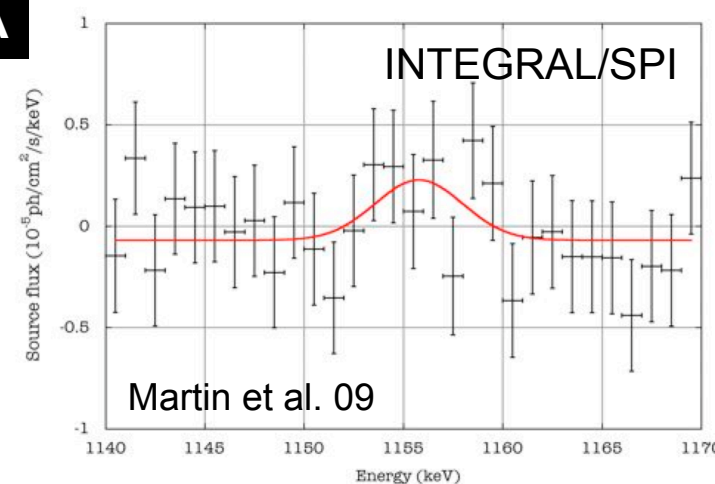
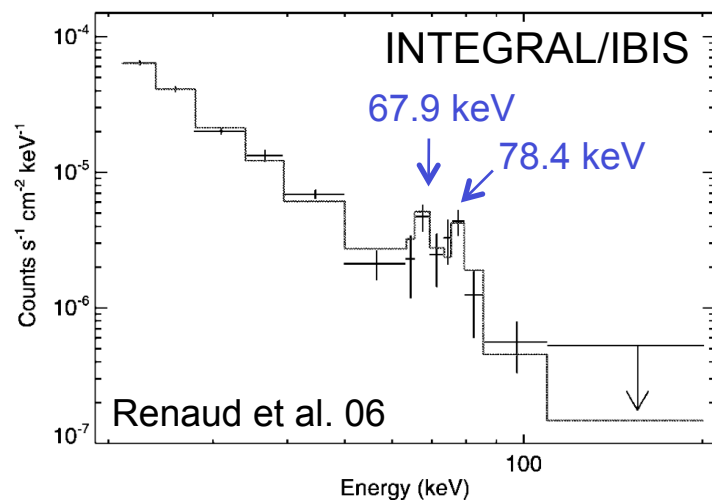
Access to the total mass of ^{44}Ti synthesized by the supernovae

=> keys to the very depths of SNe and to the physical conditions of the explosion

- 67.9 and 78.4 keV (BeppoSAX, Vink et al. 01, INTEGRAL, Renaud et al. 06) => $M(^{44}\text{Ti}) = 1.6 \cdot 10^{-4} M_{\odot}$
- 1157 keV (Comptel, Iyudin et al. 94) + search with INTEGRAL/SPI (Martin et al. 09)

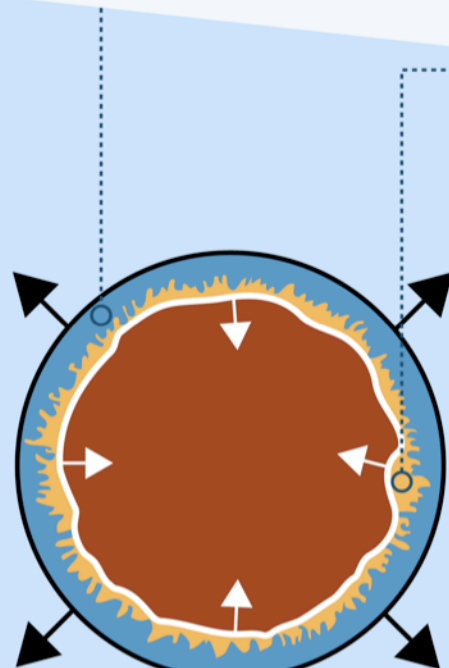


Cas A



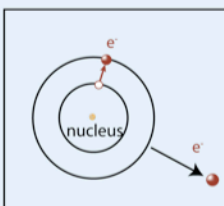
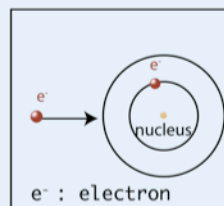
Difficult task with current hard X-ray instruments => **Nustar (2012)**

Heating of the ambient medium by the forward shock

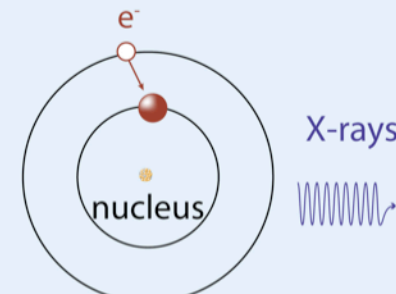


ejecta	█ unshocked █ shocked
shocks	█ reverse █ forward
ambient medium	█ shocked █ unshocked

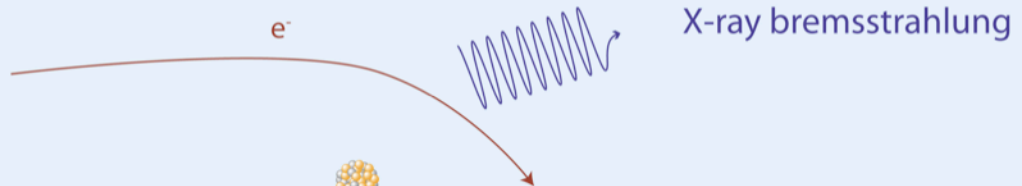
Heating of the ejecta by the reverse shock



Collisionally excited atom



Atomic deexcitation



Braking of the electron in an electric field

Supernova remnants: key ingredients to understand our Universe

Direct measurements of the composition and spatial distribution of synthesized elements in the ejected material accessible through SNRs

OBJECTIVES

- to understand how heavy elements are produced, mixed and dispersed in the ISM
- to understand the explosion mechanism of stars and their progenitors
- to provide constraints to supernova models

How: by characterizing the emission from shocked and unshocked ejecta in young SNRs

Access to the elements synthesized by the supernovae: determination of the SN type

Access to the emitting conditions in the ejecta (density, temperature): constraints on progenitor and explosion mechanism

Access to the repartition and kinematics of the synthesized elements:

- level of mixing of elemental layers and asymmetry => understanding SN explosion
- level of mixing with the ambient medium => chemical enrichment in galaxies

For either type of explosion

- Intermediate elements (Si to Ca)
- Fe production
- Asymmetries/mixing of layers

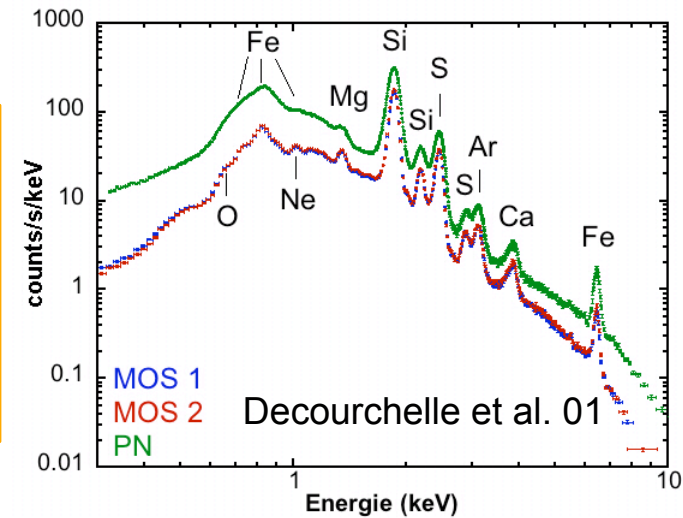
are closely related to the explosion mechanism

X-ray spatially resolved spectroscopy: a path to shocked ejecta

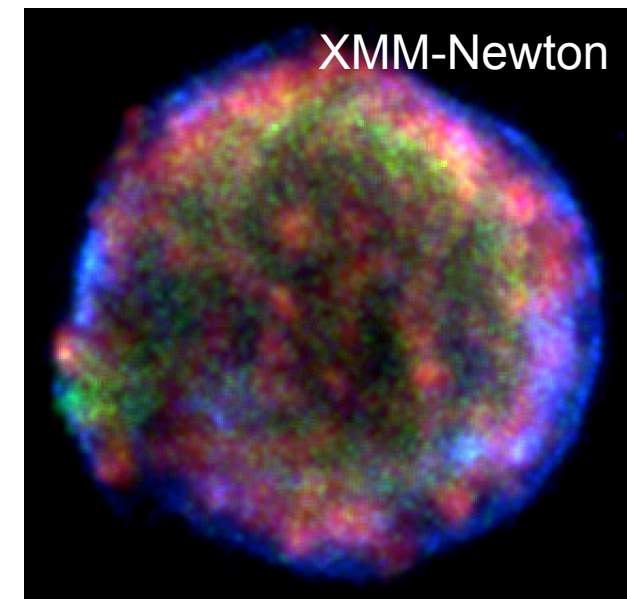
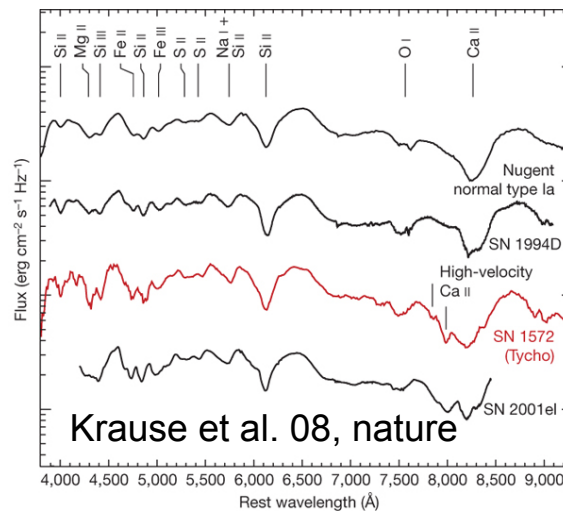
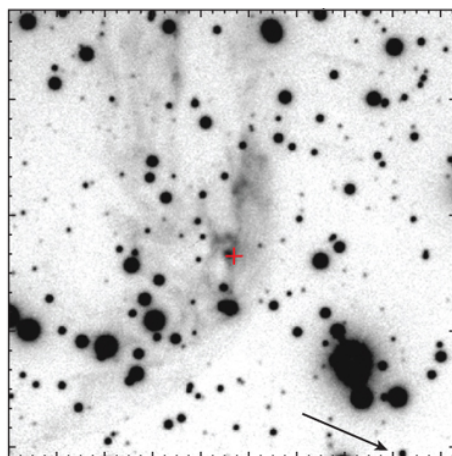
Tycho'SNR : an historical SN Ia supernova remnant (SN 1572)

Overall X-ray spectrum constrains SN type and explosion mechanism:

- delayed detonation favored for Tycho (Badenes et al. 06)
- normal type Ia confirmed by optical light echo spectrum (Krause et al. 08)



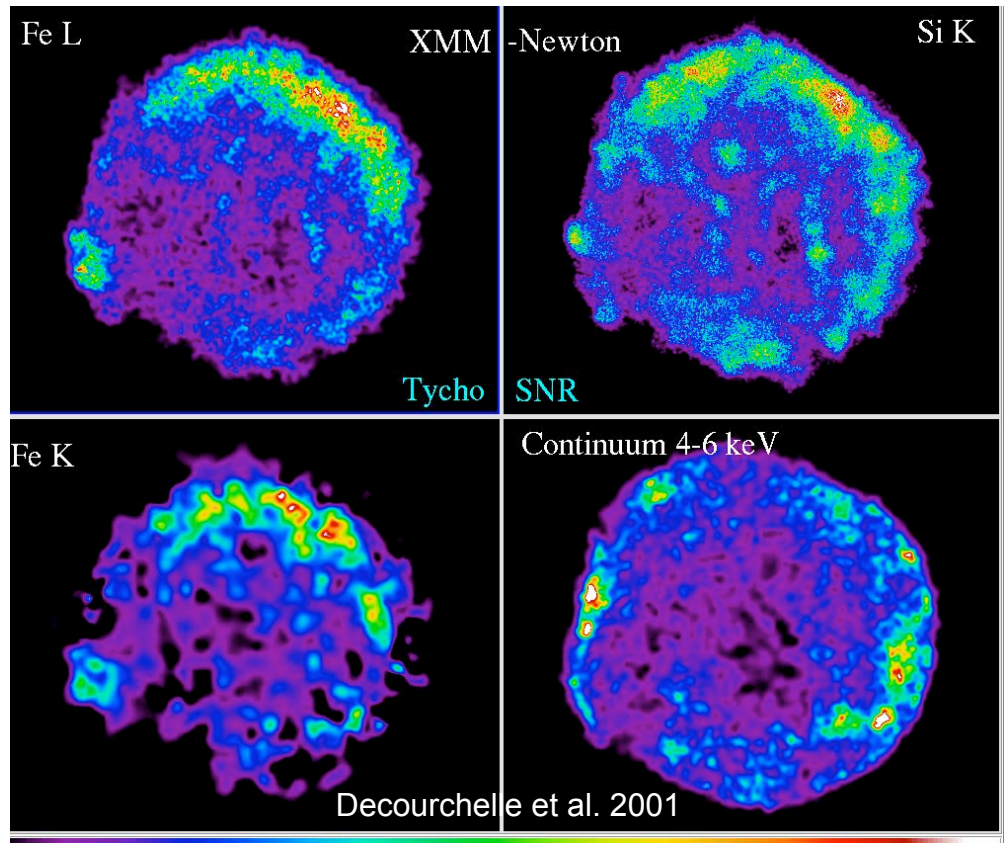
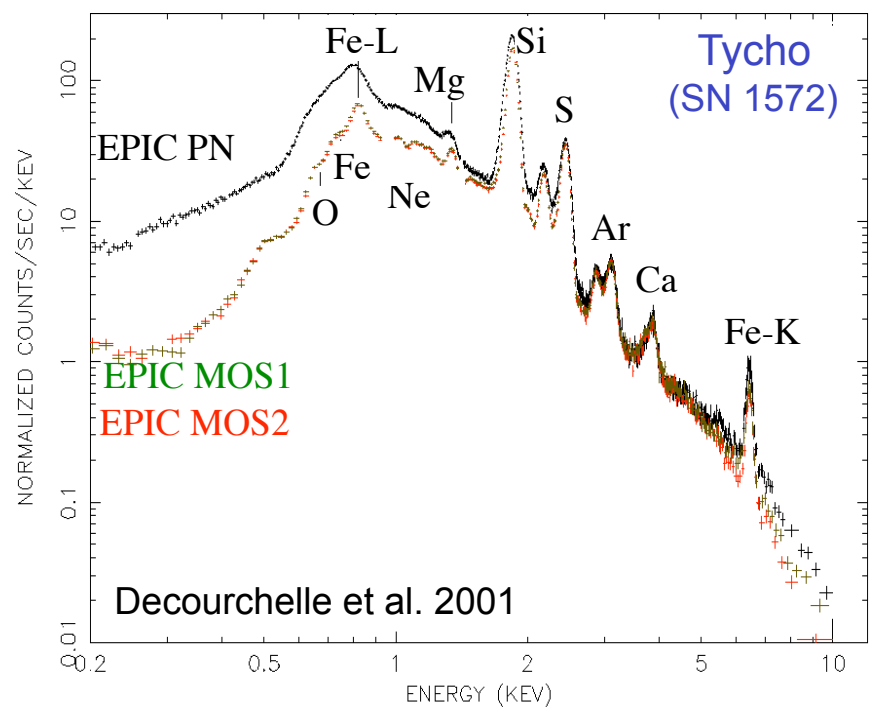
Optical light echo image and spectrum of SN 1572 compared with spectra of normal extragalactic SNe Ia



Characterization of the elements synthesized by type Ia supernovae

Goal: constrain the explosion mechanism and supernova progenitor

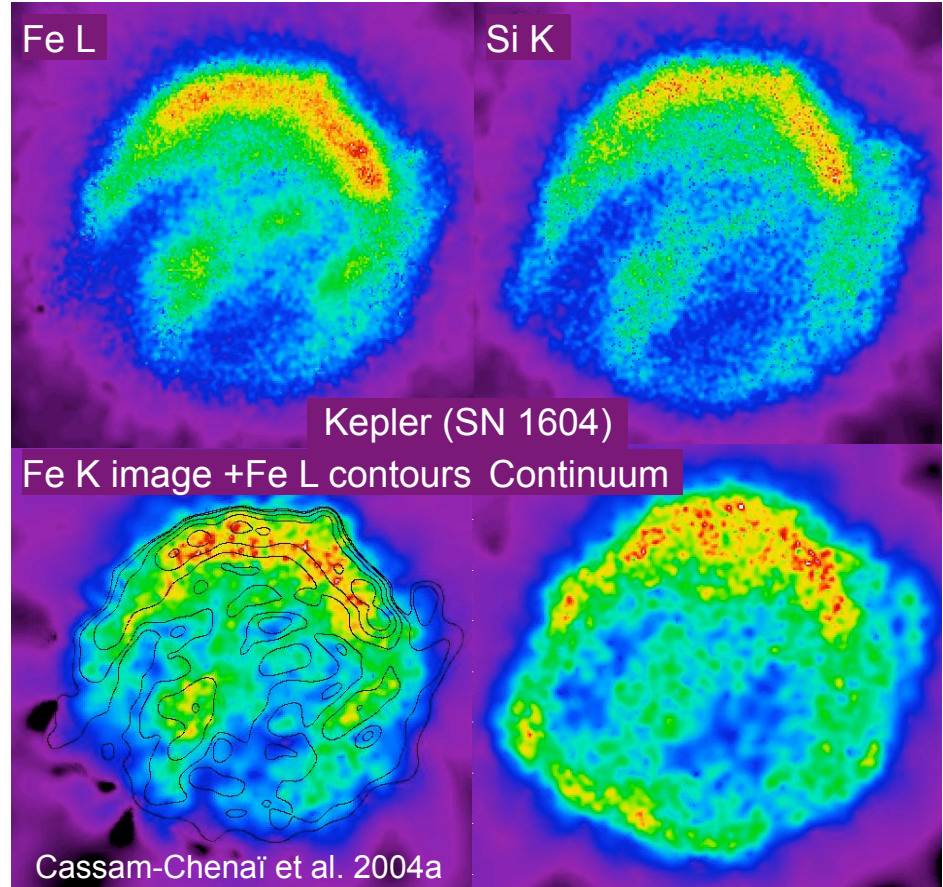
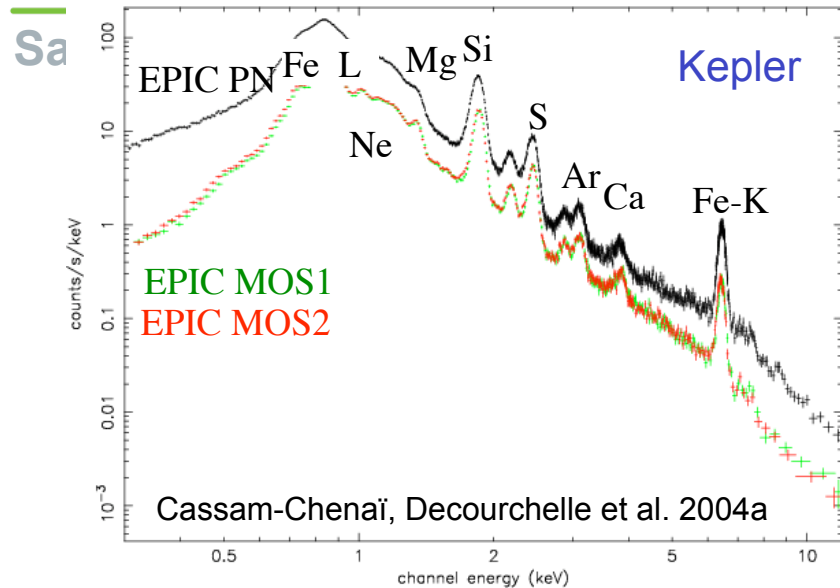
Method: characterization of the thermal emission



- Efficient overall mixing of the Si and Fe layers, but inhomogeneities at small scale.
- Fe K emission peaks at smaller radius than Fe L: higher temperature towards the interior
- Continuum emission associated with the forward shock (shown by Chandra to be nonthermal)

Characterization of the elements synthesized by supernovae

Kepler's SNR (SN 1604): a long debated historical SN type



Similarity with Tycho SN Ia

- Lines emission from Si, S, Ar, Ca, Fe
- Overall mixing of the Si and Fe layers
- Higher temperature in the interior (Fe K / Fe L)

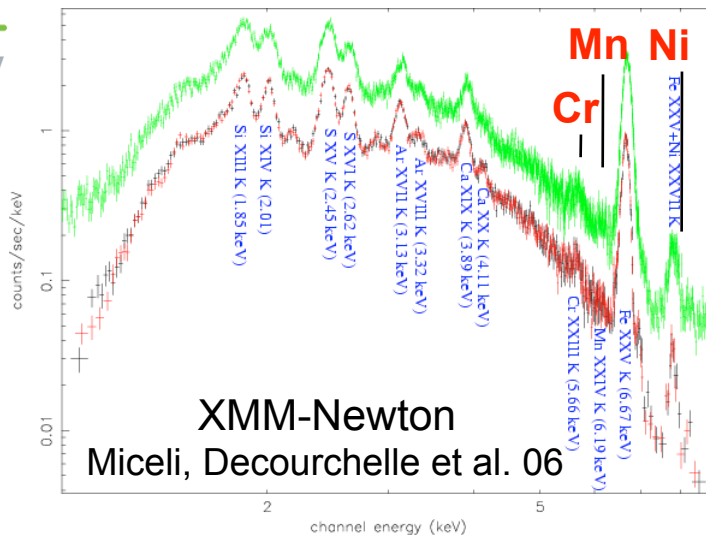
Difference: strong asymmetry of the X-ray morphology

=> circumstellar material (Cassam-Chenaï et al. 2004a)

=> SN Ia in a massive progenitor: **a different path to produce SN Ia?** (Reynolds et al. 2008)

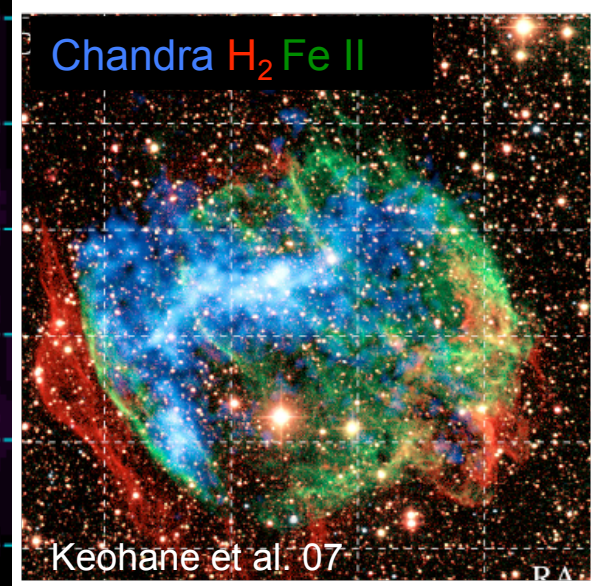
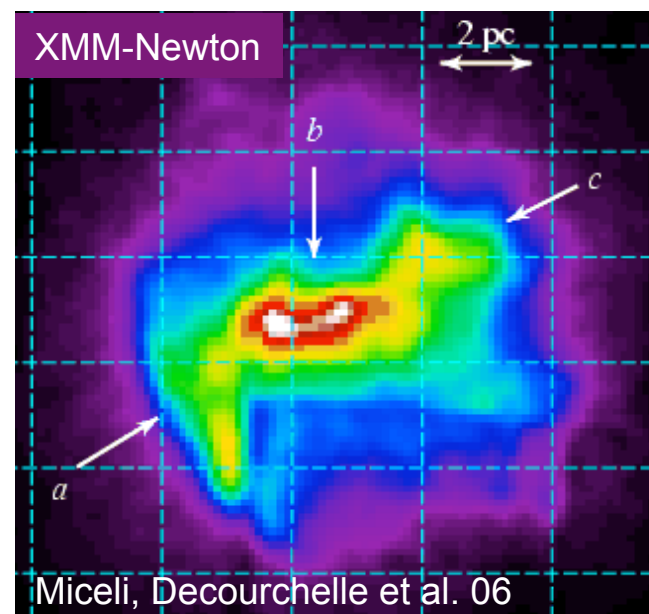
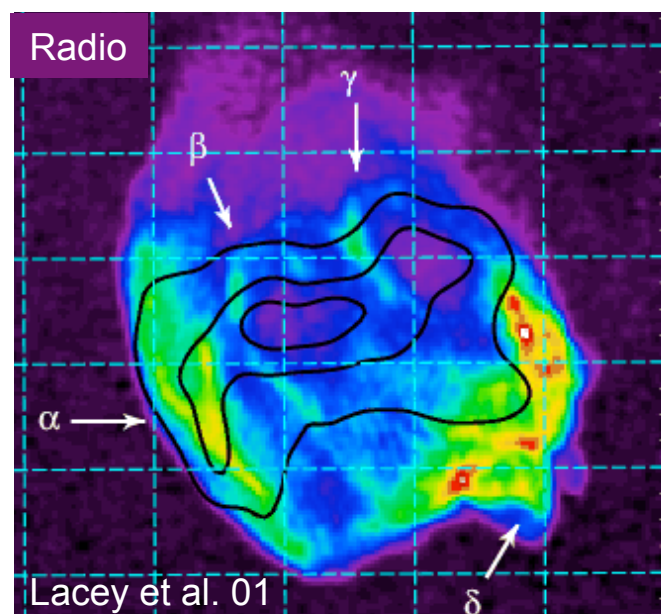
Characterization of the elements synthesized by core collapse SNe

W49B : a pure ejecta-dominated core-collapse supernova remnant

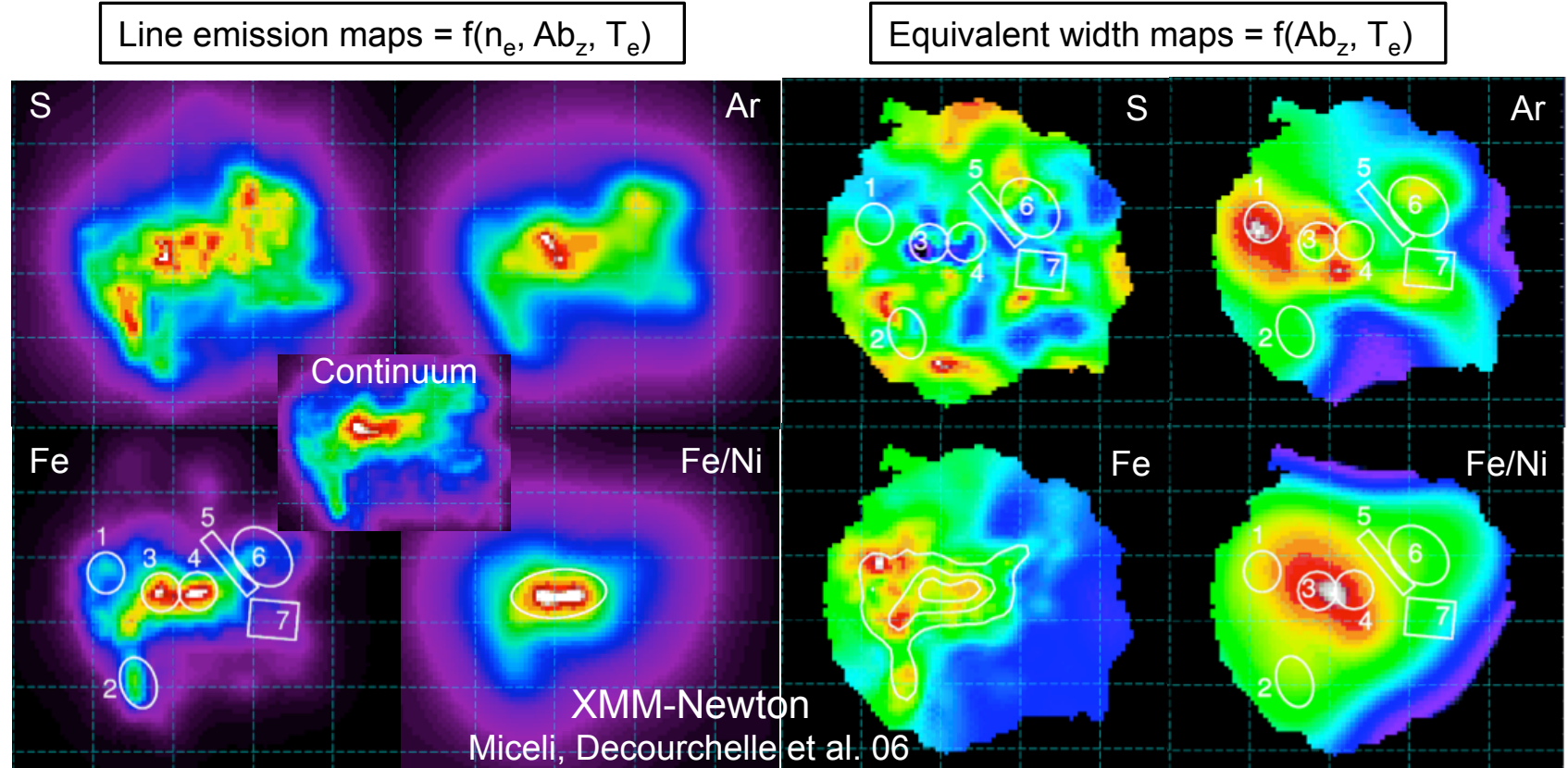


- Presence of rare elements (Cr, Mn, Ni)
- Strong bipolar X-ray ejecta emission :
asymmetry of the explosion or circumstellar
and interstellar environment ?

**How are distributed the synthesized
elements in the ejecta ?**



Distribution of the synthesized elements in W49B



Elemental distribution:

=> equivalent width images and spatially resolved spectroscopy

Chandra H₂ Fe II

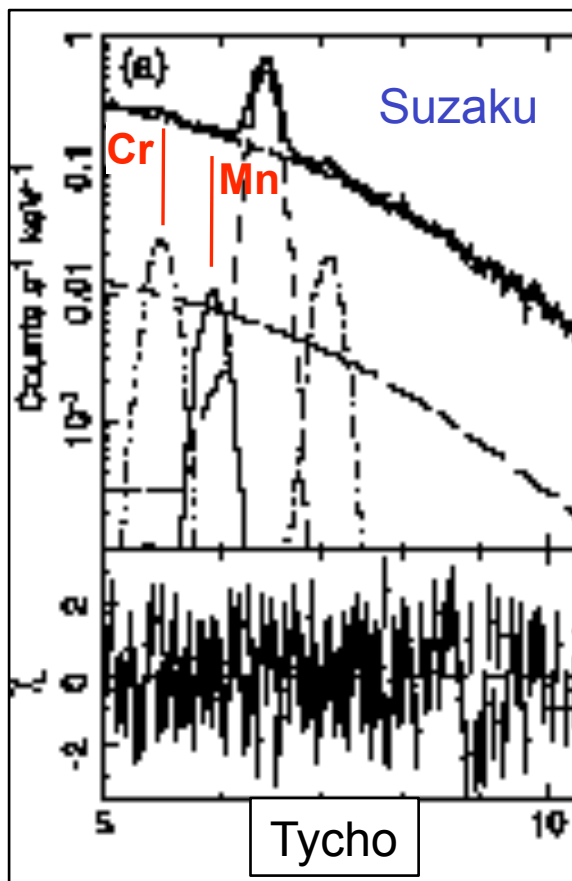
Strong asymmetry in the Fe distribution:
 Ab_{Fe} and temperature are the largest in the east side, supported by spatially resolved spectroscopy.

=> Kinematics of the ejecta required to understand the morphology

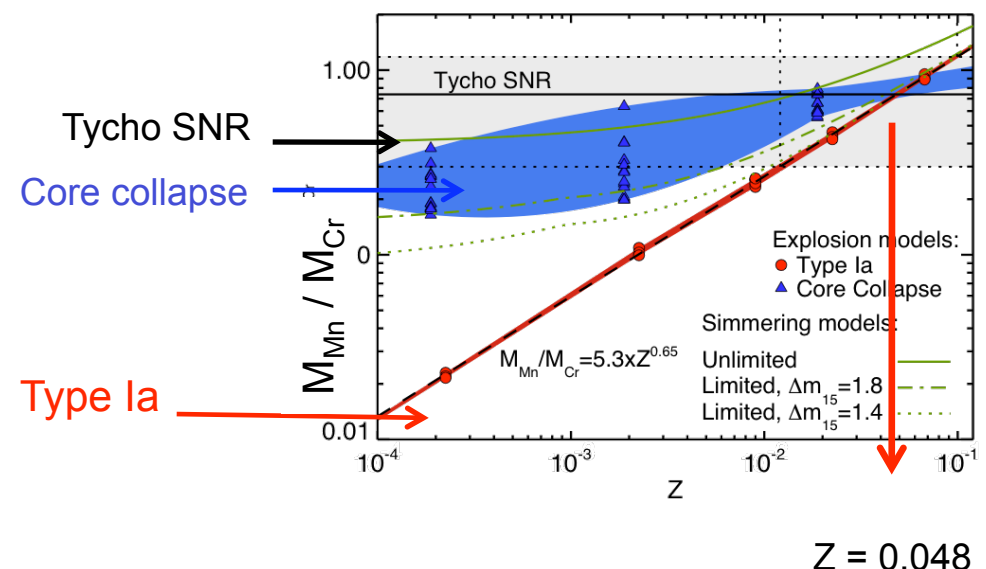
Keohane et al. 07

Presence of Cr and Mn K α lines in the X-ray spectrum of young SNRs

- W49 B (ASCA, Hwang et al. 00, XMM-Newton Miceli et al. 06)
- Tycho (Suzaku, Tamagawa et al. 09)
- Cas A, Kepler (Cr only, Chandra, Yang et al. 09)



⇒ For type Ia, Mn / Cr is a promising tracer of progenitor metallicity
(Badenes et al. 08, 09)

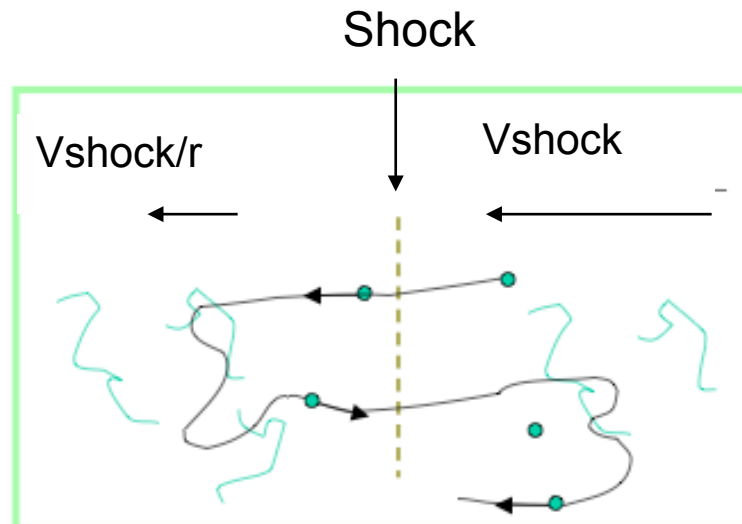


III. Accélération de particules

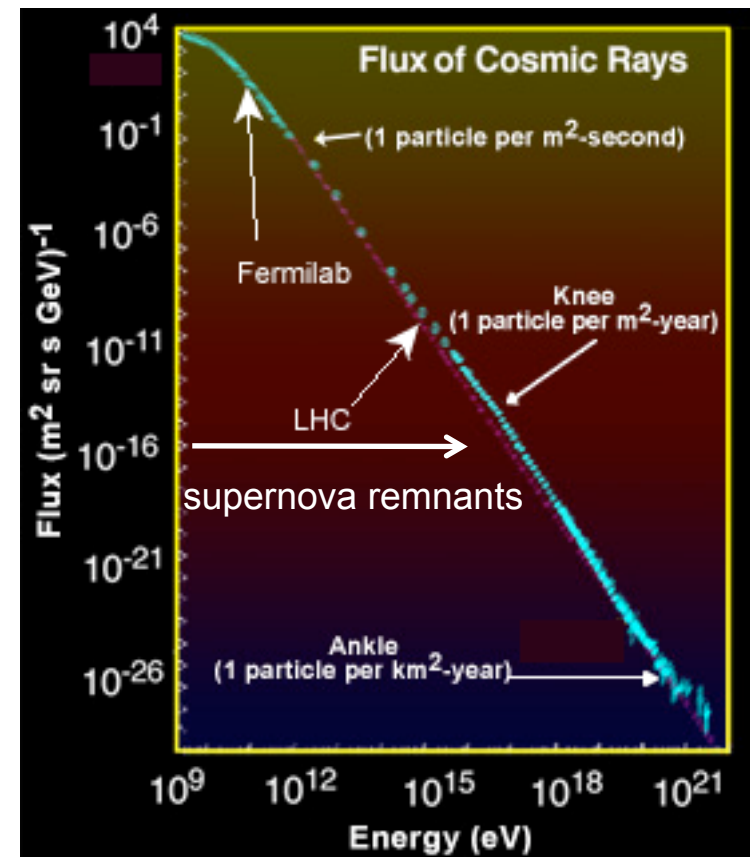
1. Origine des rayons cosmiques galactiques
2. Observations de l'accélération de particules dans les restes de supernova : de la radio au TeV
3. Caractérisation de l'accélération
 - Amplification du champ magnétique au choc
 - Energie maximale atteinte dans les restes de supernova
 - Efficacité de l'accélération : rétroaction des particules accélérées

Supernova remnants: likely the birth places of Galactic CRs up to $\sim 3 \times 10^{15}$ eV

- 10% of their kinetic energy: to maintain the pool of Galactic Cosmic rays
- High mach number shocks: 1st order Fermi mechanism through diffusive shock acceleration (1949)



First order Fermi acceleration



III.2 Observation de l'accélération de particules de la radio au TeV

Particule acceleration at the shock

ejecta unshocked shocked

shocks reverse forward

ambient medium shocked unshocked

Relativistic electron in a magnetic field

X-ray synchrotron

magnetic field line

accelerated e^-

X-ray synchrotron

Inverse Compton effect

low energy photon

γ -rays

e^-

very high energy gamma rays

Proton – proton collision

accelerated p

ambiant medium p

π^+

μ^+

ν

e^-/e^+

π^0

p

γ -rays

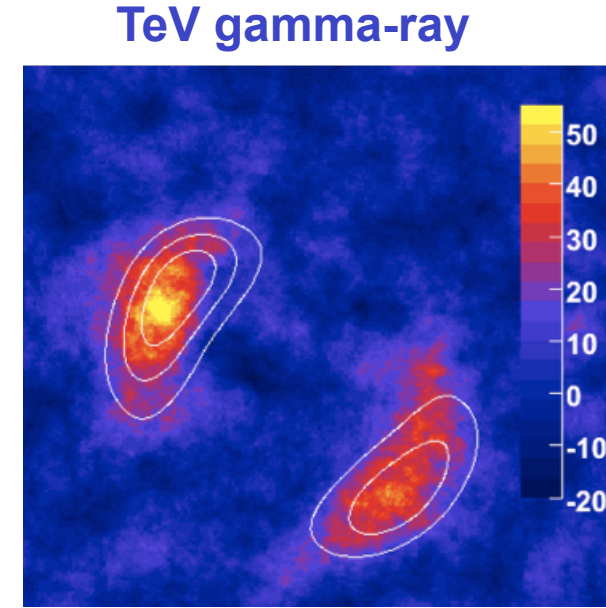
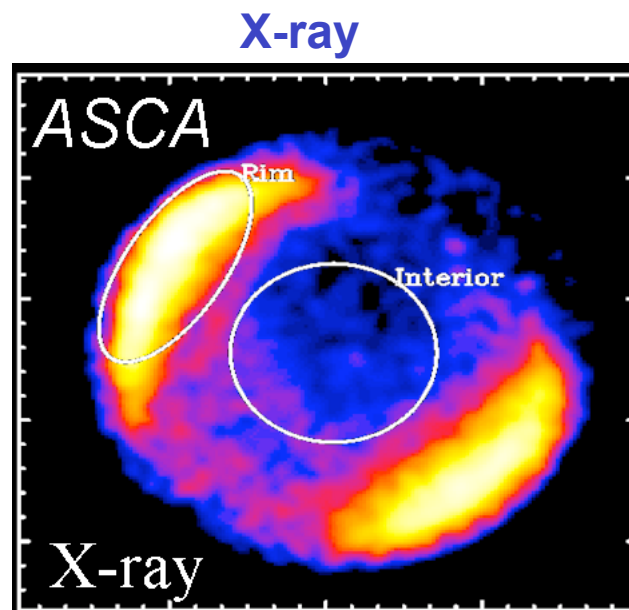
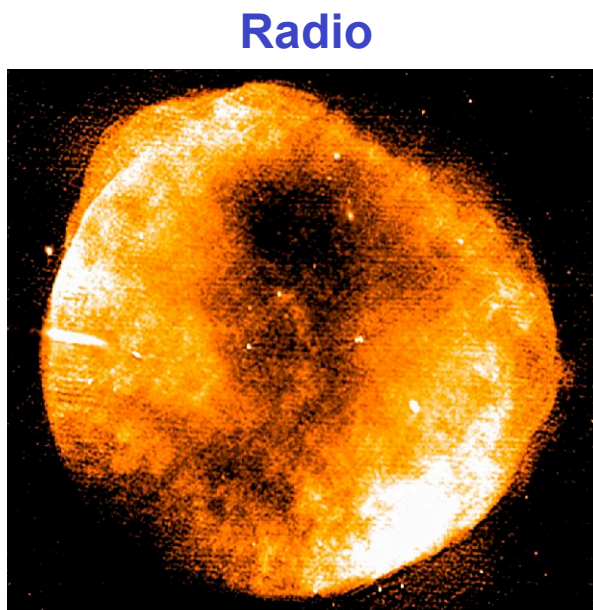
very high energy gamma rays

Graphic design by Aurélie Bordenave - Cea 2009

III.3 Emission non thermique de la radio au TeV : SN 1006

Radiative signatures at their shock:

- Radio synchrotron => electrons accelerated to GeV energies (Hanbury Brown 1954)
- X-ray synchrotron => electrons up to TeV energies in SN 1006 (Koyama et al. 1995, Nature)
- TeV gamma-ray emission => particles accelerated to TeV energies (Aharonian et al. 2004, Nature)



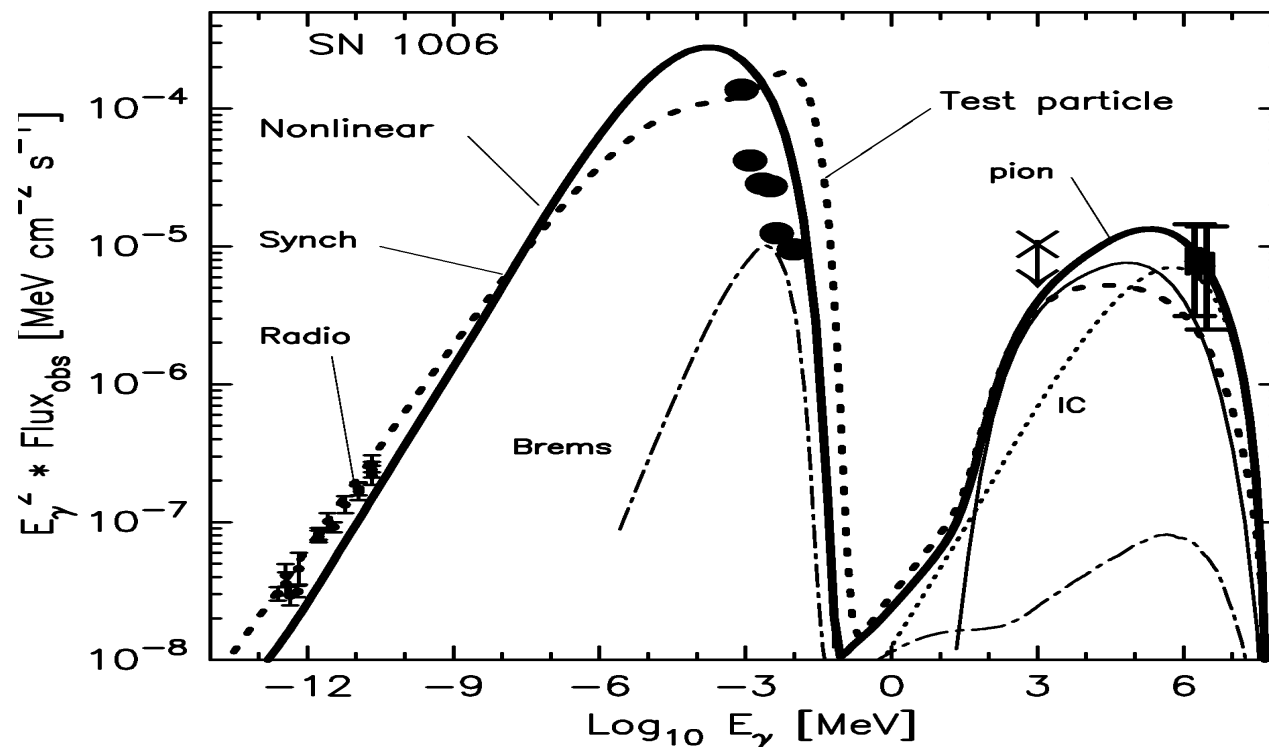
Petruck et al 08

Koyama et al. 95

Naumann-Godo et al. 09

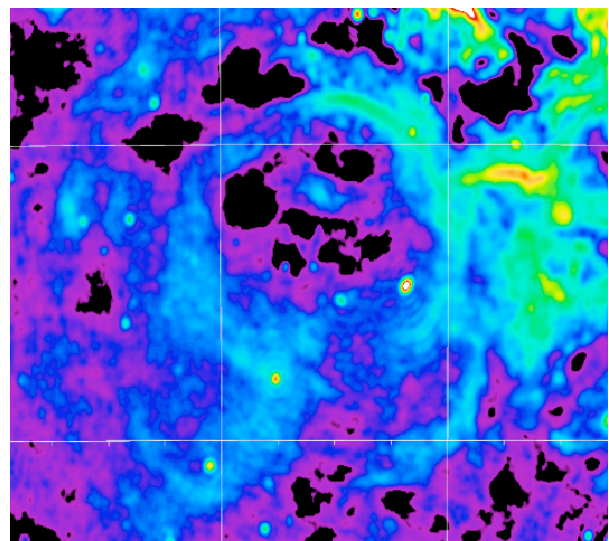
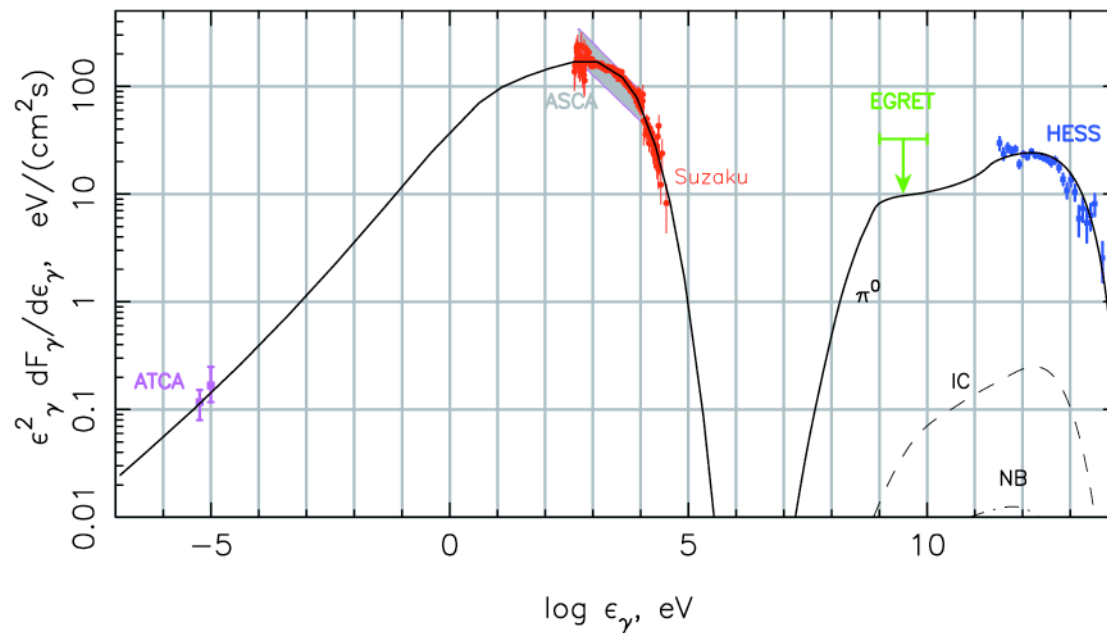
- π^0 following p-p collisions in GeV range
- Inverse Compton on CMB in TeV range

- Synchrotron from radio to X-rays
- Thermal (continuum + lines) in X-rays

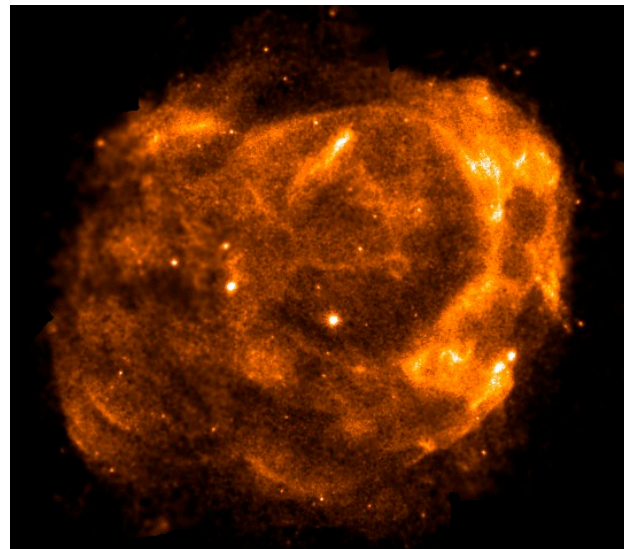


Ellison, Berezhko and Baring 2000, ApJ **540**, 292

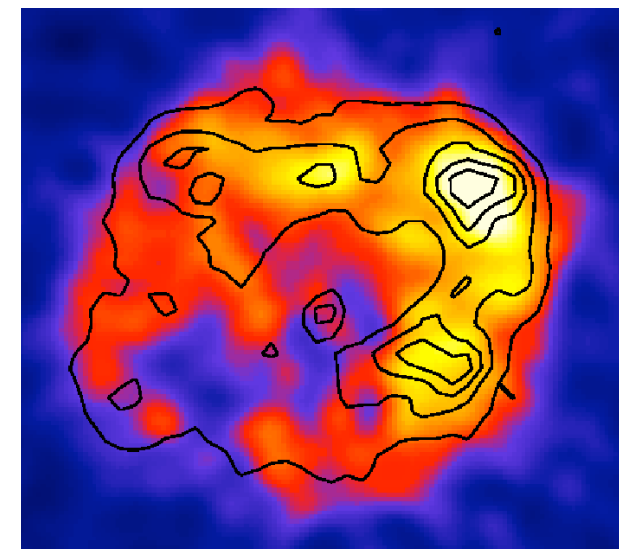
III.3 Emission non thermique de la radio au TeV : G347.3-0.5



Radio - ATCA



Rayons X - XMM-Newton



Rayons gamma - HESS

Objective : to understand the process of particle acceleration and the origin of Galactic cosmic rays

- What is the level of magnetic field amplification at the shock ?
- What is the maximum energy of the accelerated particles ?
- What is the efficiency of particle acceleration ?
- ...

Why are X-rays crucial to investigate particle acceleration ?

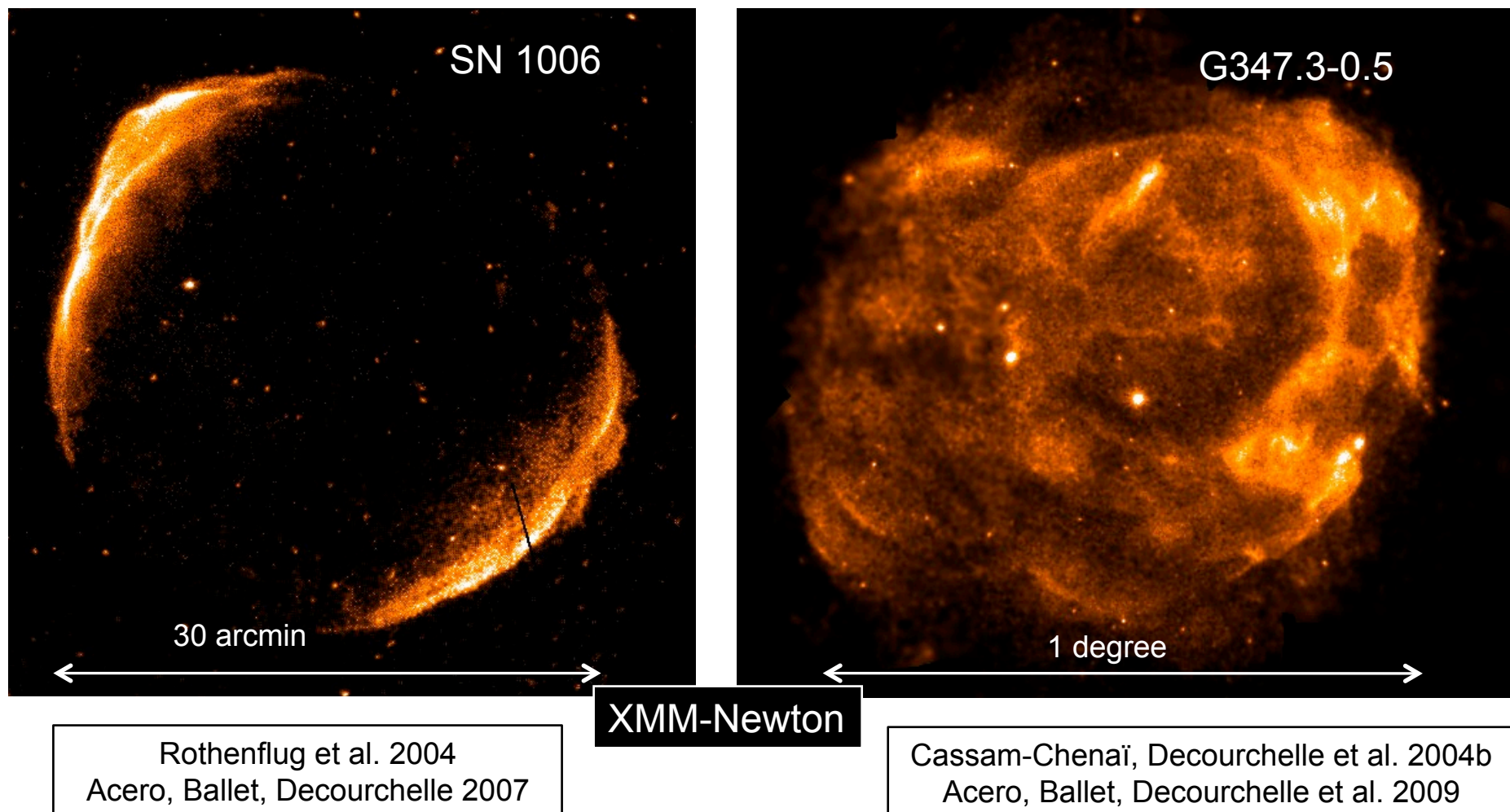
- Physics of the synchrotron emission of the electrons accelerated at the highest energy
- Physics of the thermal gas
 - Global parameters of the remnant
 - Back-reaction of accelerated protons
- Capability of performing spatially-resolved spectroscopy at small scale
(< 10 arcsec while VHE gamma-ray instruments ~0.1 deg at best)

III.3 Observations: characterization of the properties of particle acceleration

cea
Saclay

Method: characterization of the synchrotron and thermal emission

Tool: spatially resolved X-ray spectroscopy using radio and XMM-Newton data



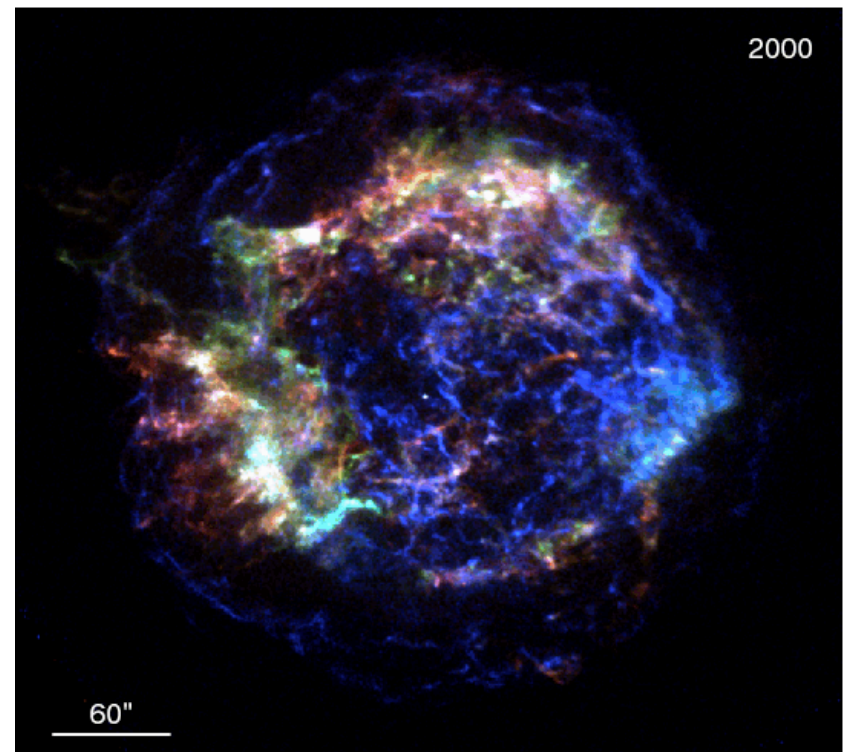
The magnetic field is a crucial parameter :

- for understanding particle acceleration
- for deriving the maximum energy of accelerated particles
- for interpreting the origin of TeV γ -rays : leptonic versus hadronic

Morphology and variability of the synchrotron emission

- Sharp filaments observed at the forward shock : width determined by synchrotron losses of ultrarelativistic electrons
 (Park et al. 09, Parizot et al. 06, Bamba 05, 04, 03, Vink & Laming 03,...)
- Fast variability of the brightness of these filaments
 (Patnaude et al. 09, Uchiyama et al. 08, 07)
- Broad band modeling of the nonthermal emission
 (Berezhko et al. 09, Voelk et al. 08,...)

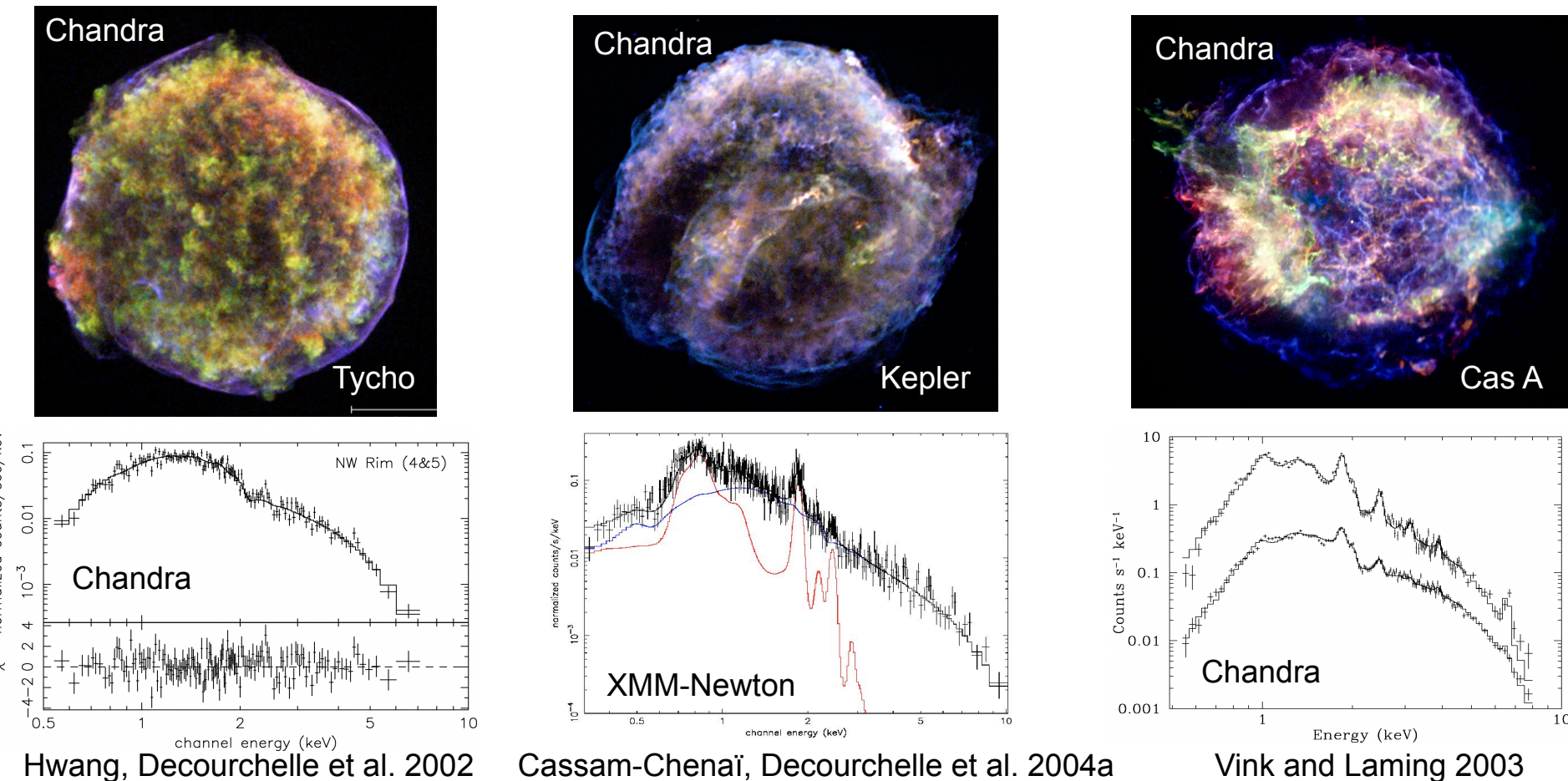
=> high value of $B_{\text{downstream}}$ ($\sim 50\text{-}500 \mu\text{G}$) which implies large magnetic field amplification



Patnaude et al. 09

III.3.1 Amplification du champ magnétique au choc : filaments fins

Sharp filaments at the forward shock all along the periphery of young ejecta-dominated SNRs, in bilateral limbs in SN 1006 and irregularly along the periphery of G347.3-0.5
=> synchrotron emission



=> width of the filament determined by synchrotron losses of ultrarelativistic electrons

III.3.2 Energie maximale atteinte dans les restes de supernova

What is the maximum energy of accelerated particles ?

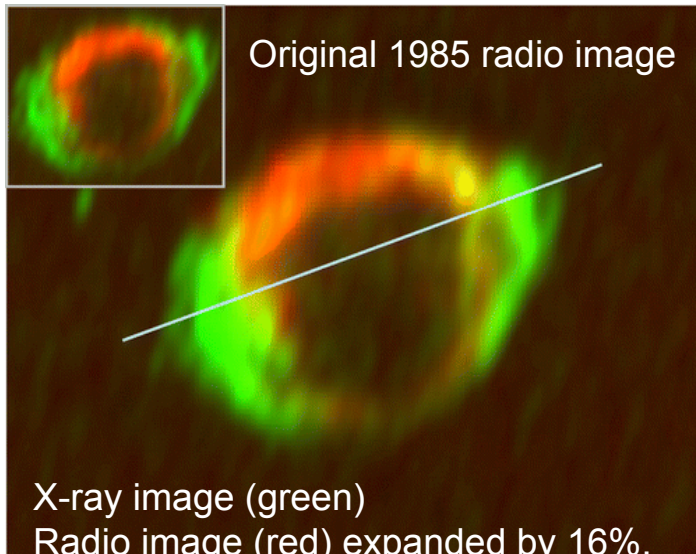
Electrons are a few % of cosmic rays but can reveal a lot on the mechanism of diffusive shock acceleration

⇒ accelerated like protons, except for the radiative losses

Spectrum of the synchrotron emission (radio + X-rays)

- Measurement of the roll-off photon energy $h\nu_{\text{roll}}$, observable in X-rays
 - Estimate of downstream magnetic field
- ⇒ Estimate of the maximum energy of accelerated electrons :

$$E_{\text{max}} = 39 (h\nu_{\text{roll}} / B_{10})^{1/2} \text{ TeV} \sim \text{few 10 TeV}$$



G1.9+0.3: the youngest observed galactic SNR
(Reynolds et al. 08, 09, Green et al. 08)

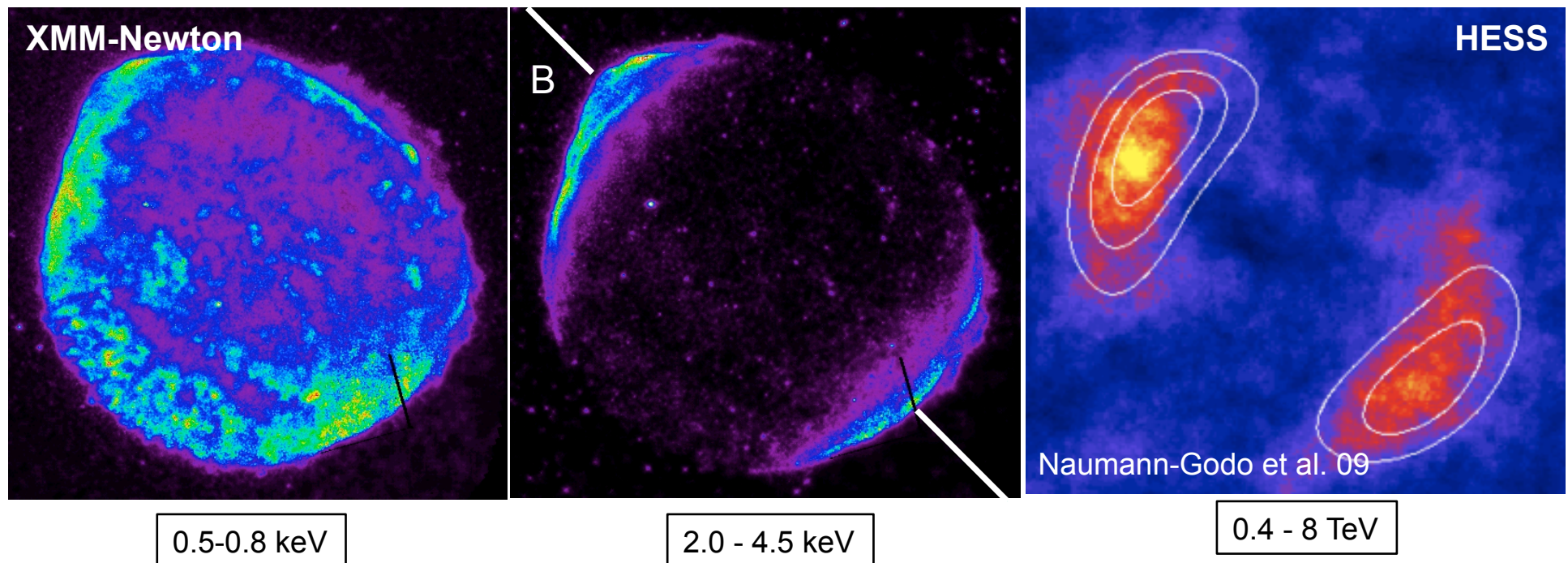
Expansion by 16 % between 1985 and 2007
=> **V_s ~ 14000 km/s for D ~ 8.5 kpc, age ~100 yr**

$h\nu_{\text{roll}} \sim 2.2 \text{ keV}$, among the highest reported

$E_{\text{max}} \sim 70 \text{ TeV assuming } B \sim 10 \mu\text{G}$

SN 1006: characterization of the geometry of the acceleration

High latitude SNRs evolving in a uniform interstellar magnetic field, like SN 1006, offer the possibility to investigate the dependence of the process of particle acceleration with B orientation



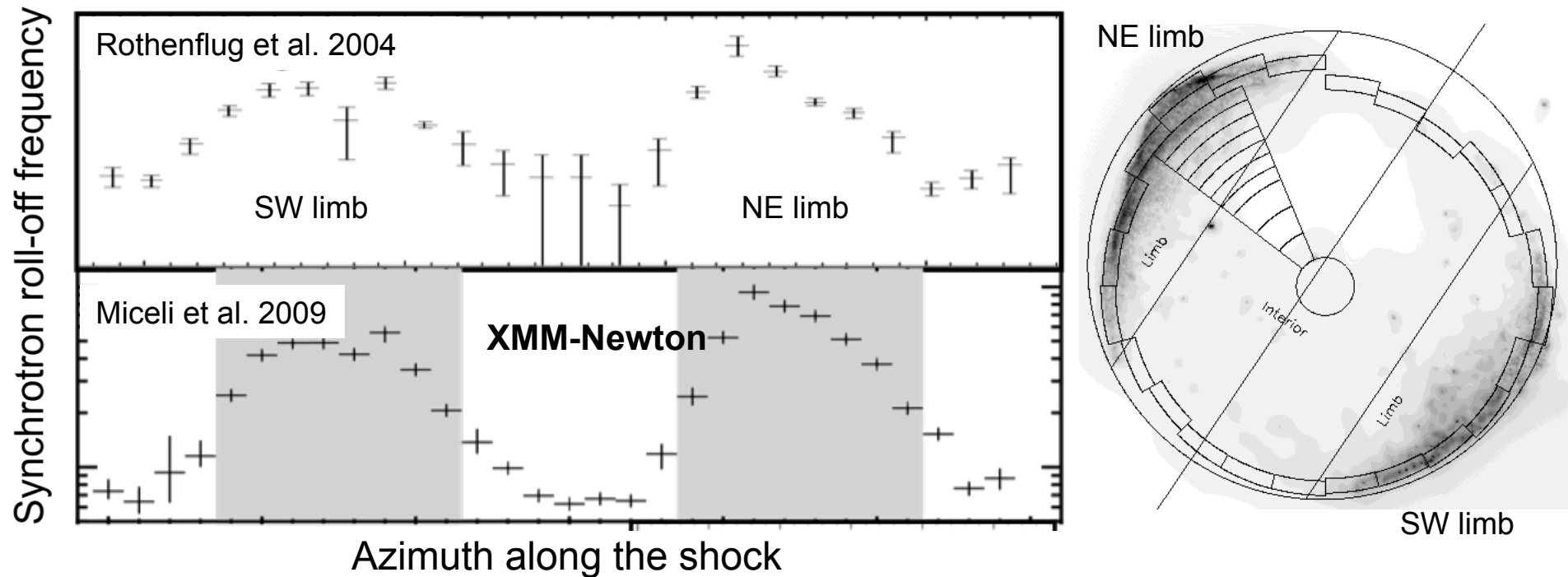
Synchrotron X-ray morphology indicates limbs are polar caps rather than an equatorial belt
(Rothenflug et al. 2004)

=> particles are accelerated where the magnetic field is parallel to the shock velocity

How does E_{\max} vary with ambient magnetic field orientation ?

Spatially resolved spectroscopy of the synchrotron emission (+ radio flux)

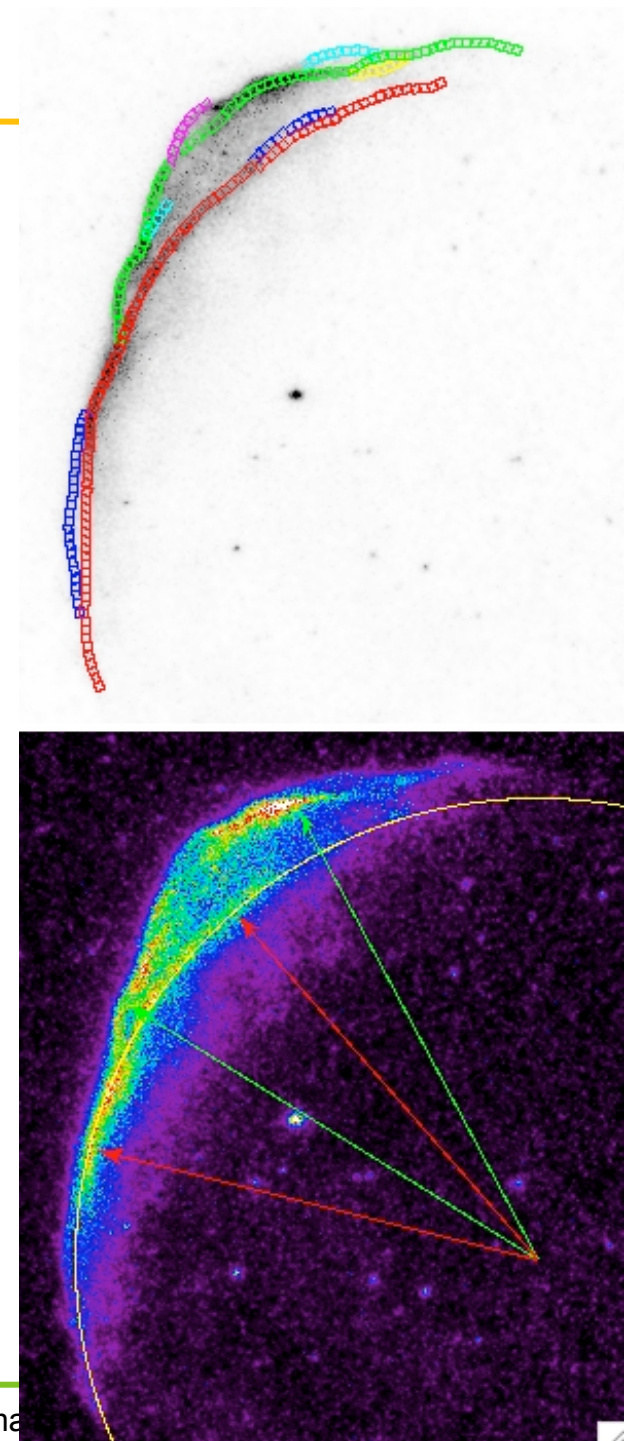
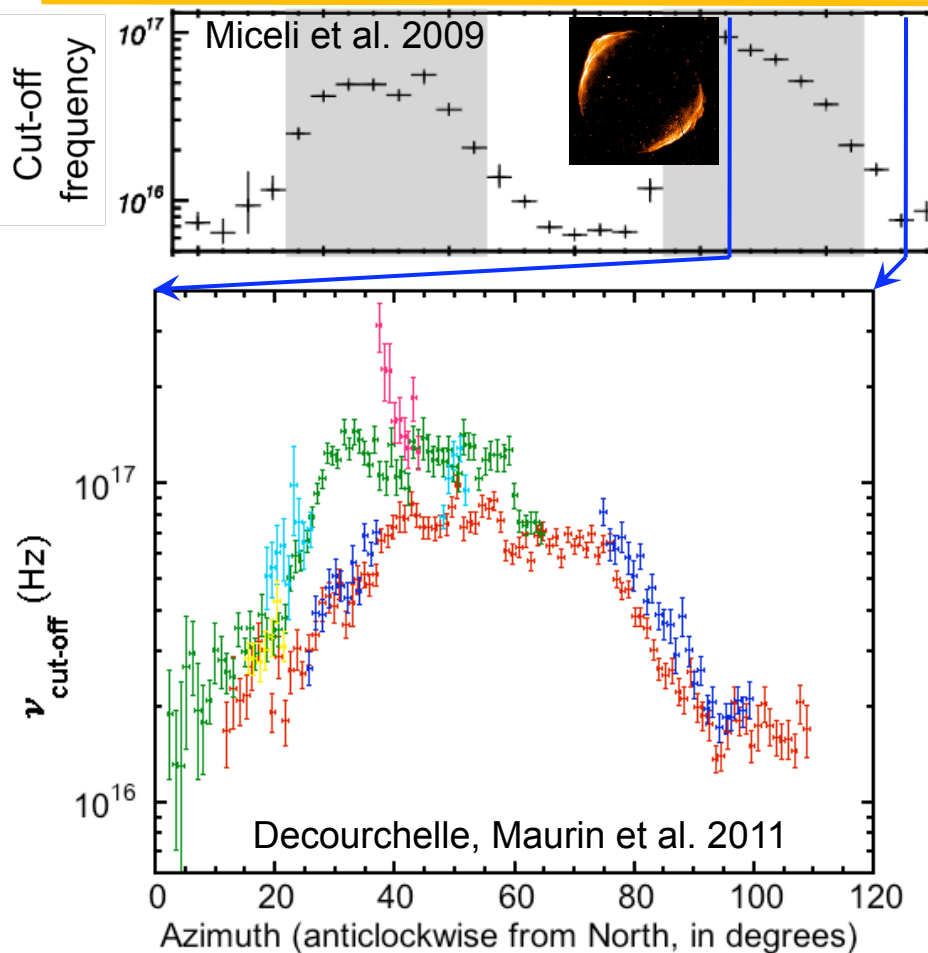
=> Measurement of the averaged azimuthal variation of the synchrotron roll-off frequency along the shock



SN 1006: very strong variations of the synchrotron roll-off frequency

=> Maximum energy of accelerated particles must be higher at the bright limbs than elsewhere

Cut-off frequency along each filament



Along the two extended filaments, cut-off frequency shows:

- a rapid increase, followed by a plateau and a rapid decrease
- increase amplitude depends on filaments (from 4 to 10)
- the most outward filaments have larger cut-off frequency

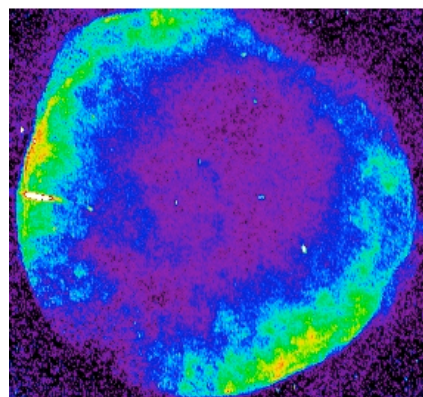
($V_s \sim 5000$ km/s, Katsuda et al. 09)

Synchrotron spectral index

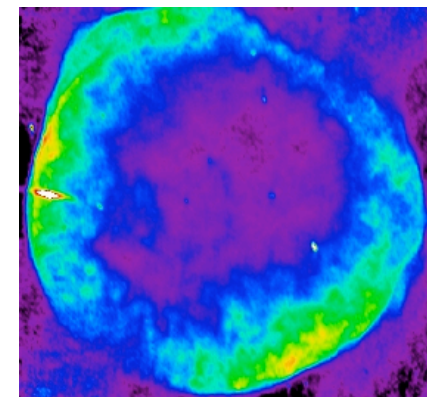
Along all filaments, same behaviour of the spectral index

- slight increase towards the pole and decrease outwards
- but exact dependence and values depend on radio maps

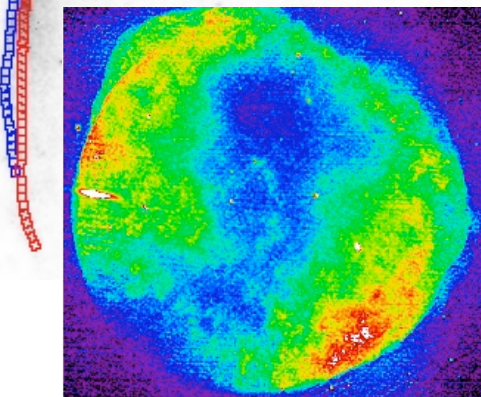
Dyer et al. 2009



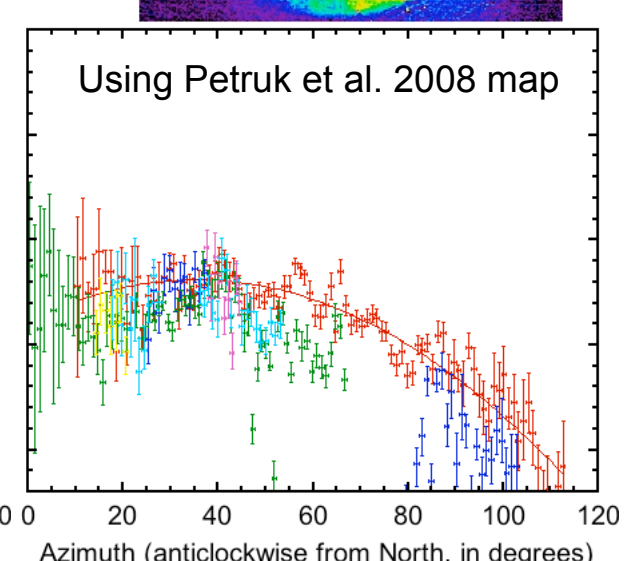
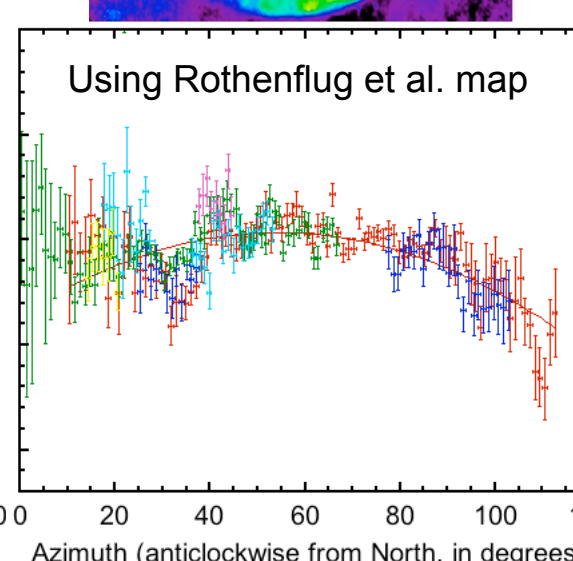
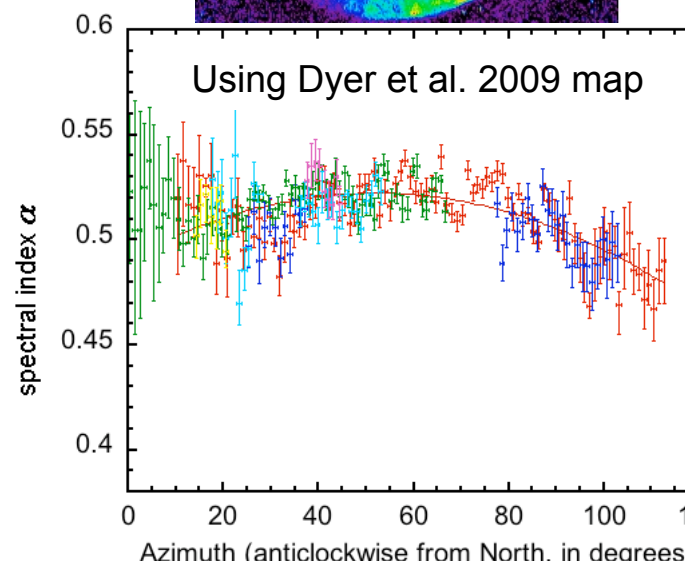
Rothenflug et al. 2004



Petruk et al. 2008



Radio
maps



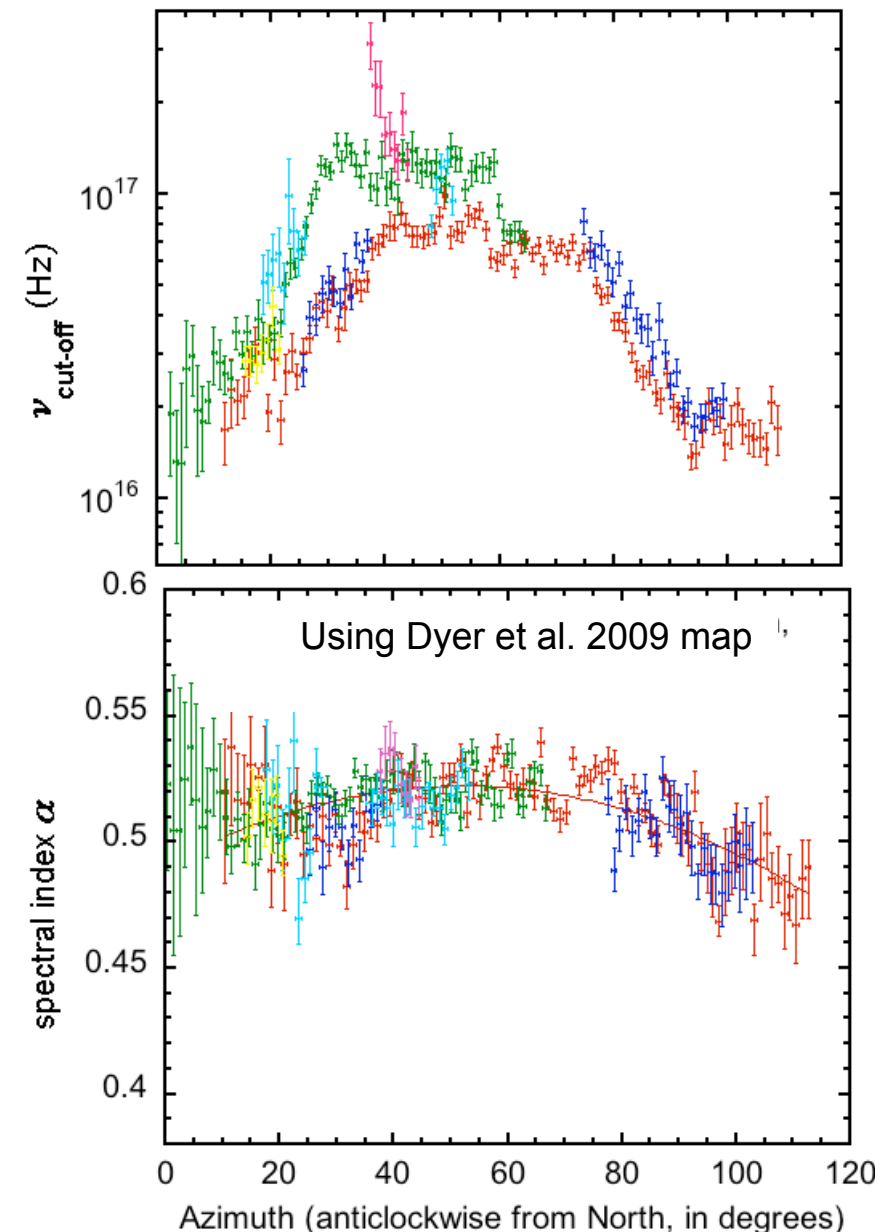
At the north-east pole:

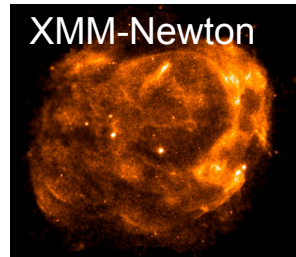
- Highest cut-off frequency
=> highest energy reached by particles
- Highest values for the outermost filaments
=> higher energy for higher shock velocity
- Plateau regime: saturation of the cut-off frequency near the pole: loss-limited ?
- Largest spectral index: highest back-reaction on the particle spectrum?
=>highest acceleration efficiency/injection

(Decourchelle, Maurin et al., 2010, in prep)

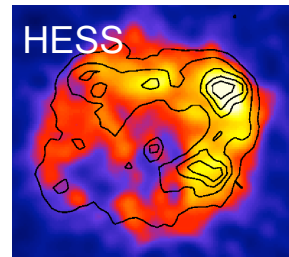
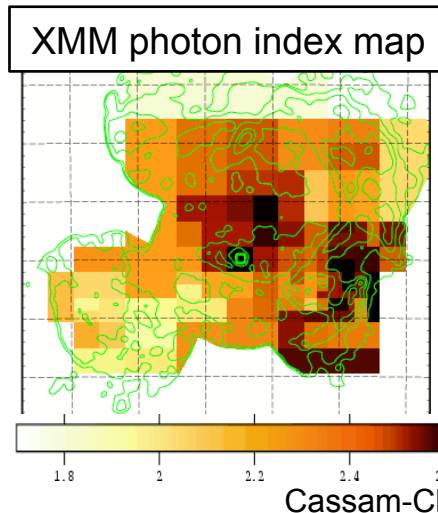
Azimuthal dependence provides very strong constraints to the acceleration mechanism

=> detailed modeling required

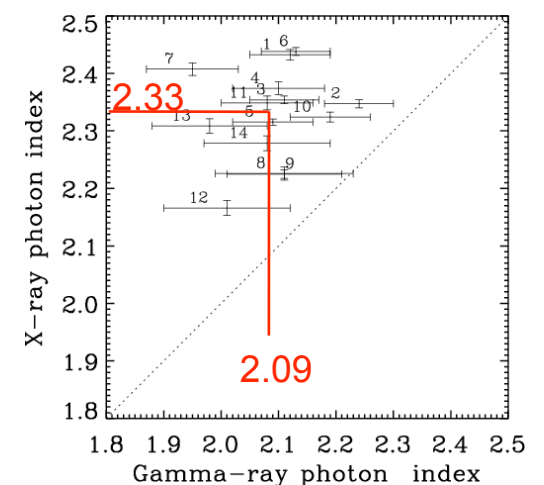
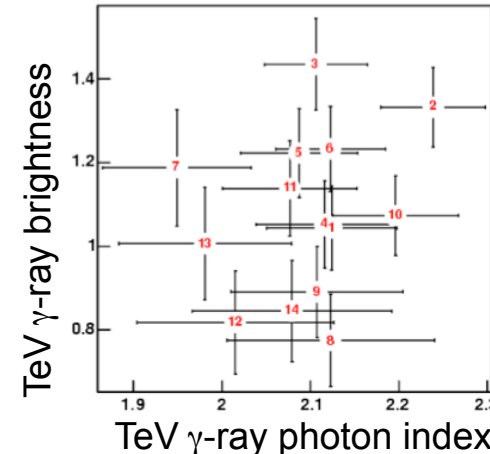
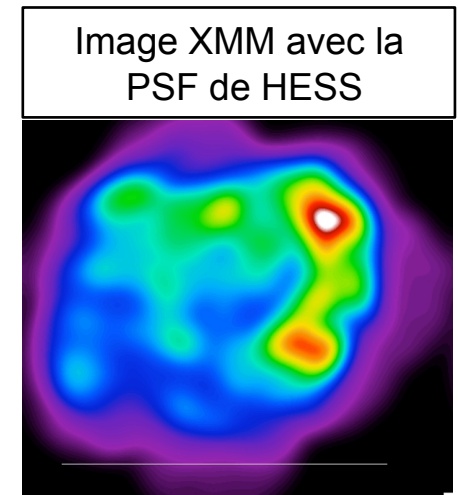
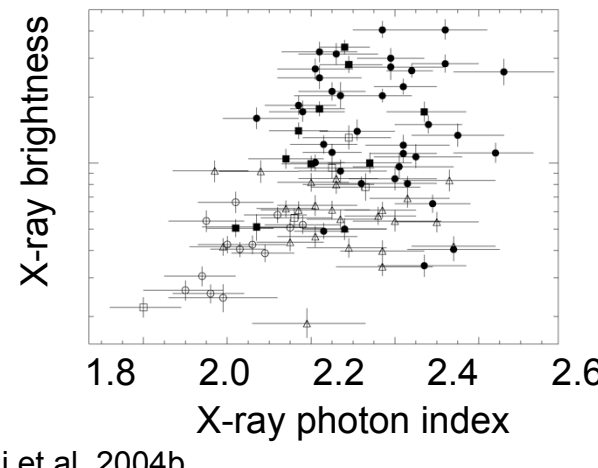
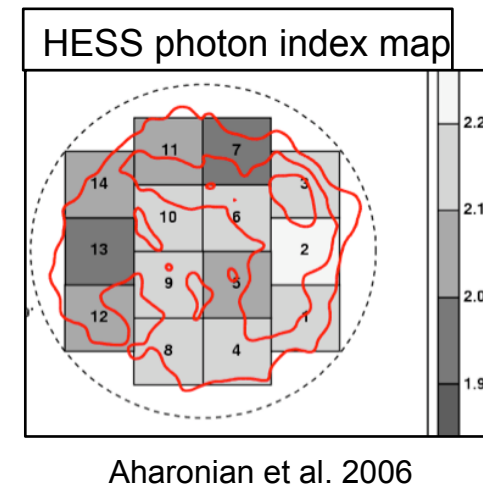




Acero et al. 2009



Aharonian et al. 2004



- Large variation of X-ray photon index [1.8-2.6], the steepest in the densest regions => [2.2-2.4]
- Average TeV γ -ray photon index [1.9-2.3], no flux correlation

High and very high energy gamma ray observation

HESS has observed several young supernova remnants with hard spectra below 1 TeV.

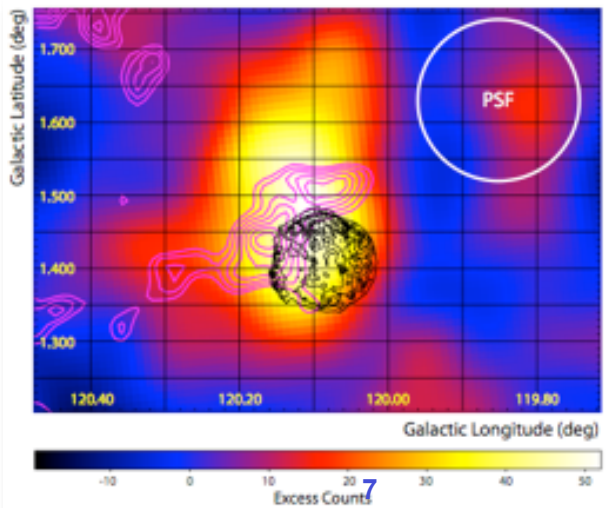
Fermi has observed several middle-aged supernova remnants with broken spectra, steep at 100 GeV

High and very high energy gamma ray observation

Tycho: Recent TeV Detection



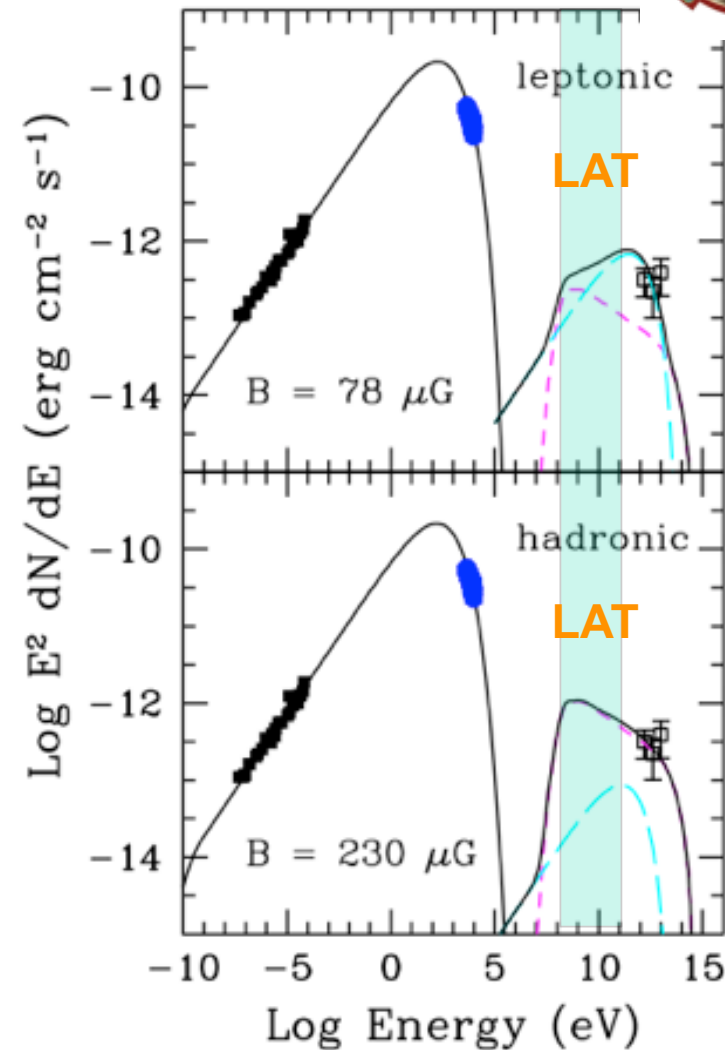
VERITAS Collaboration (2011)



Flux(>1 TeV) $\sim 1\%$ Crab
 5.0σ detection (post-trial)

B-field constraint put by X-ray
 does *not* contradict IC origin.

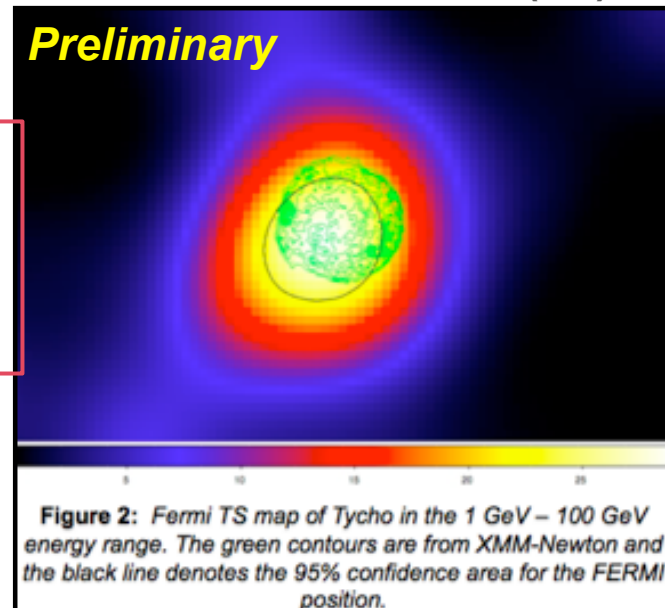
Fermi-LAT can test
 “leptonic vs hadronic”





Fermi-LAT Detection (5σ)

Preliminary

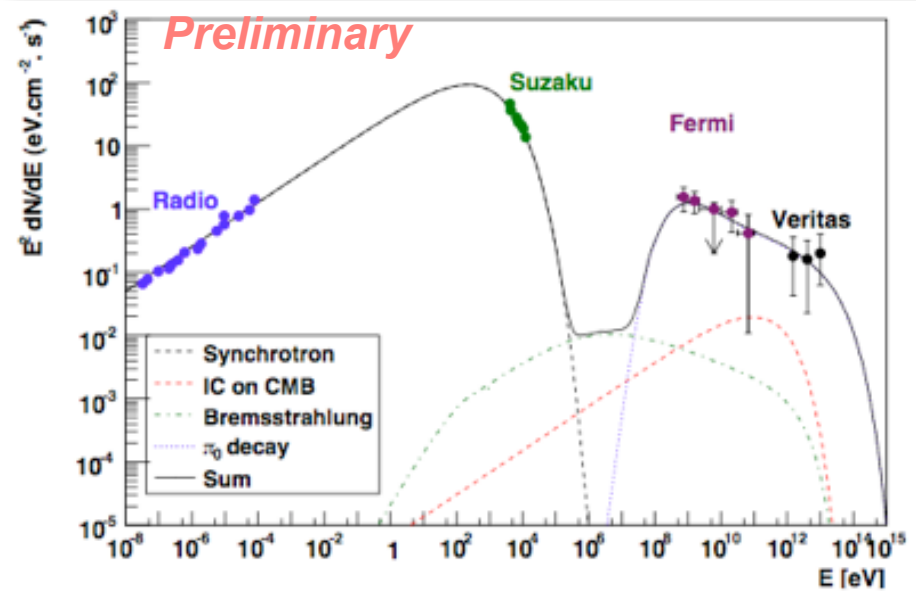


Uchiyama
Fermi
meeting
mai 2011

Tycho: New GeV Detection



See a poster by Fermi-LAT Collaboration
(Naumann-Godo+)



Case	D_{kpc}	n_H [cm $^{-3}$]	E_{SN} [10 51 erg]	$E_{p,tot}$ [10 51 erg]	K_{ep}
Far	3.50	0.24	2.0	0.150	4.5x10 $^{-4}$
Nearby	2.78	0.30	1.0	0.061	7.0x10 $^{-4}$

Photon index = 2.3 ± 0.1
(favors hadronic origin)

6-8% of E_{SN}
transferred to CRs.

High and very high energy gamma ray observation

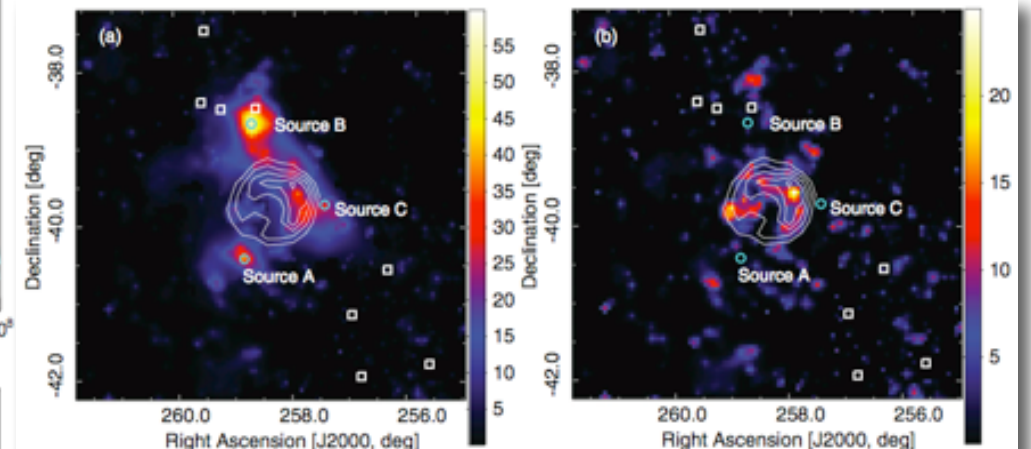


RX J1713.7-3946: LAT Results



Abdo+2011 (in press)

TS map above 0.5 GeV
(using a point source hypothesis)



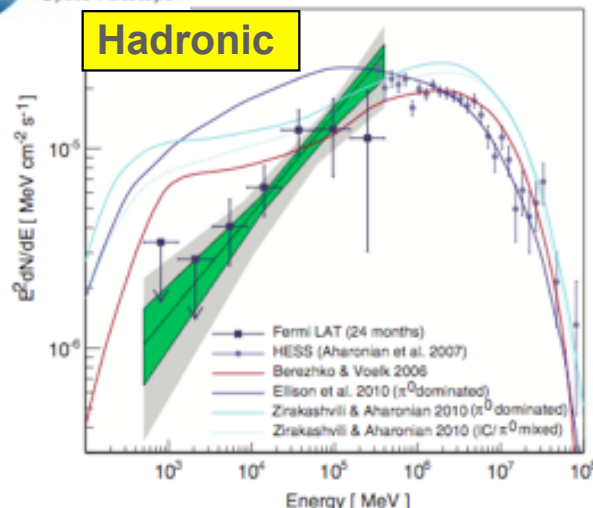
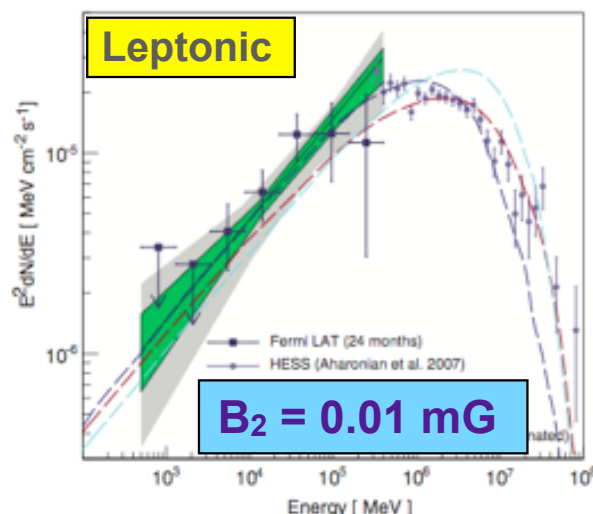
1FGL sources in BGD model

SrcA,B,C also in BGD model

Photon index: $\Gamma_{\text{LAT}} = 1.5 \pm 0.1(\text{sta}) \pm 0.1(\text{sys})$

LAT spectral shape is consistent what expected in leptonic scenarios (IC origin), though $B_2 = 0.01$ mG would be difficult to be reconciled with X-ray measurements. Hadronic origin requires very hard proton spectrum, which challenges current models.

Uchiyama
Fermi
meeting
mai 2011



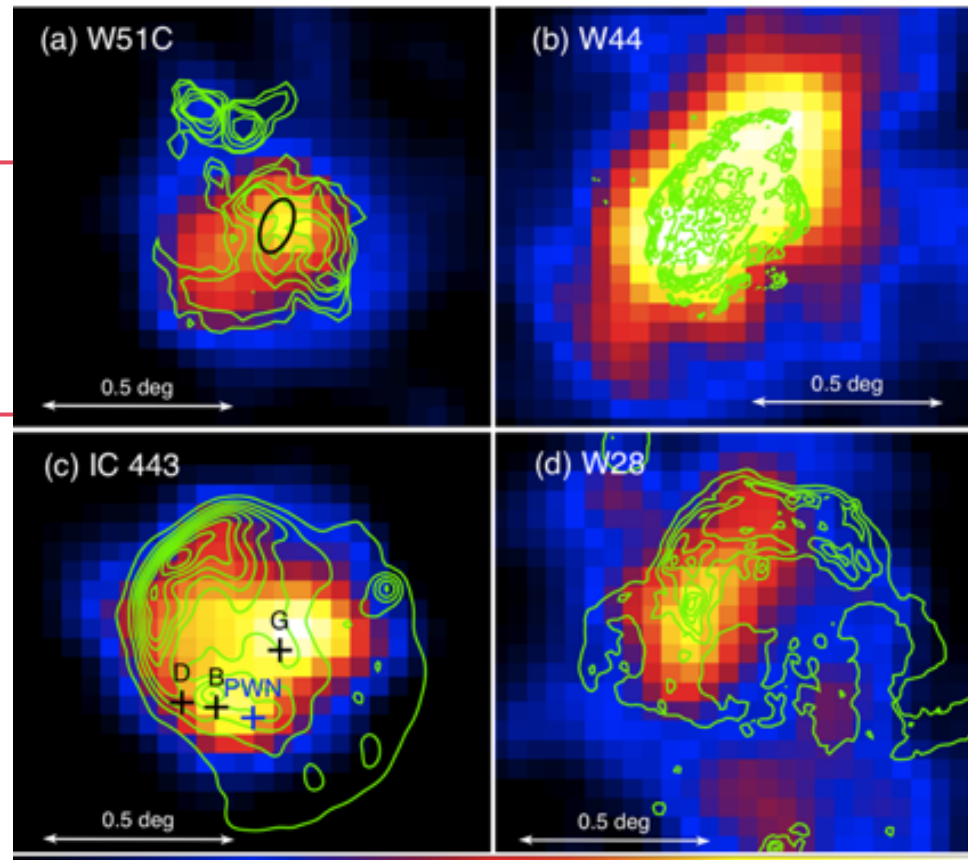


High and very high energy gamma ray observation

LAT Discoveries of MC-SNRs



Fermi-LAT Collaboration (Uchiyama+) 2011



Extended GeV emission has been discovered from several SNRs, with **molecular cloud (MC)** interactions.

GeV extension is consistent with the size of a radio remnant (except for W28).

The dominant class of LAT SNRs.

Uchiyama
Fermi
meeting
mai 2011



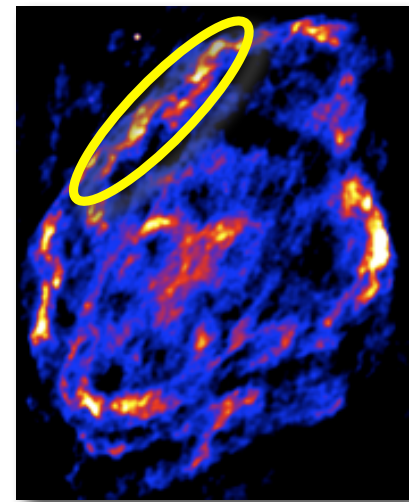
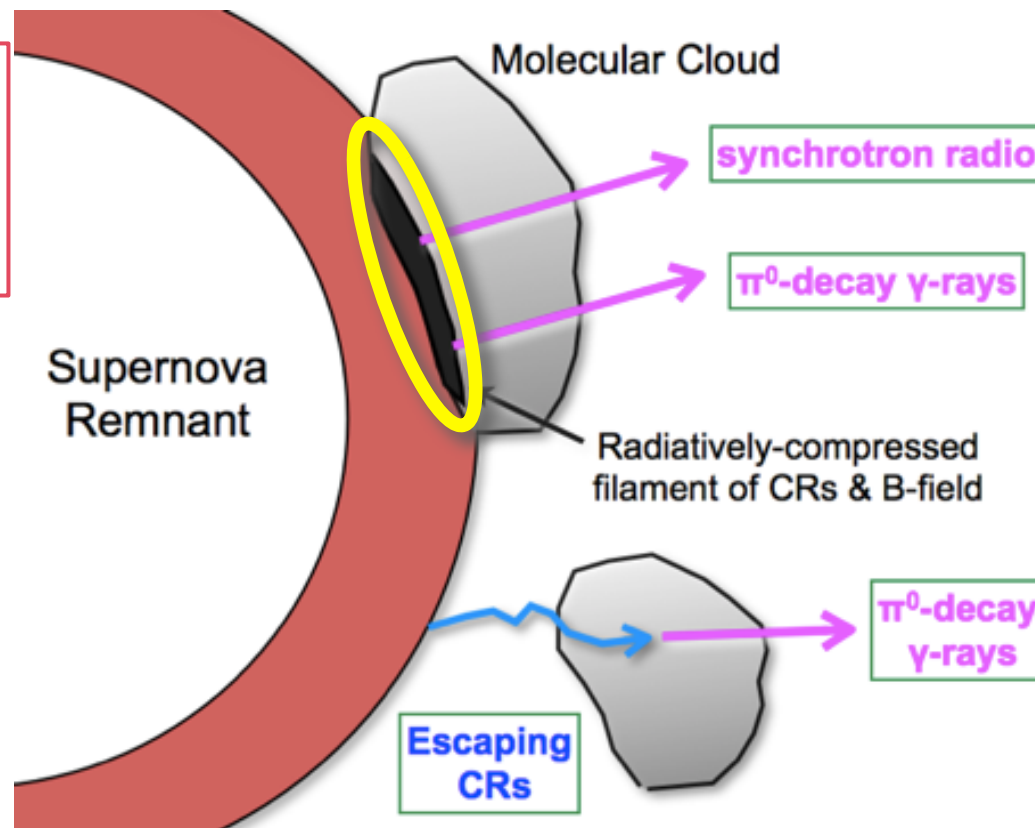
High and very high energy gamma ray observation

Gamma-ray Emission Sites



Radio & γ -ray emissions from radiatively-compressed filaments
 Crushed Cloud Model (Uchiyama+2010)

Uchiyama
 Fermi
 meeting
 mai 2011



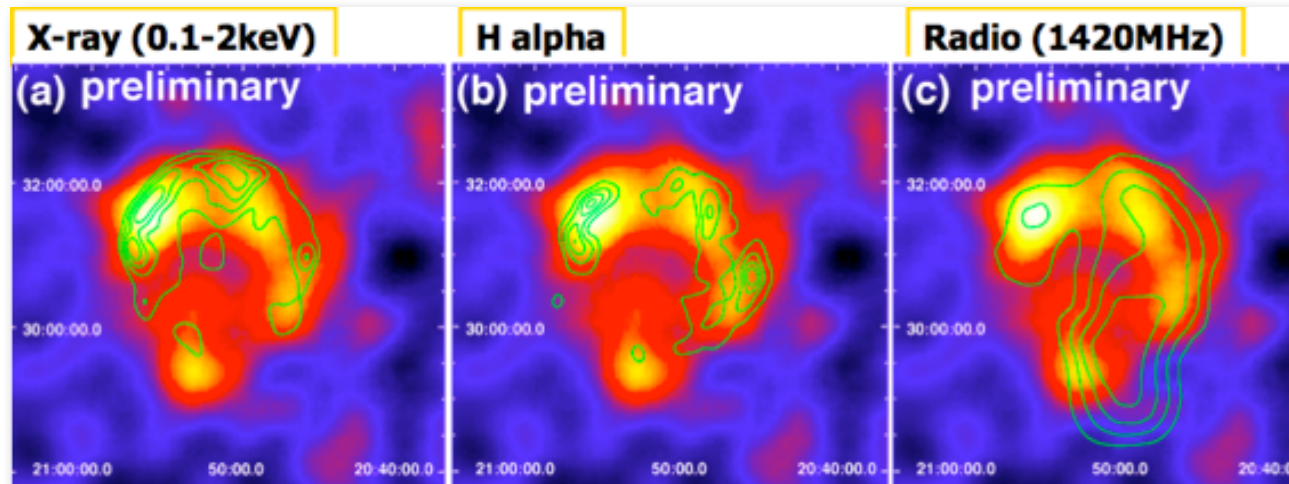
SNR W44
 synchrotron radio emission
 correlated with shocked H₂ gas

High and very high energy gamma ray observation

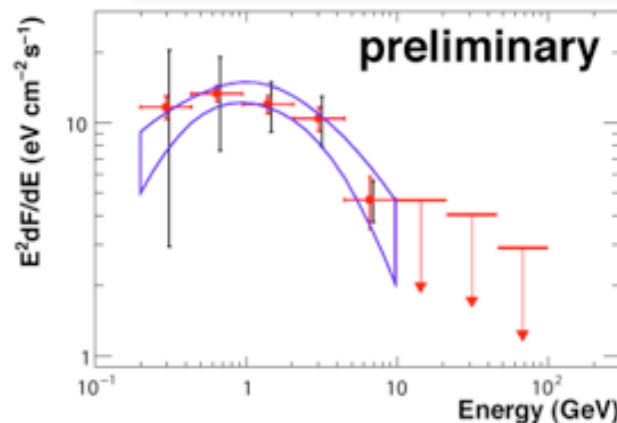
Cygnus Loop: LAT Results



Katagiri+ (submitted)



Uchiyama
Fermi
meeting
mai 2011



Correlation with X-ray and H α emissions
 → Gamma-ray-emitting particles distribute near shock waves

NOTE: southern radio emission would be another SNR.

Spectral steepening above ~ 2 GeV.
 (simple power-law disfavored at 3.5σ level)
 Gamma-ray Luminosity $\sim 1 \times 10^{33}$ erg/s (< other LAT SNRs)

28

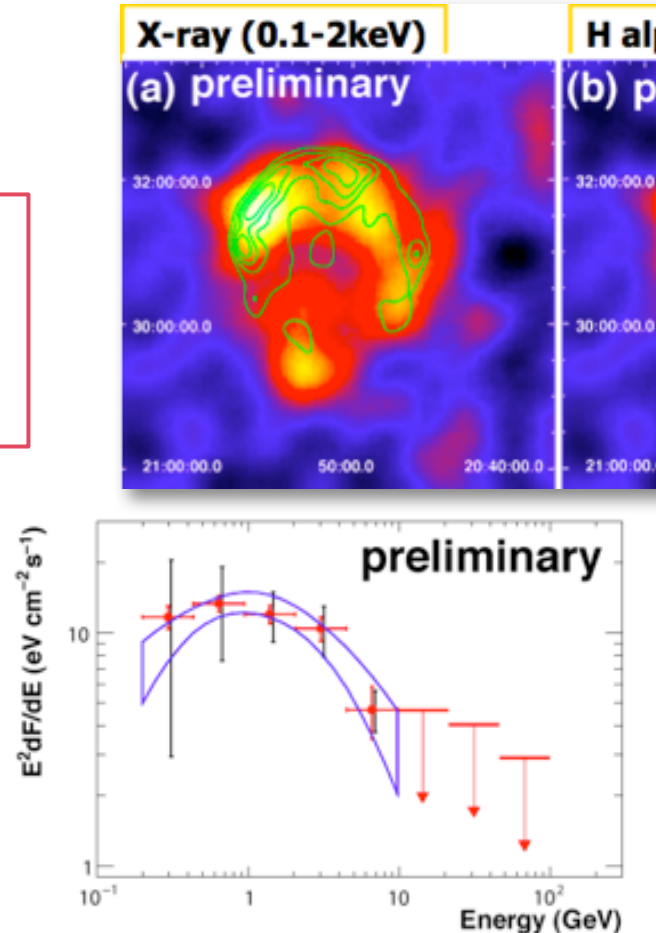
High and very high energy gamma ray observation

Cygnus Loop: LAT Results

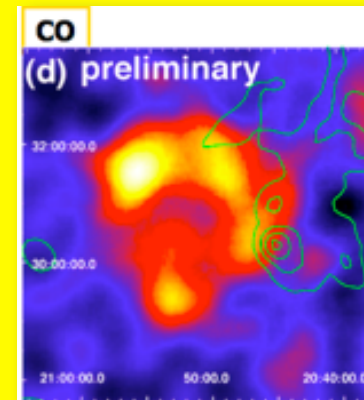


Katagiri+ (submitted)

Uchiyama
Fermi
meeting
mai 2011



Unlike other middle-aged remnants, gamma-ray emission is not due to interactions with molecular cloud.



Gamma-ray emission comes from either (1) main blast wave regions (X-ray) or (2) radiative shock region (H α).

=> traité en même temps que la modélisation

IV. Modélisation des restes de supernovae

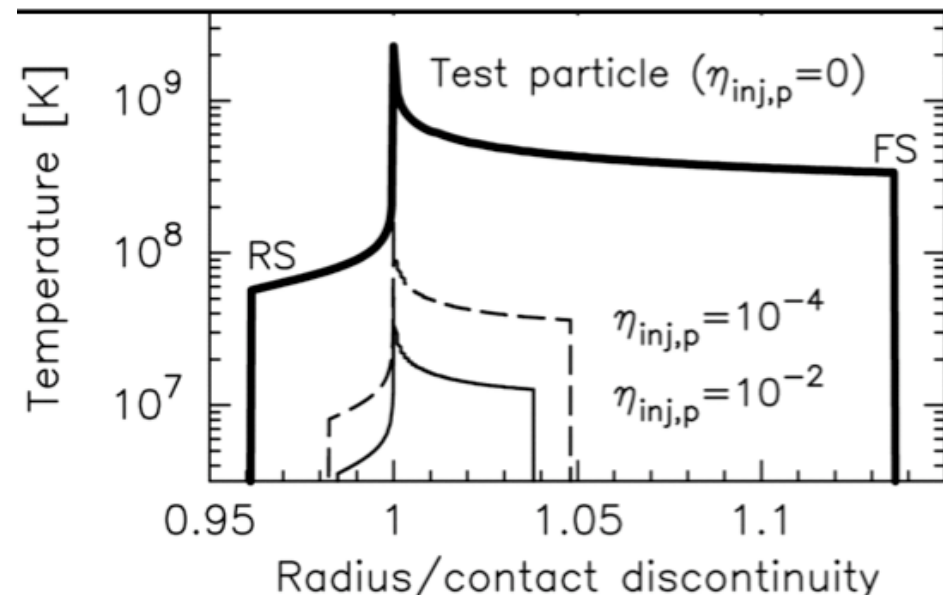
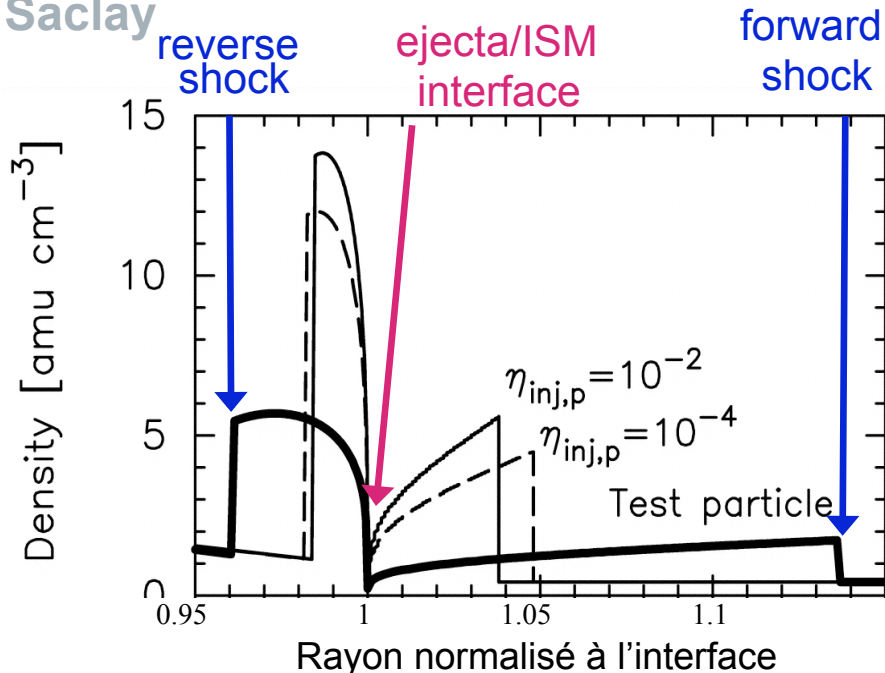
1. Modélisation 1D et contrainte observationnelle sur l'efficacité de l'accélération par rétroaction des particules accélérées
2. Modélisation 3D

IV.1 Modélisation hydrodynamique 1D avec accélération de particules : rétroaction

cea

Saclay

Context: 1D self-similar solutions including a prescribed back-reaction of accelerated particles (Chevalier 1983)



Our work: 1D semi-analytical modelling coupled to a model of particle acceleration
(Berezhko & Ellison 1999) => Decourchelle, Ballet, Ellison (2000)

If efficient ion diffusive shock acceleration:

- larger compression ratio (> 4 at the shock)
- lower post-shock temperature than for test-particle case => R. X
- Shrinking of the post-shock region => R. X

Thermal signature: a lower post-shock temperature

If efficient ion diffusive shock acceleration, lower post-shock temperature than for test-particle case
 (Chevalier 1983, Ellison et al. 2000, Decourchelle et al. 2000)

Mean test-particle post-shock temperature in 1E0102 (SMC):

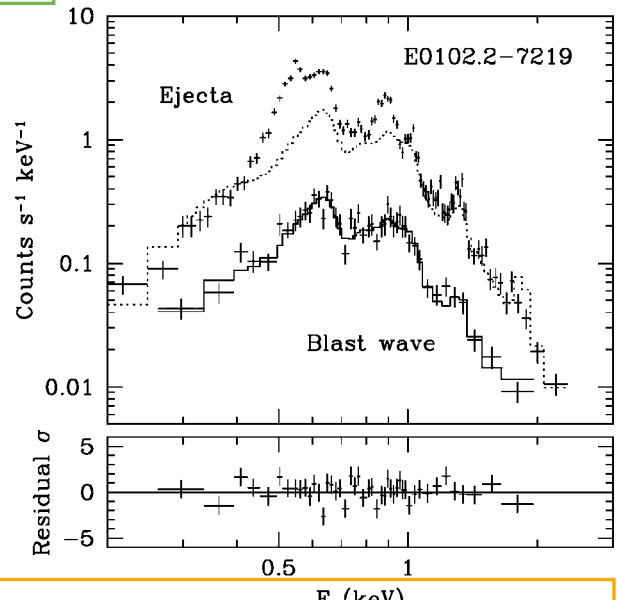
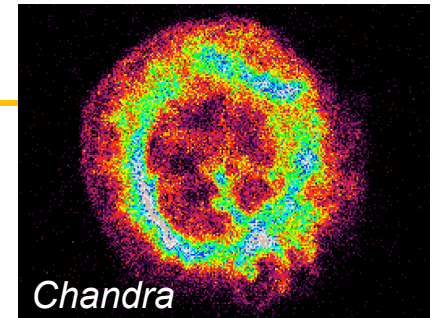
$$kT_s = 3/16 \mu m_p V_s^2 \text{ with shock velocity } V_s \sim 6200 \text{ km/s}$$

=> expected $kT_s \sim 45 \text{ keV}$

Chandra: $kT_e \leq 1 \text{ keV}$ measured

With coulomb collisions only, one expects: $kT_e > 2.5 \text{ keV}$

(Hughes, Rakowski, Decourchelle 2000)



Indication of strong back-reaction in young SNRs

- **1E0102**: post-shock kT_e from X-rays and V_s from X-ray proper motion (Hughes, Rakowski, Decourchelle 2000)
- **RCW 86**: post-shock proton temperature from H_α broad line and V_s from X-ray proper motion (Helder et al. 09): 50 % post-shock pressure in relativistic particles
- No back-reaction in the older SNR**
- **Cygnus Loop**: post-shock kT_e from X-rays and V_s from optical proper motion (Salvesen et al. 09)

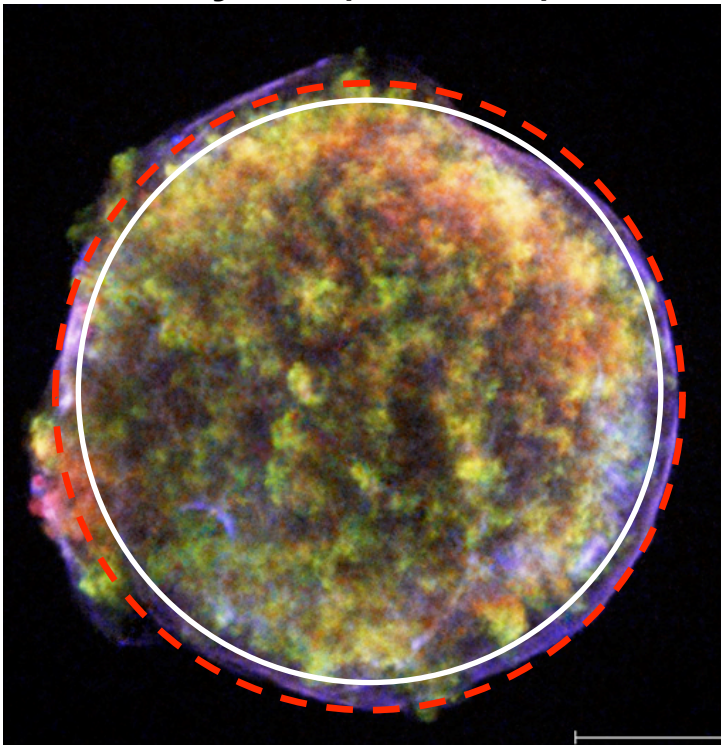
Thermal and non thermal signature: shrinking of the shocked region

If efficient ion diffusive shock acceleration: modified hydrodynamics

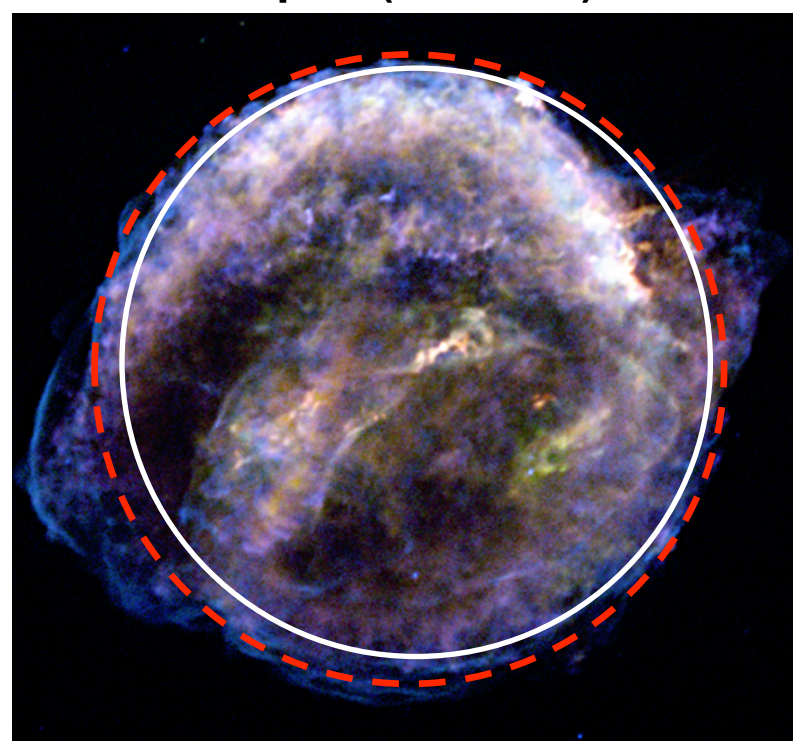
=> narrower shocked region than test-particle case

(Chevalier 83, Decourchelle et al. 00)

Tycho (SN 1572)



Kepler (SN 1604)



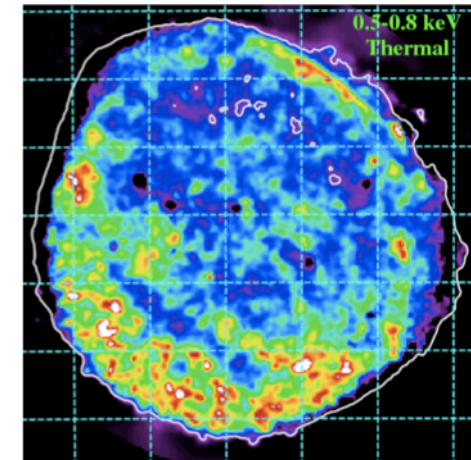
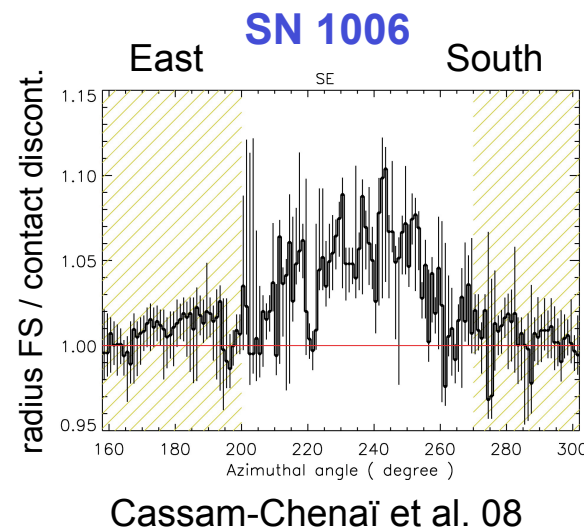
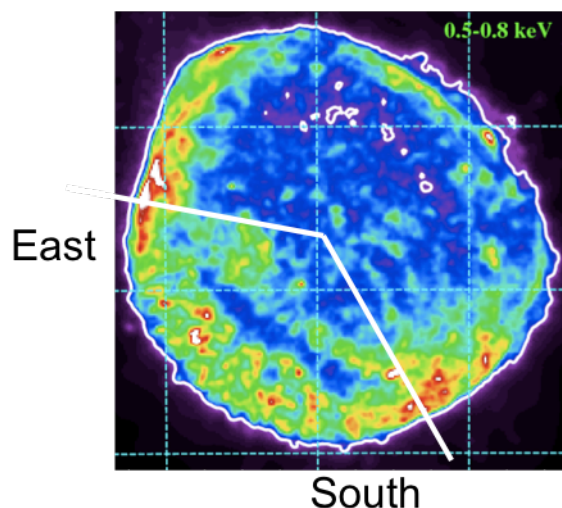
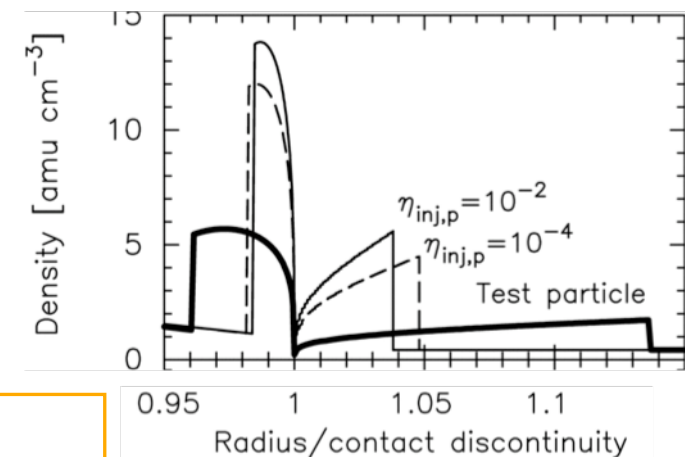
Observational diagnostic: shock very close to interface: $R_{\text{shock}}/R_{\text{interface}} < 1.1$
(Decourchelle 2005, Warren et al. 2005)

=> Efficient particle acceleration of protons at the shock

Thermal and non thermal signature: shrinking of the shocked region

**Indication of strong back reaction
in young SNRs: $R_{fs}/R_{cd} < 1.1$**

- **Tycho**: morphology (Warren et al. 05, Decourchelle et al. 05)
- **Cas A**: X-ray proper motion and morphology (Patnaude et al. 09)
- **SN 1006**: morphology (Miceli et al. 09, Cassam-Chenaï et al. 08)



Miceli et al. 09

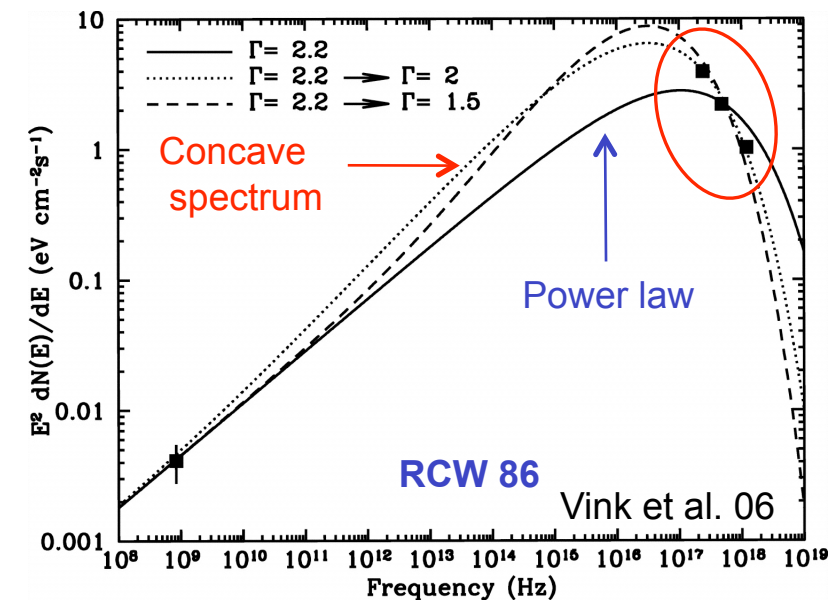
Efficiency of particle acceleration

Nonlinear diffusive shock acceleration

=> Curvature of the particle spectra (Berezhko & Ellison 99, Ellison & Reynolds 91,...)

Curvature of the spectrum : indications in a few SNRs

- **SN 1006**: combining radio and X-ray data
(Allen et al. 08)
- **RCW 86**: combining radio and X-ray data
(Vink et al. 06)
- **Cas A**: from infrared data
(Jones et al. 03)
- **Tycho and Kepler**: from radio data
(Reynolds & Ellison 92)



- Coupling of the thermal X-ray emission emission in the framework of the semi-analytical model: non-equilibrium ionization and X-ray spectra (Decourchelle, Ballet, Ellison 2000)
- Impact of a hybrid electron distribution (maxwellian plus power-law tail) on the ionization and recombination rates (Porquet, Arnaud, Decourchelle 2001)
- Coupling of the calculation of the nonthermal synchrotron emission in the framework of the semi-analytical model (Cassam-Chenaï, Decourchelle, Ballet, Ellison 2005)
- Application to the interpretation of Tycho's radio and X-ray synchrotron observations (Cassam-Chenaï, Hughes, Ballet, Decourchelle 2007)
- Development of numerical 1D simulations to extend the domain of applicability of the semi-analytical model (Ellison, Decourchelle, Ballet 2004)
- Ability of the reverse shock to accelerate particles (Ellison, Decourchelle, Ballet 2005)

- Coupling of the calculation of the nonthermal synchrotron emission in the framework of the numerical 1D code (Ellison & Cassam-Chenaï 2005)
- Coupling of the calculation of the thermal X-ray emission in the framework of the numerical 1D code (Patnaude, Ellison, Slane 2009, Patnaude, Slane, Raymond, Ellison 2010)

IV.2 Limitations of the 1D approach

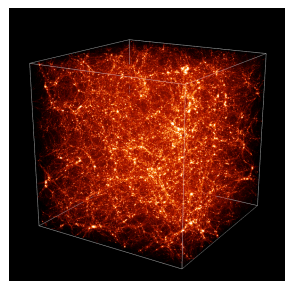
Development of hydrodynamic Rayleigh-Taylor instabilities at the interface between the ejecta and the ambient medium

=> **3D simulations required**

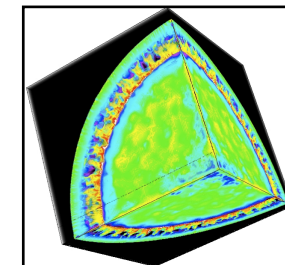
- + Explosion mechanism can be asymmetric
- + Ambient medium can be not uniform

3D simulations coupling a model of efficient particle acceleration required

=> ANR Young researcher obtained “Acceleration of protons in young supernova remnants”, 2007-2011

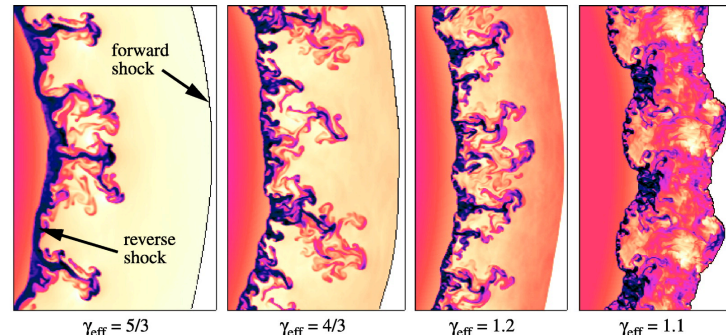


From cosmological simulations to building blocks of galaxies : supernova remnants
RAMSES code (R. Teyssier)

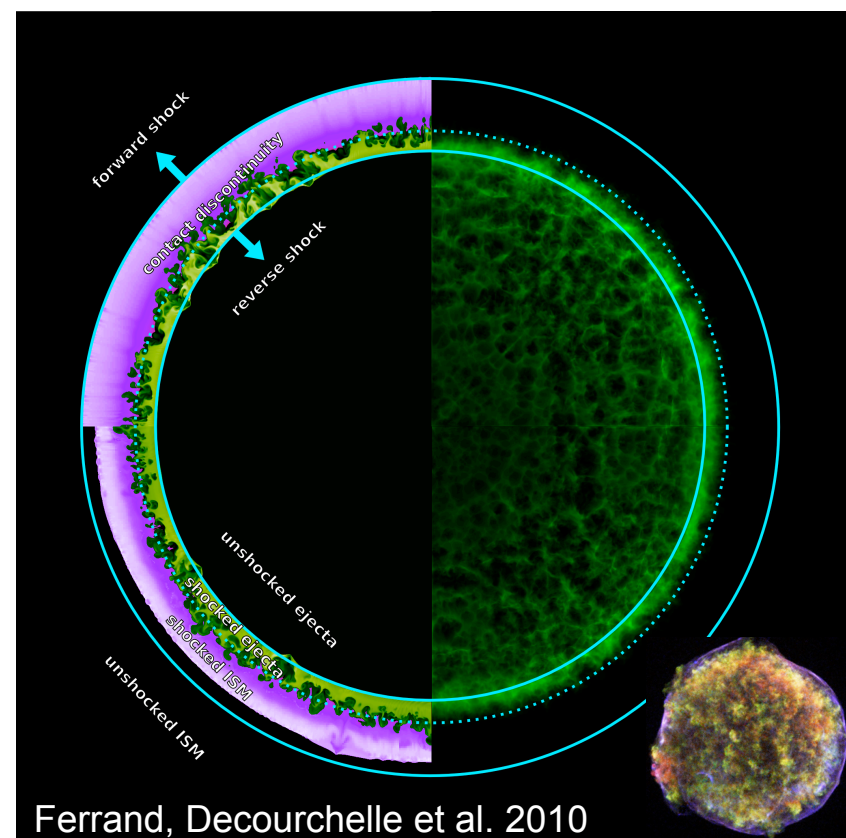
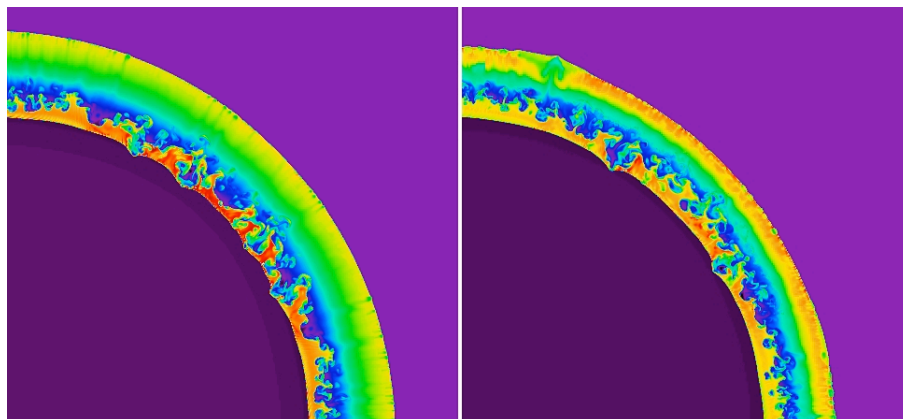


IV.2 3D numerical simulations coupling particle acceleration

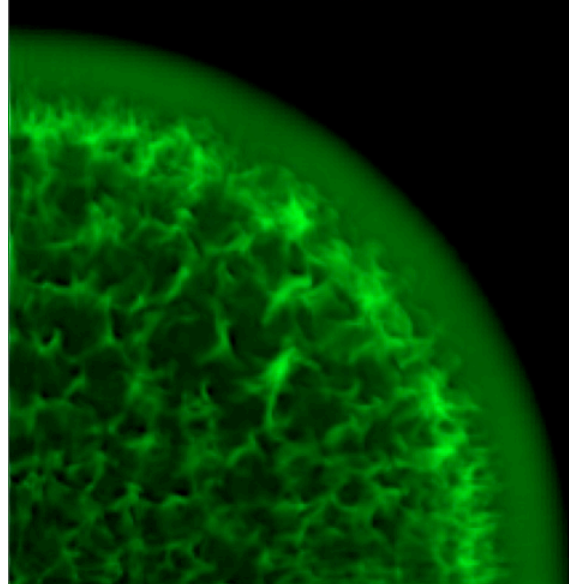
Previous work: 2D/3D simulation including arbitrarily the back-reaction of accelerated particles
 (Blondin and Ellison 2001, Wang 2010 submitted)



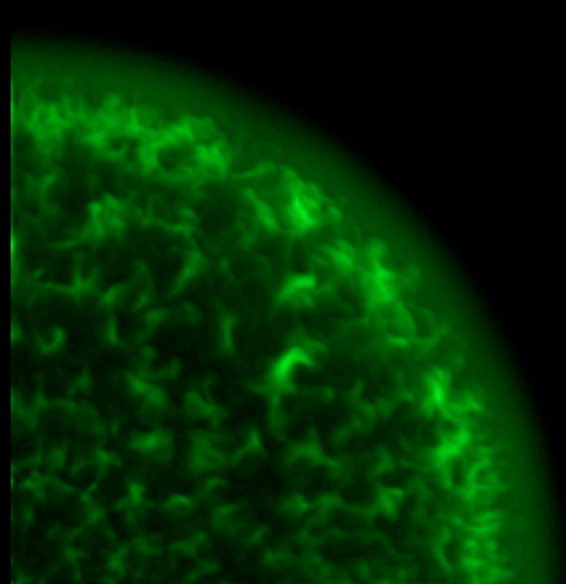
Our work (ANR): 3D simulations (1/8 of sphere) time-dependently coupled to a nonlinear acceleration model (Blasi 2002) with a simple coupling method at the shock front



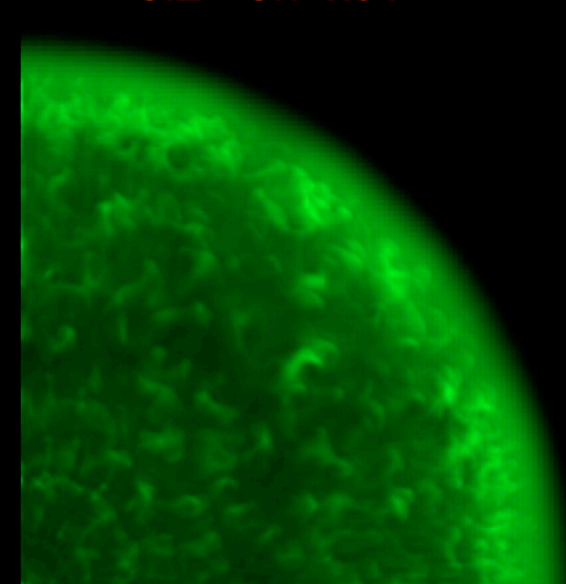
O band
500 - 800 eV



Si band
1.8 - 1.9 keV

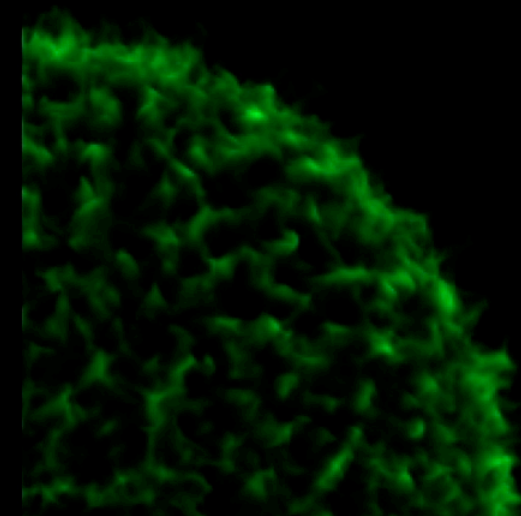
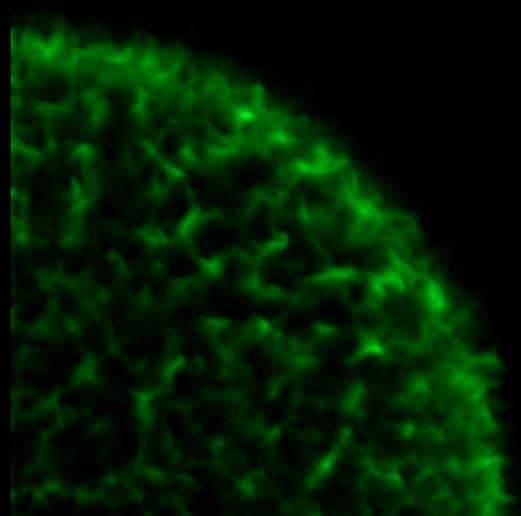
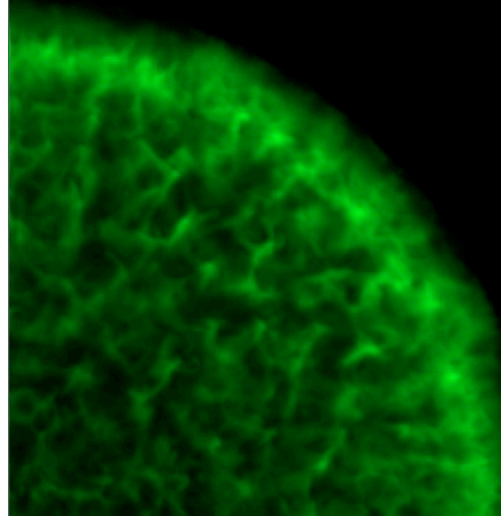


Fe K band
6.2 - 6.7 keV



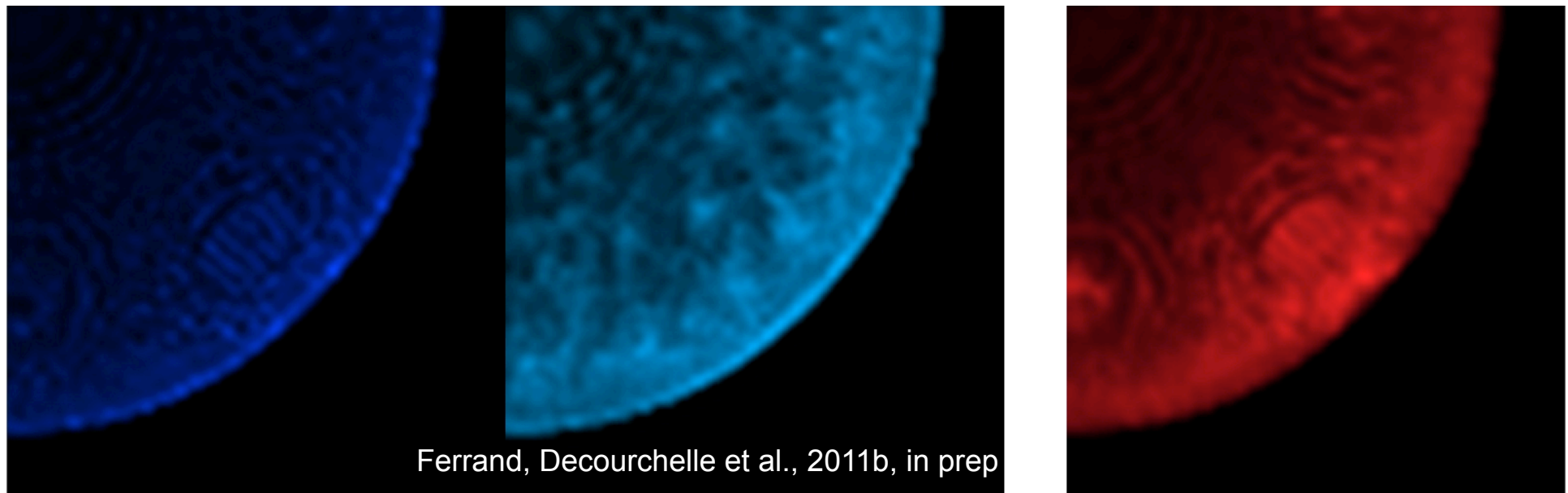
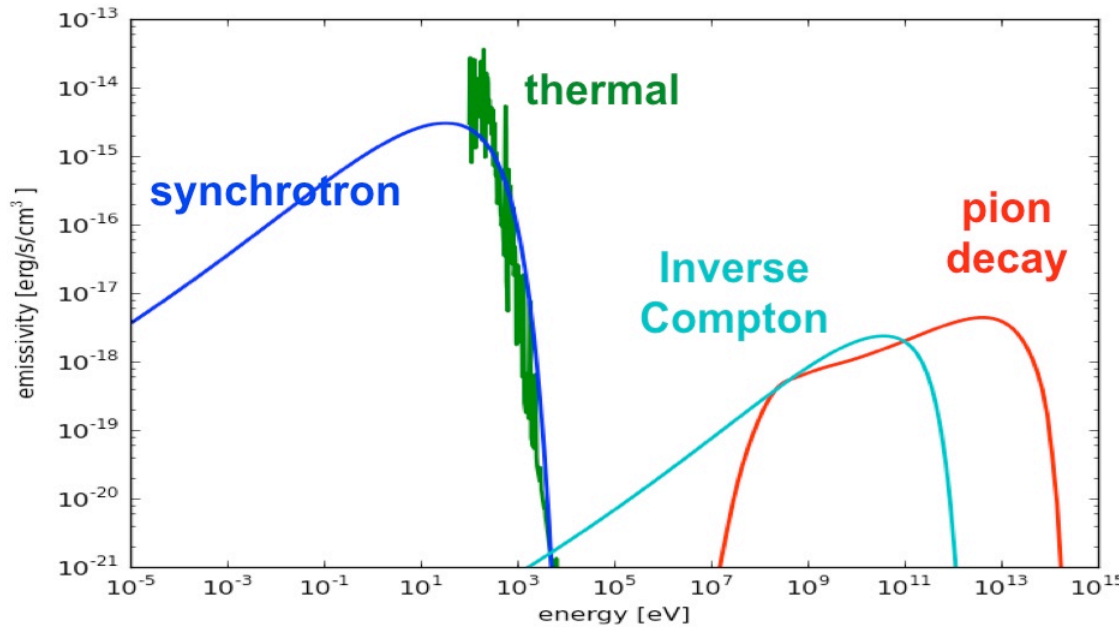
un-modified shock
(back-reaction off)

Ferrand, Decourchelle et al., 2011a, in prep

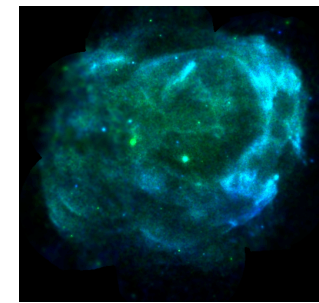
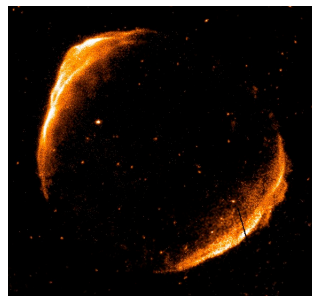
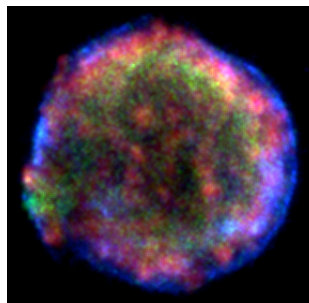


modified shock
(back-reaction on)

Projected 3D maps of non-thermal emission in young SNRs



5. Conclusions et perspectives



Observations haute énergie

=> Constraints on the models

Goal: to characterize the process at play (acceleration, heating, matter ejection and mixing)

Data: XMM-Newton, FERMI, HESS II, CTA

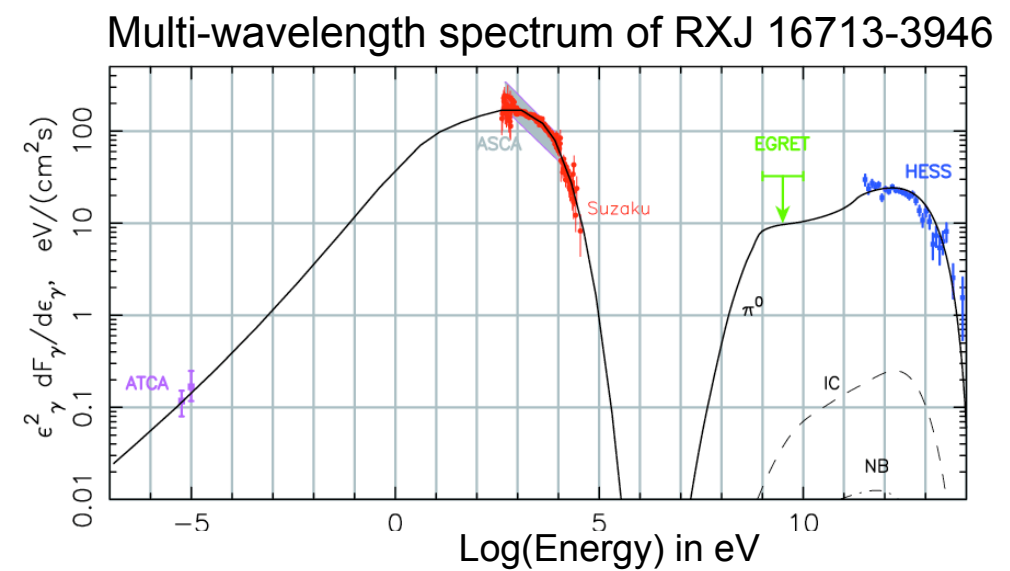
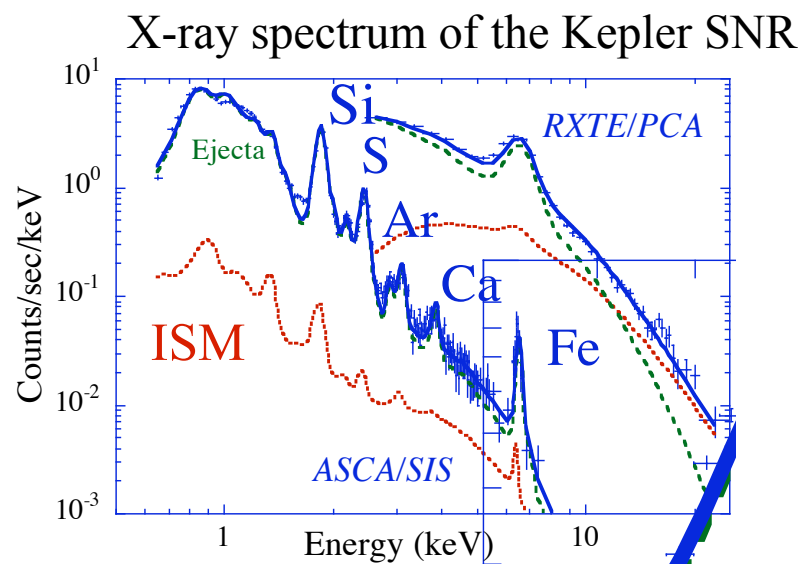
Tools:

- **Spatially resolved-spectroscopy of young supernova remnants at the smallest spatial scale achievable:** nucleosynthesis products, explosion mechanism, particle acceleration
- High-resolution spectroscopy at the shock to probe shock physics (LP SN1006)
- Combined radio and X-ray analysis to probe the accelerated electron spectrum
- Combined radio, X-ray and gamma-ray analysis to probe the accelerated electron and proton spectra

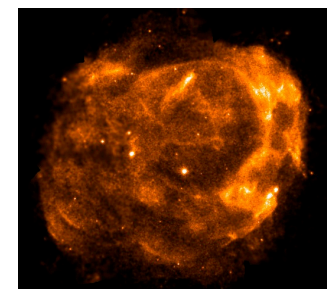
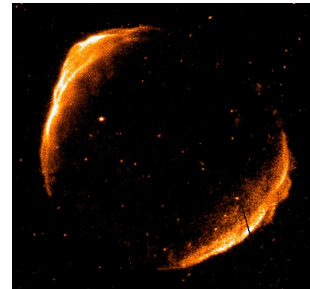
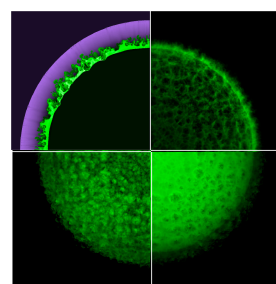
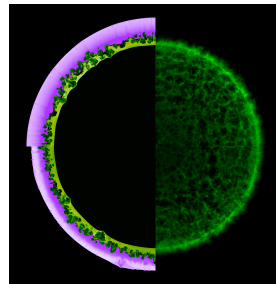
Perspectives: modelling of high-energy observations

Goal: constrain the prime parameters of the models through a consistent modelling of both the thermal and non-thermal emission of SNRs.

Tools: simple (1D) consistent models including heavy and radioactive elements, back-reaction of accelerated protons, magnetic field, accelerated particles, and emission processes.
Data: multi-wavelength spectra of supernova remnants
=> Understanding of the physics involved in various supernova remnants



Perspectives: 3D numerical simulations

**Goal:** modelling

- the geometry of the acceleration (like in SN 1006 or in ejecta-dominated remnants)
- the evolution of a remnant, including in a turbulent interstellar medium (like RXJ1713-3946)
- the impact of the evolution of supernova remnants on the large scale interstellar medium

Requirements: take into account the magnetic field orientation and pressure**Tools:** MHD simulations (code RAMSES et HERACLES)**Data:**

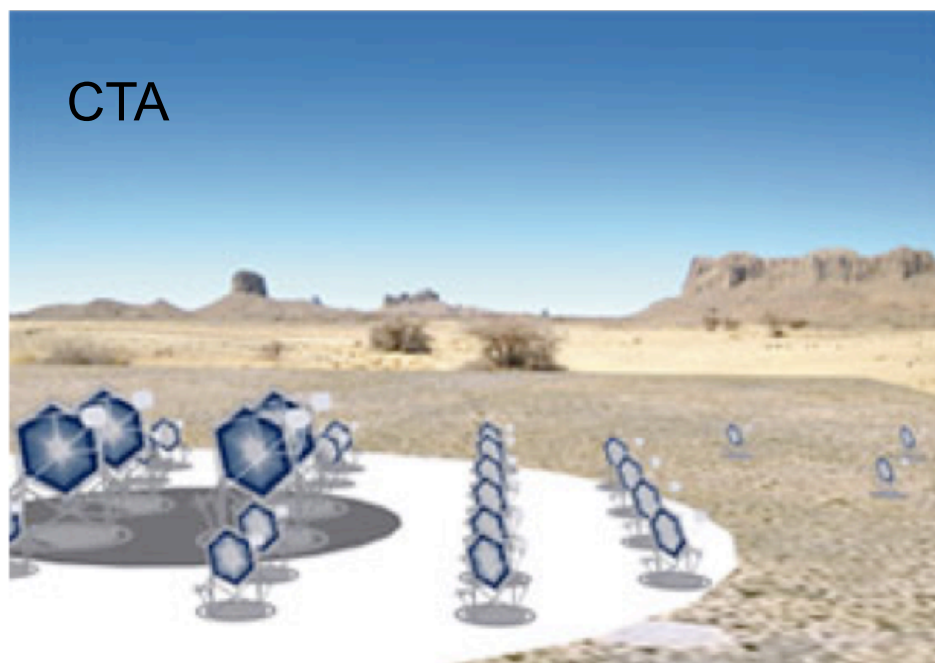
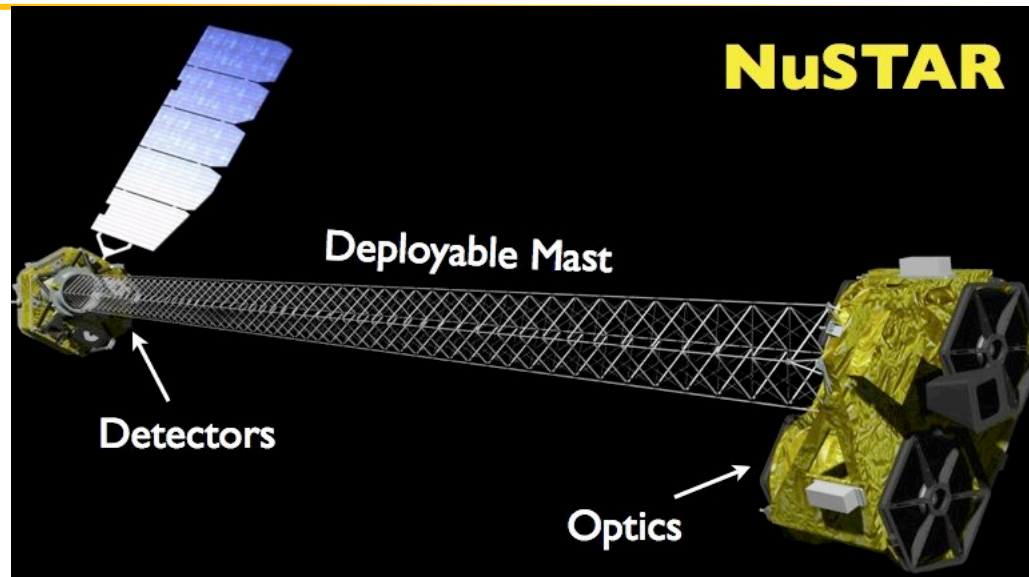
- simulations of the supernova explosion
- simulations of the turbulent interstellar medium

=> Multiwavelength spectra (radio, X et γ -rays, neutrinos)

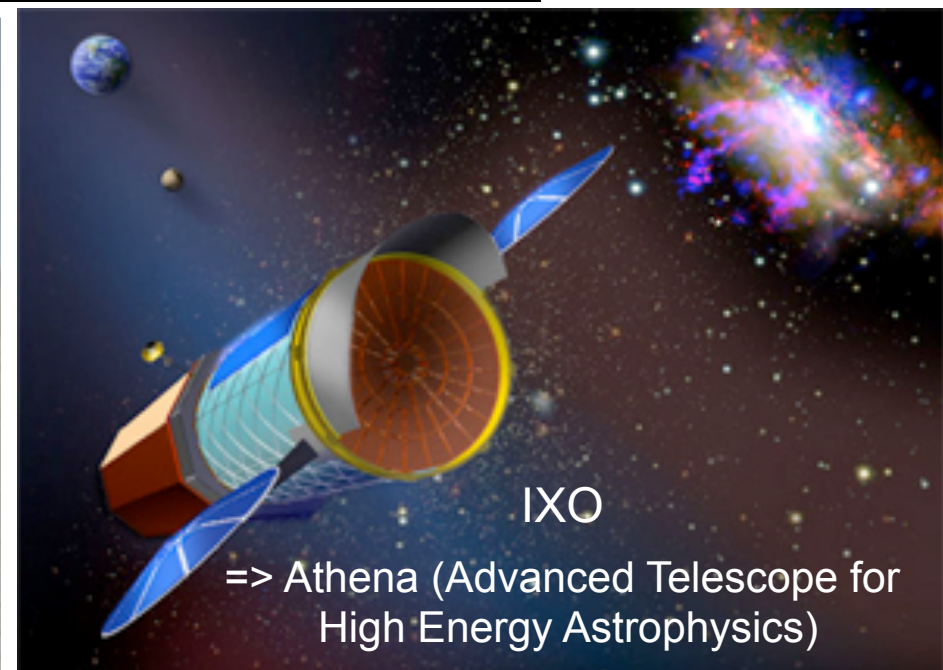
Grant: ANR blanche 2011-2014 *Cosmic rays and compressible MHD turbulence in the ISM*
LERMA / AIM / LPTA

Grant : *The youth of Cosmic Rays and their emergence into interstellar clouds*
LABEX UnivEarthS

Future facilities



CTA



Gamma-rays: access to shocked and unshocked radioactive ejecta.

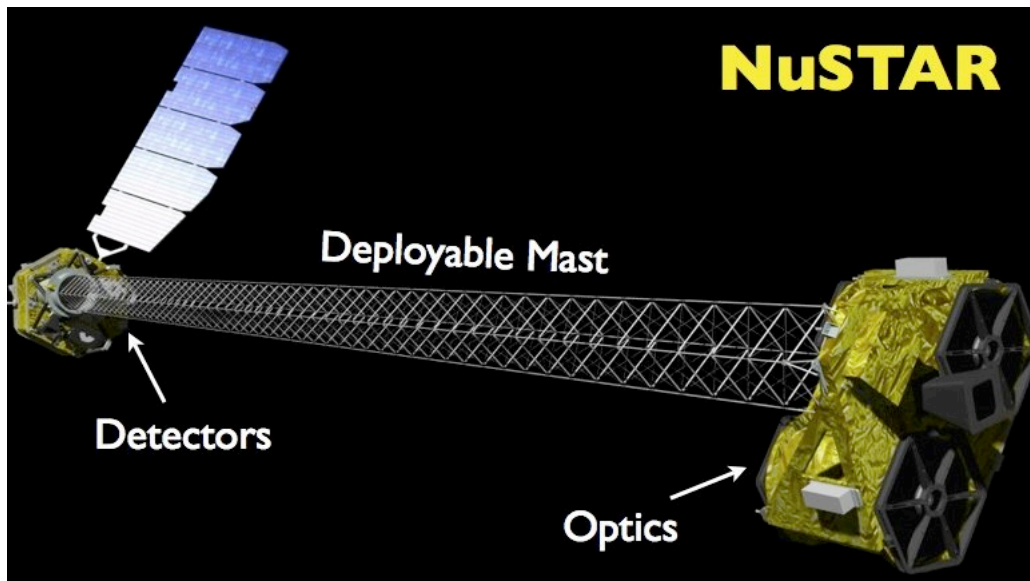
Heavy element production and explosion mechanism of supernovae

Objectives: mass of unstable freshly synthesized products (^{44}Ti) and their spatial distribution (site of alpha-rich freezeout) and constraints on the mass-cut.

Method: spectroscopy of the ejecta.

Needs: higher signal to noise spectra, higher spectral and spatial resolution to determine their mass, locate the site of alpha-rich freezeout and measure their velocity, to detect ^{44}Ti in a sample of SNRs

⇒ gamma-ray spectro-imager with low background.

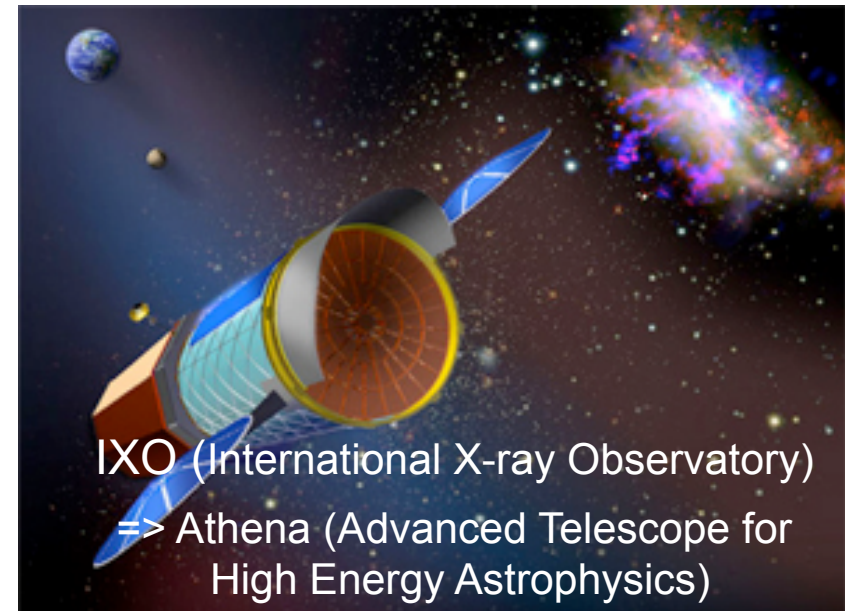
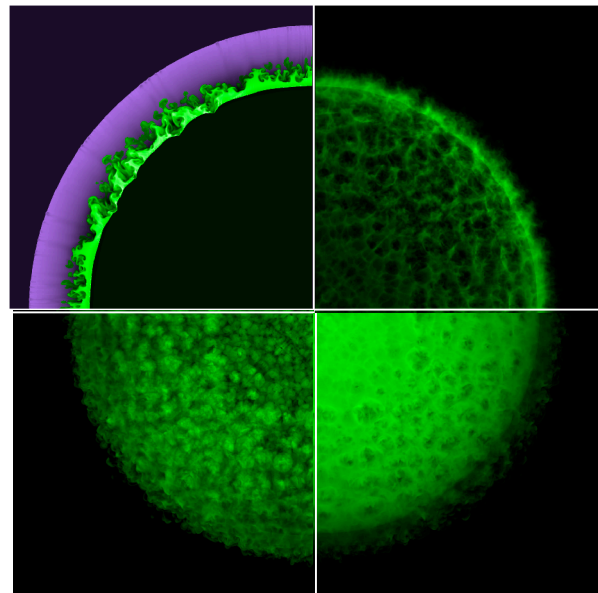


X-rays: access to high ionization states probing the shocked ejecta

Objectives: thermodynamic conditions (electron temperature, density), composition, spatial distribution and kinematics of the synthesized elements

Method: spatially resolved spectroscopy of the shocked ejecta

Needs: 3D maps of the elemental composition and kinematics through Doppler shift measurements of various lines for a sample of SNRs => energy resolution must improve from ~100 eV to ~eV range. Increased effective area to perform spectroscopic studies at a relevant spatial scale, faint lines diagnostics (Cr, Mn, ^{44}Sc) and studies of a larger sample of SNRs including extragalactic SNRs in the local group => **high throughput, high-resolution spatially resolved spectroscopy: IXO**



Objectives: caractérisation de l'émission par de la spectro-imagerie à une échelle adaptée à la source

- Spectro-imagerie des SNRs étendus les plus brillants vus pas HESS :
- Caractérisation spatiale et spectrale des restes découverts par FERMI : W51C, W44,...
- Découverte de nouveaux restes dans le plan Galactique
 - étude d'une population plus grande de restes émetteurs de gamma
 - différentes catégories, âges et processus en jeu (IC versus décroissance de pions)
- Découverte de spécimens inattendus : RSNe accélérant jusqu'à des énergies du PeV ?

